The viscosity of nanofluids: a review of the theoretical, empirical and numerical models

JOSUA P. MEYER, SAHEED A. ADIO, MOHSEN SHARIFPUR and PAUL N. NWOSU

Nanofluids Research Laboratory, Thermofluids Research Group, Department of Mechanical and Aeronautical Engineering, University of Pretoria, Pretoria 0002, South Africa.

ABSTRACT

The enhanced thermal characteristics of nanofluids have made it one of the fastest-growing research areas in the last decade. Numerous researches have shown the merits of nanofluids in heat transfer equipment. However, one of the problems is the increase in viscosity due to the suspension of nanoparticles. This viscosity increase is not desirable in the industry, especially when it involves flow, such as in heat exchanger or micro-channel applications where lowering pressure drop and pumping power are of significance. In this regard, a critical review of the theoretical, empirical and numerical models for effective viscosity of nanofluids was presented. Furthermore, different parameters affecting the viscosity of nanofluids such as nanoparticle volume fraction, size, shape, temperature, pH and shearing rate were reviewed. Other properties such as nanofluid stability and magnetorheological characteristics of some nanofluids were also reviewed. The important parameters influencing viscosity of nanofluids are temperature, nanoparticle volume fraction, size, shape, pH and shearing rate. Regarding the composite of nanofluids, which can consist of different fluid bases and different nanoparticles, different accurate correlations for different nanofluids need to be developed. Finally, there is a lack of investigation into the stability of different nanofluids when the viscosity is the target point.

Address correspondence to Mohsen Sharifpur, Nanofluids Research Laboratory, Department of Mechanical and Aeronautical Engineering, University of Pretoria, Pretoria, South Africa.
E-mail: mohsen.sharifpur@up.ac.za
Tel: +27 12 420 2448
Fax: +27 12 420 6632

INTRODUCTION

Colloidal suspension dates back to Maxwell's study in 1873 [1]. Though the idea behind his study was vivid, the imposed problems were too enormous for profitable engineering solutions [2]. In 1995, Choi [3] came up with a pioneering idea based on Maxwell's study and suspended ultrafine particles (nanoparticles) in conventional heat transfer fluids. His invention has opened up a myriad of opportunities in research and development. Nanofluids descriptively are colloidal suspensions containing metallic (Ag, Au, Al, Cu, Ni, etc.), non-metallic (single- and multi-wall carbon nanotube (SWCNT and MWCNT), Si, Graphene, etc.), metallic oxide (Al_2O_3, CuO, NiO_2,TiO_2, etc.) and oxides of non-metals (SiO_2, SiC, MgO, $CaCO_3$, etc.) nanoparticles suspended in conventional heat transfer fluids such as water, engine oil, ethylene glycol, transformer oil, gear oil or mixture of two or more heat transfer fluids [2, 3]. When compared with previous microparticle suspensions in conventional heat transfer fluids, it is a special type of fluid with numerous applications potentials because of its enhanced thermal conductivity, stability and homogeneity [3, 4]. Microscale particles in suspensions lead to abrasion, clogging of flow paths, pressure drop and high pumping power requirements, therefore, its sustainability was impossible. Besides, nanofluids can reduce the pumping power in engineering equipment significantly and do not pose the problem of clogging and abrasion of equipment flow paths [5–8]. Therefore, the design and engineering of physical systems are now being tailored towards using nanofluid as working fluid.

The impact of colloidal suspension cuts across the fields of science, biological science, medical, pharmaceutical and engineering. In the context of sustainable energy development and thermal management, nanofluids are becoming more and more significant as the need for efficient thermal management is of paramount importance. Moreover, the level of miniaturisation of devices today as technology advances is overwhelming. Devices such as microprocessors, microelectromechanical systems (MEMS), nanoelectromechanical systems (NEMS), microchannels and lab-on-chips come with high-density heat flux that needs quick heat removal for

efficient performance, stability and durability, which, from all indications, could be provided by nanofluids for now [9-12]. The following are also emerging areas of applications of nanoparticles and nanofluids: (i) they could be useful in medicine in the targeted treatment of malignant cells without damaging healthy tissues, (ii) they could also be used in the biomedical field for drug delivery for some special cases and (iii) they could also be used in surgery in order to increase the chances of survival of patients [6, 13-16].

The two most important parameters in bringing about the efficiencies highlighted above are the thermal conductivity and the viscosity of the nanofluids [17-20]. The thermal conductivity and heat capacity of the fluid determine to a great extent the heat removal capacity of the fluid. The higher the thermal conductivity, the more heat the fluid can remove from thermal systems. On the other hand, viscosity is mostly important in systems that require flow because flow properties such as the Reynolds number, heat transfer coefficients and pressure drop are very much dependent on the viscosity [21]. Therefore, if the viscosity is very high, there will be a penalty on the pumping power requirement to achieve the system's target. In the recent past, much research progress has been made on the thermal conductivity of nanofluids [22-32], which are a few of the copious works that can be found on theoretical and experimental reviews of the thermal conductivity of nanofluids. However, concerning the viscosity of nanofluids, very few theoretical models have been developed based on the unique properties of nanoparticles [2, 33]. Most theoretical models available were developed for the suspension of microparticles. Notably, there are many different types of empirical models of nanofluids, but their usage is often limited to specific types of nanofluids, nanoparticle sizes and volume fractions [34, 35]. The available review articles on nanofluid viscosity is very scarce [36, 37], and they lack the appraisal into the existing numerical works on nanofluid viscosity, which is part of the focus of this paper. Some other researchers have made efforts in partly reviewing nanofluid viscosity, however, their efforts were not exhaustive as their focus was mainly on the review of the thermal conductivity of nanofluids [38–41].

The mismatch between model and experimental results obtained from studies [42–44] on the rheological behaviour of nanofluids is of great concern. Besides, [2, 45] have shown that despite good agreement between experimental and theoretical results in certain cases, a wide range of constitutive factors need to be incorporated into the models in order to account for the rheological behaviour of the nanofluids in widely varying conditions [39]. Therefore, this work critically looks into the viscosity of nanofluids from an analytical, empirical and numerical view, points out loose ends in existing research and its methodologies and proposes an algorithm-based approach for the selection of appropriate nanofluid viscosity model(s). This review is divided into five sections, viz. 1. Introduction, 2. Theoretical background of suspension rheology, 3. Experimental studies, 4. Numerical studies and 5. Conclusion. Subsections under Section 1 are classical theoretical models, which give a detailed account of colloidal suspension viscosity models that predate the invention of nanofluids; new theoretical models, which are the models derived based on the factors that have been identified as key players in nanofluid viscosity enhancement such as particle size, zeta potential, pH and electrical double layer and empirical correlations, which are products of various experimental studies and observations that have been carried out on nanofluid viscosity. Section 3 accounts for the methods that have been used in establishing nanofluid viscosity experimentally, starting from the preparation of nanoparticles and nanofluids, characterisation and testing, nanofluid stability and its markers, factors affecting nanofluid viscosity and a cursory look into magnetic nanofluids for high-temperature lubrication application. The numerical aspect of nanofluid viscosity enhancement under Section 4 brings the following to the fore: the application of artificial neural network systems (ANNs), genetic algorithm and fuzzy logics for the prediction of the viscosity of nanofluid, with a concluding part identifying areas for further development and future research on nanofluids.

THEORETICAL BACKGROUND OF SUSPENSION RHEOLOGY

The rheology of colloidal suspension encompasses the study of the behaviours of suspension in relation to whether it is Newtonian or non-Newtonian and thus a measure of its viscosity with respect to shearing stress and shearing rate. There are a number of factors that affect colloids suspensions (micro/nanoparticles in suspensions), which are: temperature, particle volume concentration, particle size, particle size distribution (PSD), packing fraction, electrical double layer (EDL), aspect ratio of particles, particle interaction, particle agglomeration, zeta potentials, pH, nanolayer and magnetic properties of some particles [46]. As mentioned previously, the earlier classical theoretical analyses were on microparticles in suspensions and a great deal of simplification on the mechanisms of rheological behaviours was applied.

Classical Theoretical Models

Hypothetical analyses of the possible phenomena affecting the viscosity of nanofluids can be found in the literature, though they are very limited when compared with the depth of the theoretical models that can be found on thermal conductivity of nanofluids. However, several theoretical studies have been conducted into the rheology of suspensions. The fundamental work by Einstein [47] on infinite dilute suspensions of uncharged hard spheres based on the vorticity of the particle shear field was the first available theoretical work on the viscosity of suspension that gave the model in Eq. (1).

$$\mu_{eff} = \mu_o(1 + [\eta]\phi) \tag{1}$$

where μ_{eff} is the effective viscosity of the suspension, μ_o is the dynamic viscosity of the base fluid and $[\eta]$ is the intrinsic viscosity of the suspension. This linear equation is based on the assumed absence of interaction between the particles, and the coefficient $[\eta]$ is a function of shape of the particle, which for hard spheres was given as 2.5. This model was stated to be valid for solid volume concentration, $\phi \leq 2\%$.

Numerous models were developed in efforts to extend the Einstein model to concentrated suspensions [48–51] a few years after Einstein's work. Contained in Table 1 is the comprehensive list of other available classical models developed by various investigators [52–62] and are applicable to the determination of the viscosity of solid-liquid suspension. These models differ from one another, and no single model can predict data in the entire concentration range up to the maximum concentration possible.

Contrary to the uncharged particles of Einstein [47], Smoluchowski [48] presented an effective viscosity model for charged particles in electrolyte suspension given in Eq. (2). There was no explanation of how this equation was achieved:

$$\mu_{eff} = \mu_o \left[1 + 2.5\phi \left\{ 1 + \frac{1}{k\mu_o a^2} \left(\frac{\zeta D_E}{2\pi} \right)^2 \right\} \right] \tag{2}$$

where k is the specific conductivity of the electrolyte, a the radius of the solid particles, D_E the dielectric constants of the water and ζ the zeta potential of the particle with respect to the electrolytic medium. There was no explanation of how this equation was achieved and this was buttressed by researchers in the past [63, 64]. Based on experimental data, Bull in 1940 [64] suggested that the effective viscosity of suspension of egg albumen varies with the square of the electrophoretic mobility (a measure of zeta potential). However, the analytical works of Smoluchowski [48] gave effective viscosity of suspension with the square of zeta potential as well, unfortunately when this equation was applied to Bull's experimental data, it exaggerated the predictions. Therefore, Bull [64] proposed a simple model for effective viscosity at isoelectric point to be:

$$\frac{\mu_s}{\phi} = 0.0112 \frac{\mu_e}{\sqrt{k}} \tag{3}$$

where μ_s is the specific viscosity, μ_e the electrophoretic mobility and k the specific conductivity. Booth [63] in 1950 studied the overprediction (of viscosity of suspension with respect

to the effect of electroviscous force between particles and the suspending medium) made by Smoluchowski's model. Therefore, Booth made a quantitative recalculation of the electroviscous force effect on effective viscosity, which predicted the data of Bull [64] with a good degree of accuracy and the model is given as:

$$\mu_{eff} = \mu_o \left[1 + 2.5\phi \left\{ 1 + \sum_{1}^{\infty} b_I \left(\frac{e\zeta}{k_b T} \right)^I \right\} \right] \tag{4}$$

where b_I is the characteristics of electrolyte, e is the electronic charge on particles, k is the Boltzmann constant and T is the absolute temperature.

In 1922, Jefferey [49] furthered the work of Einstein for suspensions that contain ellipsoidal particles. Based on the principle of dissipation of energy, the model presented was not different from Einstein's Eq. (1). However, the intrinsic viscosity was provided with two limits (minimum and maximum) for both prolate and oblate spheroids of different ellipticity of the meridian section. Therefore, as the particles approach the sphere in shape, the difference in the limits of the intrinsic viscosity diminishes and hence reduces to Einstein's model. Ward and Whitmore [65] experimented on microsphere-aqueous suspension in a bid to verify the Einstein equation. They concluded that the intrinsic viscosity given by Einstein is a function of PSD ratio, which is approximately 4.0 for an infinitely diluted suspension with PSD ratio 1:1 and approximately 1.9 for PSD ratio exceeding 3:1. At the ratio of 1.5:1, the Einstein intrinsic value of 2.5 was obtained. This was corroborated by the work of Vand [52]. Williams [66] also concluded that PSD is a key parameter affecting the viscosity of solid-liquid suspension after experimenting with different size (4, 8 and 12 μm) categories of glass spheres in an ethylene glycol-water mixture. He tried to fit the data obtained into the equations of Mooney [53] and Roscoe [54] with relatively good success. Maron and Fok [67] held that the duo of Mooney and Roscoe models did not satisfactorily predict the experimental data of Williams [66], hence tried to fit the data with models of Maron and Fok [67] that had been successfully tested with lattices and latex mixtures. After treating the

experimental data with the least-squares method to obtain model constants, they clearly showed that if the intrinsic viscosity of Einstein's model were to be between 3.15-3.35, the equations of Mooney [53] and Roscoe [54] would have given a perfect fit to Williams's data.

Applying a different viewpoint, Batchelor [55] considered the influence of interparticle interactions to obtain the model in Eq. (5), for the relative viscosity of solid-liquid suspension for a case of volume fraction, $\phi \leq 4\%$. Within the limits of a very low particle concentration, this model approaches Eq. (1), which means Batchelor's model does not differ from Einstein's model, i.e. at low volume concentration, the assumption of non-interaction of particles as assumed in [47] is also inherently considered and this is an ideal situation.

$$\mu_{eff} = \mu_o \left(1 + [\eta]\phi + k_H \left([\eta]\phi\right)^2\right) \tag{5}$$

where k_H is the Huggin's coefficient known also as the interaction parameter, this coefficient accounts for interparticle interaction as opposed to hydrodynamic effects [68]. The semi-empirical relationship proposed by Krieger and Dougherty [56] for shear viscosity covering the full spectrum of particle volume concentrations is expressed as:

$$\mu_{eff} = \mu_o \left(1 - \frac{\phi}{\phi_m}\right)^{-[\eta]\phi_m} \tag{6}$$

where ϕ_m is the maximum particle volume fraction at which flow can still occur (i.e. the concentration at which the relative viscosity approaches infinity asymptotically), the intrinsic viscosity [η] was given as 2.5 for monodispersed suspensions of hard spheres. However, in practical situations, particles are polydisperse in nature. Hence the assumption made by Krieger and Dougherty [56] is not valid for all particulate suspensions and this has been accentuated with underpredictions of this model when applied to viscosity data, for example, when it was applied to Al_2O_3-water nanofluid data [69].

Currently, there is a lack of unified models that can be used to predict the viscosity of colloids. Most of the available classical models are built around particle volume concentration and when tested, they all give different predictions as depicted in Fig. 1. The insets of Fig. 1 show the degree of variations among the models. There is no clear-cut phenomenon to explain the erratic nature of nanofluid viscosity data presented by different investigators. However, using these models to predict the recent experimental data as depicted in Fig. 2 and Fig. 3 (for Al_2O_3-water and TiO_2-water respectively) shows their inability to accurately predict the suspension's viscosity. Generally, the discrepancies in reported viscosity data have mostly been ascribed to agglomeration formation. Chen et al. [68], based on this widespread assertions, extended the theoretical work of Krieger and Dougherty [56], which was based on packing fraction of monodispersed particles without agglomeration. Chen et al. [68] assumed that if particle agglomerates were spherical, the sphere would be of different sizes. Thus they derived a modified Krieger and Dougherty equation as presented in Eq. (7), based on maximum packing fraction of agglomerates and the fractal index of the agglomerates, which is an indication of degree of variation in the packing fraction from the centre of the agglomerates to the outer edge.

$$\mu_{eff} = \mu_o \left(1 - \frac{\phi_a}{\phi_m}\right)^{-[\eta]\phi_m} \tag{7}$$

ϕ_a is given by $\phi_a = \phi/\phi_{ma}$, where ϕ_{ma} is the packing fraction of the aggregates. The viscosity was assumed to follow a power law with a fractal index, *D*. Consequently, ϕ_a becomes $\phi_a = \phi(a_a/a)^{3-D}$, where a_a/a is the ratio of effective radii of aggregates and primary nanoparticles.

In an attempt to bring together the two separate views, namely that (i) PSD affects the viscosity of suspension and further that (ii) agglomeration, which is a function of interaction between particles, affects the viscosity of suspension, Farris [70] suggested that agglomeration alone could not describe the evolution of viscosity of nanofluids and that PSD was seen to play a role in the viscosity trend. Therefore, if the PSD is discrete, the global relative viscosity of the non-interacting

monodispersed system of particles in suspensions may be calculated as the product of each independent viscosity as shown in Eq. (8) [70].

$$\eta_r = \left(\frac{\mu_1\phi_1}{\mu_o}\right)\times\left(\frac{\mu_2\phi_2}{\mu_o}\right)\times\cdots\cdots\times\left(\frac{\mu_z\phi_z}{\mu_o}\right) \tag{8a}$$

In general form $$\eta_r = \prod_{i=1}^{z}\eta_r\left(\phi_i\right) \tag{8b}$$

where ϕ_i is the z^{th} class corresponding particle fraction and z stands for the different average particle sizes contained in the distributions. The viscosity of each monodispersed suspension can also be related to the maximum particle volume fraction, ϕ_m with the proposed model in [71] given as:

$$\eta_r\left(\phi_i\right) = \left[1+0.75\left(\frac{\phi_i/\phi_m}{1-\phi_i/\phi_m}\right)\right]^2 \tag{9}$$

Chong et al. [71] determined experimentally the maximum particle volume fraction for a monodispersed system of glass beads sized in microns using a specially developed orifice viscometer. They reported ϕ_m for their experiment as 0.605 and further proved that plotting the $\phi\eta_r/\left(\eta_r-1\right)$ vs ϕ and extrapolating up to the point where the two axes variables meet will give the ϕ_m for any suspension. Storms et al. [72] expanded the work of Chong et al. [71] to understand the effect of plydisperity (size ratio and % volume fraction of smaller particles) on the viscosity of suspension. It was found that the viscosity is dependent on the size ratio and % volume fraction of the small particles present. The model in Eq. (10) predicted the experimental data of Chong et al. [71] with good accuracy:

$$\eta_r\left(\phi_i\right) = \left[1+\frac{R\phi_i}{1-\phi_i/\phi_m}\right]^{3.3\phi_m} \tag{10}$$

where R is an adjustable parameter and varies from 0.7 to 1.25 depending on the size distribution. If ϕ_m is taken as 0.605 as Chong et al. [71] proposed, the exponent in Eq. (10) becomes 2. It should be noted that Eqs. (9) and (10) are modified versions of the Eilers equation given below.

$$\eta_r = \left[1 + \frac{2.5\phi}{2\left(1-\phi/\phi_m\right)}\right]^2 \tag{11}$$

Determining ϕ_m for monodispersed and bidispersed suspension, Dames et al. [73] applied an empirical model in Eq. (12) to determine the maximum packing fraction for particle sizes R_{large} = 270 nm and R_{small} = 80 nm:

$$\phi_{\mathrm{m}} = \phi_z - \left(\phi_z - \phi_m^{mono}\right)^{\left(0.27\left(1-\frac{D_5}{D_1}\right)\right)} \tag{12}$$

where $\phi_z = 1-\left(1-\phi_m^{mono}\right)^z$ and $D_x = \dfrac{\sum_{i=1}^{z} N_i d_i^x}{\sum_{i=1}^{z} N_i d_i^{x-1}}$

where ϕ_m^{mono} is the maximum packing fraction of a monodispersed system and it is taken as 0.63, z is the number of modal suspensions (mono, bi or multi), D_x is the *x-th* moment of particle size distribution, i.e. D_1 is the number average of the particle diameter. For a multidispersed mixture of spherical particles, the technique given in Muralidaharan and Runkana [74] and Servais et al. [75] can be used to determine ϕ_m from the minimum value of P_i:

$$\phi_{\mathrm{m}} = \min\left(P_i\right) \tag{13}$$

where P_i is the packing fraction of each class size i, calculated based on the following:

$$P_i = \sum_{j=1}^{n} \gamma_{ij} \nu_j \tag{14}$$

γ_{ij} is the binary packing coefficient of classes i and j, and ν_j is the volume fraction of the class j. The procedures for calculating these two quantities are detailed in [74, 75].

It should be noted that all of these earlier works were done before the invention of nanofluids and as such were basically on the suspension of microsolids and rigid spheres in fluid medium. However, knowledge and ideas have been borrowed from these past works for the recent analyses of the thermophysical properties of nanofluids. Again, some of these models were first published more than 80 years ago. Therefore, the useability of these classical models on nanofluids is a subject that should be critically analysed [76] because many factors that affect colloids in suspensions have been greatly oversimplified in order to achieve a presentable solution.

New Theoretical Models

Researchers have tried to predict the viscosity of nanofluids using the classical models on viscosity of suspension without success. These models all predate the invention of nanofluids. Therefore, some very salient characteristics such as nanolayer, pH, electrical double layer (EDL), zeta potentials, temperature, capping layer, interparticle spacing and particle magnetic properties that influence the thermal properties of suspensions were not considered.

Chen et al. [68], based on an earlier work, considered an important factor (agglomeration) because it affected the viscosity of nanofluids. After substituting some empirical data that described the extremes of nanoparticle agglomeration, the viscosity of nanofluids given in Eq. (15) was derived.

$$\eta_r = \left(1 - \frac{\phi}{0.605}\left(\frac{a_a}{a}\right)^{1.2}\right)^{-1.5125} \tag{15}$$

Hosseini et al. [33] obtained a new dimensionless model for predicting the viscosity of nanofluids. The relative viscosity was a function of formulated dimensionless groups, which contains the following parameters: (i) viscosity of the base fluid, (ii) the hydrodynamic volume fraction of nanoparticles, (iii) diameter of a nanoparticle, (iv) thickness of the capping layer, and (v) temperature as dimensionless groups π_1, π_2, π_3 and π_4 respectively as presented in Table 2. The model (Eq. 16) is the result of the combination of the dimensionless groups:

$$\mu_{nf} = \mu_o . \exp\left[m + \alpha\left(\frac{T}{T_o}\right) + \omega(\phi_h) + \gamma\left(\frac{d_p}{1+r}\right)\right] \quad (16)$$

where μ_{nf} is the viscosity of the nanofluids, μ_o is the viscosity of the base fluid, ϕ_h is the hydrodynamic volume fraction of nanoparticles, d_p is nanoparticles diameter, r is the thickness of the capping layer, T_o is a reference temperature taken to be 20 ^{o}C, and T is the measured temperature. In this model, m is referred to as system property constant, which is a function of types of nanoparticles, types of base fluids and the interactions between them. α, ω, γ are empirical constants obtainable from the experimental data. However, there was no indication of how these constants were derived and this makes the testing of these models against similar or other nanofluids a problem. The model was also tested with limited samples of Al_2O_3-water-based nanofluids, although it claimed good agreement with the experimental data tested.

Recent literature revealed that the theoretical analysis of the effective viscosity of nanofluids can be approached as either a single-phase problem or as a two-phase problem. Masoumi et al. [2] analysed the dispersion of nanoparticles in a fluid medium as a two-phase problem and considered five parameters as affecting the effective nanofluid viscosity. The following parameters: nanoparticle size, temperature, nanoparticle density, nanoparticle volume fraction in the fluid medium and fluid physical properties were considered. Using the Brownian velocity relation presented by Prasher et al. [77] in Eq. (17), the effective viscosity was derived as presented in Eq. (18). A creeping flow assumption around the spherical nanoparticle was used in their derivation and they introduced a correction factor, also based on very limited data to take care of the simplification of their assumption. The model was tested in predicting effective viscosity of CuO-H_2O, CuO-EG, TiO_2-EG, CuO-EG/H_2O and Al_2O_3-H_2O nanofluids and according to the results presented, there was an acceptable level of agreement between the model and the experimental data used.

$$V_B = \frac{1}{d_p}\sqrt{\frac{18k_bT}{\pi\rho_p d_p}} \tag{17}$$

$$\mu_{nf} = \mu_o + \frac{\rho_p V_B d_p^2}{72C_1\delta} \tag{18}$$

where k_b is the Boltzmann constant, T is the temperature, ρ_p is the particle density, δ is the distance between the centres of particles, V_B is the Brownian velocity, C_1 is the correction factor, and d_p is the particle diameter. V_B, δ and the constant were C_1 defined as:

$$\delta = \sqrt[3]{\frac{\pi}{6\phi}}d_p \tag{19}$$

$$C_1 = \mu_o^{-1}\left[\left(c_1 d_p + c_2\right)\phi + \left(c_3 d_p + c_4\right)\right] \tag{20}$$

constants $c_1 - c_4$ are obtainable from experimental data. It should be stated here that this is one of the very few theoretical analyses of nanofluid viscosity existing in the literature. However, the required procedures as described by the authors to obtain this set of constants will not allow for reproducibility of these constants and hence C_1 may be difficult to calculate for other nanofluids different from those in their work. We believe a better presentation of these constants can be made, in fact, to our knowledge, the model has not been cited much in comparison with experimental data by other investigators since its publication.

Empirical Models

Ward in [78] recommended that experimental results should be expressed in the form of Eq. (21) to allow easy comparison with theoretical models. He further noted that the intrinsic viscosity should be determined experimentally, because it is difficult to evaluate the intrinsic viscosity from the power of three and above theoretically [79].

$$\mu_{eff} = \mu_o\left(1 + [\eta]\phi + [\eta]^2\phi^2 + [\eta]^3\phi^3 + [\eta]^4\phi^4 + ..\right) \tag{21}$$

Cheng and Law (CL) [80] reanalysed effective viscosity of suspensions based on Einstein's model to provide an exponential formula for the effective viscosity of nanofluids for volume fractions higher than Einstein's concentration regime. The CL model (Eq. 22), though similar to the general model expression given by Batchelor [55] and Lundgren [57], however, provided the coefficient of volume fraction up to the power of five. When compared with the experimental data reported by Ward in [78], they are in close agreement.

$$\mu_{eff} = \mu_o \left(\begin{array}{l} 1 + 2.5\phi + \left(\frac{35}{8} + \frac{5}{4}\beta \right)^2 \phi^2 + \left(\frac{105}{16} + \frac{35}{8}\beta + \frac{5}{12}\beta^2 \right)^3 \phi^3 \\ + \left(\frac{1155}{128} + \frac{935}{96}\beta + \frac{235}{96}\beta^2 + \frac{5}{48}\beta^3 \right)^4 \phi^4 + \\ \left(\frac{3003}{256} + \frac{1125}{64}\beta + \frac{1465}{192}\beta^2 + \frac{95}{96}\beta^3 + \frac{1}{48}\beta^4 \right) \phi^5 + ... \end{array} \right) \tag{22}$$

where β is the diffusion exponent. Avsec and Oblak [45] emphasise that Ward's model as presented in Eq. (23) is of little importance to nanoscale viscosity (nanoviscosity) and presented a new model (Eq. 24) with a simple twist to Ward's expression. This was derived using statistical mechanics owing to the possibility of modelling particulate interaction (nanolayer interaction effect) with statistical mechanics.

$$\mu_{eff} = \mu_o \left(1 + 2.5\phi + (2.5)^2 \phi^2 + (2.5)^3 \phi^3 + (2.5)^4 \phi^4 + ... \right) \tag{23}$$

$$\mu_{eff} = \mu_o \left(1 + 2.5\phi_{eff} + (2.5)^2 \phi_{eff}{}^2 + (2.5)^3 \phi_{eff}{}^3 + (2.5)^4 \phi_{eff}{}^4 + ... \right) \tag{24}$$

where $$\phi_{eff} = \phi \left(1 + \frac{h}{a} \right)^3 \tag{25}$$

ϕ_{eff} is the effective volume fraction, h is the thickness of the nanolayer and a is the particle radius.

Apart from the theoretical models presented above, most of the available models for the determination of nanofluid viscosity are correlations from very limited experimental data. These models are not hybrid because they are in most cases developed from experimental data with a

confined volume fraction of nanoparticles, a few nanoparticle types (at most three for a model), a small spectrum of the nanoparticle size and mostly spherical or assumed spherical in shape [81–86].

It has been observed by investigators through experimental studies that the temperature of medium of study, volume fraction, shear rate and size of nanoparticles affect the effective viscosity of nanofluids [36, 87, 88]. However, an exhaustive examination of the existing empirical models shows that in the majority of the correlations, researchers refrained from providing the effect of temperature, shear rate and size of nanoparticles as they affect nanofluid viscosity in their correlations.

Nguyen et al. [87], after a comprehensive investigation of the dynamic viscosity of alumina-water nanofluids considering different nanoparticle volume fractions, sizes and temperatures, only provide individual correlation equations for nanofluid viscosity based on the volume fraction and temperature respectively. In fact, the models with temperature can only predict for 1%-4% volume fraction, which was even inadequate for their experimental data. Similarly, Vakili-Nezhaad and Dorany [89] provided two empirical models for the same nanofluids (SWCNTs/lube oil) based on volume fraction and temperature. The correlations are polynomial function of volume fraction and temperature as given below:

$$\mu_{nf} = \mu_o \left(1 + 1.59\phi - 16.36\phi^2 + 50.4\phi^3\right) \tag{26}$$

$$\mu_{nf} = \mu_o \left(1048 - 30.3T + 0.2T^2\right) \tag{27}$$

Eqs. (26) and (27) are valid for 0.01-0.2% volume fraction and 25-100 ^{o}C temperature respectively. Rashin and Hemalatha [35] on the viscosity of CuO-coconut oil also proposed two separate models to predict the mass fraction and temperature dependence of their experimental data. The mass fraction model, similar to Batchelor's equation [55], is presented alongside the temperature model in Eqs. (28) and (29):

$$\mu_{nf} = \mu_o \left(1 + A\varphi - B\varphi^2\right) \tag{28}$$

$$\mu_{nf} = Ce^{-0.03T} \tag{29}$$

where φ is the mass fraction of nanoparticle to base fluid, T is the temperature in Kelvin, *A, B* and *C* are parameters from regression analysis and unique to 20 nm CuO-coconut oil nanofluids at a temperature range of 35-55 ^{o}C. Many other researchers just present their model as a linear or polynomial function of the volume fraction without considering the effect of at least temperature [90–94].

Heyhat et al. [21] presented a volume fraction exponential correlation relating the viscosity of alumina-water nanofluid at volume fraction of 0.1-2%. The correlation (Eq. 30) averaged the effect of volume fraction over the temperature range experimented (20-60 ^{o}C):

$$\frac{\mu_{nf}}{\mu_o} = Exp\left(\frac{5.989\phi}{0.278-\phi}\right) \tag{30}$$

In 2012, Suganthi and Rajan [95] proposed a modified form of Einstein's equation (Eq. 31a) by replacing the volume fraction with agglomerate volume fraction similar to Chen et al. [68]. This was done in order to account for the effect of agglomeration on the viscosity of nanofluid.

$$\mu_{nf} = \mu_o\left(1+2.5\phi_a\right) \tag{31a}$$

where ϕ_a is related to ϕ using:

$$\frac{\phi_a}{\phi} = \left(\frac{D_a}{d_p}\right)^{3-D} \tag{31b}$$

Generally, in nanofluids, agglomerates are of different sizes. Therefore, Eq. (31b) can be rewritten in a more broad form:

$$\left(\frac{D_a}{d_p}\right)^{3-D} = \sum_i^N\left(\varphi_i\left(\frac{D_{ai}}{d_p}\right)^{3-D}\right) \tag{31c}$$

where φ_i is the mass fraction of the aggregate *i*, D_{ai} is the diameter of the aggregate *i*, *N* is the number of aggregates present and *D* is the fractal dimension. The diameter of the nanoparticle

(ZnO) used is 35-40 nm. As the volume fraction increases up to 2%, the authors proposed a modified Batchelor's equation [55] as shown in Eq. (32) to take care of the effect of particle-particle interactions:

$$\mu_{nf} = \mu_o \left(1 + 2.5\phi_a + 6.1\phi_a^2\right) \tag{32}$$

Recently, Suganthi et al. [96] proposed a temperature-based power law correlation (Eq. 33) to relate the effect of temperature on the viscosity of ZnO-propylene glycol (PG) nanofluid. Their previous models (Eqs. 31 and 32) could not be applied here, probably because the trend of ZnO-PG with increase in volume fraction is directly opposite to the trend in their experiment on ZnO-water nanofluid [95]:

$$\mu_{nf} = A\theta^{-B} \tag{33}$$

where θ is in degree Celsius, A and B are empirical constants, and are different for different volume fractions. Singh et al. [97] offered a correction based on the Arrhenius functional form (Eq. 34) to predict the temperature dependence of 170 nm SiC-water-based nanofluid at volume fraction of 1.8, 3.7 and 7.4%:

$$\mu_{nf} = \mu_{\infty,T} \exp\left(\frac{E_a}{R_g T}\right) \tag{34}$$

where $\mu_{\infty,T}$ is the viscosity at "infinite temperature", E_a is the activation energy to viscous flow, R_g is the universal gas constant and T is the temperature in Kelvin. The viscosity at infinite temperature and the activation energy can be obtained from experimental data, using the logarithmic form of the Arrhenius equation [98]. Also, Abareshi et al. [43] were able to fit their experimental data at different volume fractions into the Vogel-Fulcher-Tammann (VFT) equation [99], which took care of the temperature effect on nanofluid viscosity alone as shown below.

$$\frac{\mu_{nf}}{\mu_o}(T) = Ae^{\left(\frac{B}{T+T_o}\right)} \tag{35}$$

Eq. (35) was fitted for the two limiting volume fractions to produce two sets of the empirical constants *A, B* and T_o. The problem with generating correlation through regression analysis of a single parameter such as temperature is that when large numbers of volume fractions are involved, the empirical constants become huge and untidy. This is also dependent on the number of constants in the proposed model. For instance, Zyla et al. [100] proposed a nine-order polynomial correlation to fit the viscosity of Y_2O_3-diethylene glycol (DIEG). The variable in their correlation is the temperature of the nanofluid. The concentration studied was in five levels (5:5:25%). Therefore, according to their model Eq. (36), the empirical constants totalled 50.

$$\eta_r = a_0 + a_1 T + a_2 T^2 + a_3 T^3 + a_4 T^4 + a_5 T^5 + a_6 T^6 + a_7 T^7 + a_8 T^8 + a_9 T^9 \qquad (36a)$$

In a more general form:

$$\eta_r = \sum_{i=0}^{9} a_i T^i \qquad (36b)$$

where a_i's are the experimental constants and T is the temperature in degree Celsius.

Kulkarni et al. [101] gave a correlation, which is one of the few empirical works that take care of both the temperature and volume fraction effect on the nanofluid viscosity. Another of such is the work of Namburu et al. [34], in which they tried to fit their experimental data to existing equations in the literature. However, the failure of the exercise spurred a new correlation given in Eq. (37), which considered both temperature and volume fraction effects.

$$Log\left(\mu_{nf}\right) = Ae^{-BT} \qquad (37a)$$

Eq. (37a) is an empirical model with a correlation coefficient $R^2 = 0.99$, developed for CuO-EG nanofluids with volume concentration of CuO ≤ 6.12%. Constants A and B were calculated with the correlations below:

$$\left.\begin{aligned} A &= 1.8375\phi^2 - 29.643\phi + 165.56 \\ B &= 4\times10^{-6}\phi^2 - 1\times10^{-3}\phi + 1.86\times10^{-2} \end{aligned}\right\} \qquad (37b)$$

where $R_A^2 = 0.987$ and $R_B^2 = 0.988$. Nguyen's correlation [87] performed better than most of the classical models. However, Yiamsawas et al. [102] showed that Nguyen's correlations under predicted their alumina-EG/water experimental data, because Nguyen's correlation considers separately the volume fraction and temperature effects on the nanofluid viscosity. Consequently, the correlation below was developed to predict the viscosity of titania-EG/water (20:80) and alumina-EG/water (20:80) with volume fraction range of 1-4%. The experiments were conducted between 15-60 ^{o}C, and the diameters of the titanium oxide and aluminium oxide used were 21 and 120 nm respectively.

$$\mu_{nf} = A\phi^B T^C \mu_o^E \tag{38}$$

where μ_o is calculated based on this expression; $\mu_o = 2.3775 - 0.0461T + 0.0003T^2$, *A, B, C* and *E* are empirical constants obtained from regression analysis. Lately, Hemmat Esfe and Saedodin [103] offered a two-variable correlation (namely temperature and volume fraction) for ZnO-EG nanofluids. The correlation (Eq. 39) has an average deviation of 2% from the experimental data, and the stability region over which it was tested is $25 \leq T \leq 50^{o}$C and $0.25 \leq \phi \leq 5\%$:

$$\frac{\mu_{nf}}{\mu_o} = 0.9118e^{\left(5.49\phi - 0.00001359T^2\right)} + 0.0303ln\left(T\right) \tag{39}$$

Azmi et al. [104] offered a water-based correlation based on the combined effects of volume fraction, temperature and nanoparticle size on the effective viscosity of nanofluids. Using data available in the literature on Al_2O_3, CuO and SiC with particle size ranging from 20-170 nm and volume fraction ≤ 4%, they proposed the following correlation:

$$\frac{\mu_{nf}}{\mu_o} = C_1\left(1+\frac{\phi}{100}\right)^{\alpha}\left(1+\frac{T_{nf}}{70}\right)^{-\lambda}\left(1+\frac{d_p}{170}\right)^{-\sigma} \tag{40}$$

where C_1 is empirical constant and the exponents α, λ and σ are 11.3, 0.038 and 0.061 respectively. To test the performance of this model, they carried out new experiments on water-based nanofluids of Al_2O_3, ZnO and TiO_2. Generally, the model is valid for water-based nanofluids of Al_2O_3, CuO, Sic, ZnO and TiO_2 with particle diameter between 20-170 nm and volume fraction $\phi \leq$ 4%. Khanafer and Vafai [105] also developed a three-parameter correlation to predict the viscosity of Al_2O_3-water nanofluid. Their correlation shown below is valid for volume fraction between 1-9%, temperature between 20-70 ^oC and nanoparticle diameter between 13-131 nm.

$$\mu_{nf} = -0.4491 + \frac{28.837}{T} + 0.574\phi - 0.1634\phi^2 + 23.053\frac{\phi^2}{T^2} + 0.0132\phi^3 - 2354.735\frac{\phi}{T^3} + 23.498\frac{\phi^2}{d_p^2} - 3.0185\frac{\phi^3}{d_p^2} \qquad (41)$$

The model above predicted the viscosity changes with temperature of some data in the literature with good accuracy. However, the performance of the model was not tested against volume fraction increase.

Numerous studies have shown that the addition of nanoparticles to a Newtonian base fluid sometimes turns the fluid to non-Newtonian. An example of this is the recent works of Yu et al. [106] on aluminium nitride nanofluid and Halelfadl et al. [107], and Aladag et al. [108] on alumina and carbon nanotube water-based nanofluids. In most situations, despite the non-Newtonian nature of nanofluids, researchers will only provide correlations considering temperature and volume fraction or both. According to Syam Sundar et al. [109], it is important to study the behaviour of nanofluids with respect to change in shear rate, therefore empirical correlations should be designed taking cognisance of this parameter. Hernández Battez et al. [88] investigated the rheology of ZnO and ZrO_2 suspended in Newtonian polyalphaolefin (PAO 6) base fluid. At low shear rates (0-700 s^{-1}), all nanofluid samples behaved as Newtonian fluid; however, at higher shear rates (10^6 -10^7 s^{-1}), non-Newtonian shear thinning characteristics with varying trends were observed. This suggests that the effect of shear rate is significant in the characterisation of nanofluid viscosity. Therefore, the following correlations were proposed for the two types of nanofluids (ZnO and ZrO_2) respectively:

$$\eta_r(cp) = 52.80 - 9.76\times10^{-7}\dot{\gamma} + 0.172\varphi - 0.912T + 1.02\times10^{-8}\dot{\gamma}T + 4.24\times10^{-3}T^2 \quad (42)$$

$$\eta_r(cp) = 53.78 - 9.25\times10^{-7}\dot{\gamma} + 0.202\varphi - 0.937T + 9.65\times10^{-9}\dot{\gamma}T + 4.39\times10^{-3}T^2 \quad (43)$$

In the equations above, $\dot{\gamma}$ is the shear rate, φ is the mass fraction and *T* is the temperature. The correlations factored in the effect of shear rate using the least-squares approach with correlation coefficients $R^2 > 0.995$ in both cases. Earlier, Phuoc and Massoudi [110] noted that the addition of nanoparticles created yield stress within the Fe_2O_3-water/dispersants (polyvinylpyrrolidone, PVP and polyethylene oxide, PEO) nanofluids. They described the dependence of the yield stress on volume concentrations as $\tau_o = \psi e^{n\phi}$. Using the Casson equation (for flocculated suspended particles) described by $\tau^{1/2} = \tau_o^{1/2} + \mu_\infty^{1/2}\dot{\gamma}^{1/2}$ to determine the suspension viscosity at an infinite shear rate for their base fluid plus dispersants, they found that the viscosity values predicted with Casson's equation were two orders of magnitude lower than the viscosity of the base fluid. Moreover, the model does not consider the effect of particle concentration. Therefore, the following correlation was proposed to characterise the combined effects of shear rate and volume fraction on the viscosity of Fe_2O_3-water/(PVP and PEO) nanofluids:

$$\mu_{nf} = \mu_\infty + \left(\frac{\psi e^{n\phi}}{\dot{\gamma}}\right)^{1/2}\left[\left(\frac{\psi e^{n\phi}}{\dot{\gamma}}\right)^{1/2} + 2\mu_\infty^{1/2}\right] \quad (44)$$

The data used for the correlation in Eq. (44) were taken at 25 ^oC, where μ_∞ is the intrinsic viscosity at infinite shear rate, ψ and *n* are empirical constants dependent on the intercept of the plot of $\left(\mu_{nf}\dot{\gamma}\right)^{1/2}$ against $\left(\dot{\gamma}\right)^{1/2}$ for all the volume fractions of nanofluids. A summarised description of the above empirical models and other empirical models [32, 44, 81–83, 85–87, 90–92, 94, 101, 109, 111–114] with regards to the concentration regime, particle size, temperature and remarks is presented in Table 3.

EXPERIMENTAL STUDIES

There are copious experimental studies on nanofluid thermal properties and their behaviours. These studies mainly cut across the determination of nanofluid thermal conductivity [115–117], convective heat transfer [118, 119], performance in heat pipes and microchannels [120–122], its effectiveness in solar heaters and solar-related devices [123–126] and its behaviour in car engine radiators [76, 127]. Few of these works focused on the viscosity of nanofluids and recently there has been some new development in the experimental field, as researchers are now investigating the thermal diffusivity and electrical conductivity of nanofluids and how these properties affect thermal properties [128, 129]. For consistency in this review, the following are the experimental works done on the viscosity of nanofluids:

Methods of Preparation of Nanoparticles and Nanofluids

The preparation of nanofluids can be classified into two groups: (i) preparation of dry nanostructures and subsequent dispersion of the nanostructures in the base fluids, and (ii) an infused method of preparing nanostructures in its intended base fluid medium. The first approach is called the two-step method, in which case, nanostructure preparation is the first step to the development of nanofluids. Nanostructures of sizes ranging from 1nm-100 nm are desired for nanofluids [17, 130] and a wide range of nanostructures exist today, ranging from nanowires, nanorods, nanofibres, nanocylinders, nanograins to nanoparticles [98, 131, 132], which can either be developed from the smallest unit of matter (known as the bottom-up method) or fractured down from bigger lumps to nano-sized particles (known as the top-down method) [133–135]. The most common methods of nanostructures synthesis are broadly classified into physical and chemical methods. Some of the physical methods are pulsed laser ablation [136–138], laser deposition and matrix assisted pulsed laser evaporation (MAPPLE) [130, 139], and ball milling [133–135], while the chemical methods are chemical precipitation [140–142], sonoelectrochemical synthesis [143–148], spray pyrolysis [149, 150], chemical vapour deposition [151–153] and thermal decomposition [154]. Details on other methods under these categories can be found in the past

publications [38, 155, 156]. After the synthesis of the desired nanostructure, the nanostructures are dispersed in any intended base fluid medium using assisted dispersion with magnetic stirrer, high shear homogeniser, high-pressure homogeniser and/or ultrasonication (probes and baths) [157, 158]. The production of nanofluids by this first method is very popular and by far the most economical method which has been transformed to industrial scale of production. However, there is a problem of stability with nanofluid prepared using this method. The second method is called the single-step method because the process of preparing nanostructures (nanoparticles in most cases) is infused into preparation of the nanofluids without any intermediate product, i.e. no dry nanoparticles are produced, rather the nanofluids are produced in the form of a continuous process [159, 160]. Nanofluids from this method are by far more stable, but it is very costly, which is one of the hindrances why it is yet to reach commercialisation.

Worthy of mention is the biological method of synthesis of metallic nanoparticles. Using different biological substances such as algae [161], fungi [162, 163], plant extracts [164–168], bacteria [169–171], yeast [172–175] and marine sponge [176] have been used to synthesise two metallic nanoparticles, which are silver (Ag) and/or gold (Au). Thakkar et al. [177] established in their work the need for eco-friendly metallic nanoparticle synthesis, vis-à-vis energy saving, poisonous gas reduction and decline in the usage of toxic compounds. Therefore, a comprehensive usage of different micro-organisms for the production of non-toxic metallic nanoparticles was highlighted. Similarly, Elumalai et al. [164] and Krishnaraj et al. [165] synthesised silver nanoparticles from different leave extracts and both studied their antibacterial activities. Table 4 gives an overview of the classifications and different methods that have been used in the synthesis of nanostructures.

Nanofluid Stability

The versatility of nanofluids cuts across all phases of science and technology in human developments and this is what makes it one of the most popular and fastest-growing research entities in the world today. This versatility has also faced many challenges, most of which have

been met to a reasonable degree. However, the problem of the stability of nanofluids still persists. Like stability in many other engineering systems, a stable nanofluid is when nanoparticles are continually in their Brownian motions without cohesion and devoid of flocculation, agglomeration and ultimately sedimentation. It may be said that at very low nanoparticle volume concentration, stability does not pose a big threat in the face of the present methods of preparation of nanofluids. However, in the case of increasing volume concentration as desired by many applications, instability becomes very pronounced vis-à-vis flocculation, agglomeration, settling down and ultimately phase separation. Though, when first prepared with any combination of the different dispersion methods available [157] (especially the two-step method), it displays good dispersion, mostly because of the high shear, pressure or energy impacted into the homogenisation process. However, with time, agglomeration formation occurs [178] as shown in Fig. 4. The time difference between t_o when a homogeneous suspension is formed and t_3 when full-phase separation occurs is a function of compositions, i.e. particle volume concentration, nanoparticle type, type and concentration of surfactant, shape of particle, type of system (stationary or dynamic), method of preparation, temperature of the suspension and density difference between the nanoparticles and base fluid. For example, exploring three different dispersion methods, namely ultrasonication, ball milling and high-pressure homogenisation (HPH), Fedele et al. [157] prepared deionized water (DI-water) based nanofluids of CuO, TiO_2 and single-wall carbon nanohorns (SWCNHs) to study their stability. With sedimentation rate as stability marker, and applying static and shake dynamics (i.e. samples were prepared and divided into two, first sets were kept stationary while the second sets were shaken before measurement), they measured using dynamic light scattering to monitor the variation in size of dispersed nanoparticles and SWCHNs over a period of 30 days. From their findings, CuO and TiO_2 dispersed using ball milling sedimented four days after preparation whereas the same nanoparticles dispersed through ultrasonication lasted more than 15 days in suspension. On addition of surfactant to the unstable TiO_2-water nanofluids at varying %weight,

the nanofluid was made stable for more than 30 days without any sign of agglomeration or precipitation.

Zamzamia et al. [158] formulated 90 days stable nanofluids of Al_2O_3 and CuO in ethylene glycol and tested both in double-pipe and plate heat exchangers. Also, employing wet ball milling, Samal et al. [179] produced and dispersed nanoparticles of Al-Cu alloy in DI-water to study its stability at different pH. By measuring the zeta potential of the nanofluid as the pH is varied, their results showed that pH is a major driver of stability of the nanofluid, with or without the addition of surface active agents (surfactant). This is because pH modification has a direct link with the electrostatic condition of the interface between the suspended particles and the fluid medium. In another pH influence investigation, Wang et al. [180] systematically prepared optimised Al_2O_3-water and Cu-water nanofluids by the two-step method using the zeta potential, nanoparticle size and absorbency of the nanofluids as stability indicators. They varied the pH and surfactant concentration (in this case, sodium dodecylbenzene sulfonate (SDS)) to synthesise a stable nanofluid as indicated by the measured values of zeta potential and absorbency. However, at the optimised pH and surfactant concentration that depicted stable nanofluids from the above-measured parameters, the measured size of nanoparticles in suspension was more than the starting materials by a factor of 7.4 for Al_2O_3 and 7.5 for Cu. Although, the sizes were the minimum considering the sizes reported with pH and surfactant variations, the sizes also coincided with the optimised pH and surfactant concentration. Because the measured size was bigger than the size of the starting materials, one of two things could be inferred here, namely that the reported starting materials were not actually the size reported or there was agglomeration within the nanofluids prepared as the time given for sonication might not have been enough (in this case one hour).

In stability characterisation, the key marker of stability from the available systematic experimental investigations [157–159, 179, 180] can be narrowed down to the following: visual inspection for sedimentation, sedimentation rate measurement, turbidity, zeta potential, absorbency of nanofluids,

transmittance and size measurement against time after preparation (for detecting agglomeration and/or reduction in nanoparticle population). Some researchers have also deduced that rheological characteristics, i.e. Newtonian, signify stable nanofluids and non-Newtonian characteristics signify otherwise [181]. All these characterisation procedures have their deficiencies, which are still preventing the report of either qualitative results or a report that represents the actual situation that is encountered in real-life application. For instance, visual observation of sedimentation is relative to the eyes and as such lacks substance in reporting the stability of nanofluids. However, it can be used as a secondary means of characterisation (i.e. to back up a quantitative report on stability). Also, the quantitative approaches available such as turbidity measurement, zeta potential, absorbency and nanoparticle size measurement all have restrictions. Either the volume concentration must be in dilute regime (usually $\leq 1\%$), which is not always the case in real-life applications or the opacity of the nanofluids is disrupting the proper measurement, in which case it must be diluted as well. The idea of dilute concentration of samples in order to measure any of these stability markers may not represent what is obtainable in the industry where a concentration of up to 10% might be required for application in heat exchangers and other engineering problems. Moreover, some nanoparticles are opaque in nature, e.g. Fe_2O_3, Fe_3O_4 Cu and CuO.

Experimental Set-ups

Measuring nanofluid viscosity seemingly looks very simple when the scale and sensitivity of equipment requirement are compared with other aspects of the thermal properties of nanofluids. Nevertheless, it is important to state that a good knowledge of the design of experiment and control of variables to stability is required to be able to measure and report accurate data. At least five types of viscometers with different principles of operations have been used in viscosity measurements, viz. capillary tube viscometer [42, 94], vibro-viscometer [17, 182], rotating viscometer which includes cone-plate, flat plate and concentric geometries [18, 32, 43, 44, 68, 76, 81, 82, 85, 86, 183–187], falling ball/falling piston viscometer [87] and cup-type viscometer.

Chen et al. [68] formulated an ethylene-glycol-based TiO_2 nanofluid from dry nanoparticles using the two-step method and in the absence of dispersant. After sonication of the nanofluid samples for 20 h each, samples were subjected to a rheological test using Bolin CVO rheometer that works based on the principle of controlled shear stress. Al_2O_3-EG/water nanofluids were prepared and sonicated in the presence of oleic acid as the surfactant, for 3 h. The suspension was further agitated magnetically for 1 h to obtain a uniform homogenisation after which a rheological test was performed between the temperatures of 20 ^oC-100 ^oC using the Brookfield programmable viscometer (model: LVDV-II-Pro), which works by controlling the spindle shearing rate [76]. Chandrasekar et al. [32], with a similar set-up, measured the viscosity of Al_2O_3-water without dispersant and sonicated for a period of 6 h. Table 5 shows various pieces of equipment that have been used in the measurement of viscosity of different nanofluids with their measurement principle. In a rather different set-up, Lee et al. [182] used a vibro-viscometer operating on a constant resonance frequency to determine the viscosity of aqueous SiC nanofluids.

Parameters Involved in the Effective Viscosity of Nanofluids

Temperature

The reduction in the viscosity of conventional heat transfer fluids such as water, EG, PG, PAO, engine oil and grease is an established phenomenon. The rate at which this occurs is commensurate with the intrinsic properties of the fluid (intermolecular bond strength) [182]. Nanofluids, which are a better replacement for these conventional fluids, have hardly been in use for two decades and have drawn the attention of many in the industry, research centres and academia. In order to understand and maximise the potential of these superfluids, a number of investigations into their behaviours at different elevated temperatures have been carried out. Heating of fluids generally supplies the molecules of the fluid with higher energy. This increase in energy contributes to increased random motion and weakening of intermolecular forces holding the fluid molecules. This phenomena result in a reduced resistance of the fluid to shearing flow, and by implication, a reduction in viscosity is experienced.

It is important to note that the behaviour of the viscosity of nanofluids to change in temperature does not in any way differ from the behaviour of the conventional fluid as stated in the paragraph above. Kumaresan and Velraj [185] presented the relationship between temperature and the viscosity of MWCNT-water/EG-based nanofluid at 0.15%, 0.30% and 0.45% particle volume fractions. An increase in viscosity of the nanofluid at temperature below 25 ^{o}C was initially observed, however, further increase in the temperature witnessed corresponding reduction in viscosity of their nanofluid samples. In another recent report by Aladag et al. [108], CNT-water-based nanofluid was investigated for its rheological properties at low temperature (2-10 ^{o}C). The characteristic of the measured viscosity with respect to temperature increase was not different from the behaviour of conventional heat transfer fluid as widely reported in literature. However, one may conclude that the addition of surfactant in the experiment carried out by Kumaresan and Velraj [185] might probably be responsible for the initial behaviour of the nanofluid.

With a much different type of nanofluid, Sahoo et al. [86] considered Al_2O_3-EG/water nanofluid for its rheological characteristics. They found that it exhibited non-Newtonian behaviour at a very low temperature. This behaviour specifically fitted into the characteristics of a Bingham plastic and was more pronounced as the concentration of the nanoparticles increased. Nevertheless, as temperature increased across the volume fraction investigated, the viscosity of the nanofluid decreased exponentially. Similar results were obtained by Syam Sundar et al. [188] when they investigated the viscosity of nanofluids synthesised from magnetic Fe_3O_2 and EG-water mixture. The temperature of their investigation started from 0 to 50 ^{o}C at maximum volume fraction of 1.0%. Varying the % weight composition of the EG-water mixture (60:40, 40:60 and 20:80) did not have any impact on the viscosity-temperature trends of the nanofluids. In fact, if the base fluid involved was the highly viscous type such as glycerol, the addition of nanoparticles did not impair the established relationship between the viscosities of nanofluids and temperature as shown in Fig. 5 [189].

Volume fraction

Volumetric concentration is the amount of nanoparticles dispersed in base fluid, usually less than 10% volume of the base fluid. Adequate research efforts have gone into discovering the effects of volume fraction of nanoparticles on thermophysical behaviours of nanofluids. Most investigations reported so far show that an increase in volume fraction of nanoparticles increases the viscosity of nanofluids [190]. For example, Chevalier et al. [94] studied the rheological behaviours of SiO_2-ethanol nanofluids in microchannels and observed a constant Newtonian behaviour of the nanofluid over the range of volume fraction studied (1.1%-7%) and shear rate values of 5×10^3-5×10^4 s^{-1}. Regarding the evolution of viscosity of the nanofluid with the said volume fraction range, there was a direct relationship, i.e. as the volume fraction was increased, the viscosity also increased. Corcione [111] analysed different experimental data from diverse literature for possible parameters that affect the viscosity of nanofluids. His observation centred on the significant increase in the viscosity as the volume fraction increases. Phuoc and Massoudi [110] observed experimentally that for Fe_2O_3-deionised water, the nanofluid volume concentration of Fe_2O_3 is a critical parameter that influences the viscosity of the nanofluid. Across the shear rate range (13.2-264 s^{-1}) tested at room temperature, there was a noticeable viscosity increase for 1%-4% volume fraction concentration. Likewise, viscosity of Al_2O_3-PG at three different volume fractions was experimentally investigated by Prasher et al. [191]. Their experimental data were comparable with data from Das et al. [192] and Wang et al. [193], showing the strong dependence of viscosity enhancement on volume concentration. It was further reported that at volume fraction of less than 4% investigated, the Al_2O_3-PG nanofluid behaviour was Newtonian and viscosity increased with an increase in volume fraction. Some of the most recent works also corroborate this finding [21, 194, 195], except for a more recent experimental work by Suganthi et al. [96] on the viscosity of ZnO-PG nanofluid. Contrary to most publications, the authors discovered that the addition of ZnO nanoparticles to PG up to 2% volume fraction reduced the viscosity below the viscosity of the base fluid (PG). They offered an explanation in line with the bonding characteristics created between the ZnO

nanoparticles and the PG molecules. The hydrogen-bonding network that existed between the PG molecules was weakened by the introduction of ZnO nanoparticles, which translates to viscosity reduction. The effect is similar to the influence of increased temperature on the intermolecular bonding of nanofluids.

Generally, the observed increase in viscosity with volume fraction of nanoparticles could be explained in view of the fact that an increase in volume of particles dispersed in base fluid will result in a pronounced drag effect on individual particles due to Brownian motion. Therefore, the overall drag effect present in the medium will be increased, which, in turn, will lead to an increase in dissipation of energy and the consequence of this is the observed increase in the nanofluid viscosity. Furthermore, it can be explained by exploring the particle surface charge mechanism in relation to the suspension medium. When charged nanoparticles are dispersed into polar base fluid for instance, the attraction of counterion onto the nanoparticle surface is likely to occur and this process creates the formation of electrical double layer (EDL). An increase in nanoparticle concentration will reduce the interparticle distance and by extension the distance between the EDLs. Therefore, the force of interaction between the EDLs known as electroviscous force introduces an additional increase in viscosity [132]. Other forces such as solvation, hydration, hydrophilic and hydrophobic forces become very important and influence the rheology of nanofluids when the interparticle distance is reduced due to an increase in volume fraction [196]. Particle agglomeration has also been argued as one of the causes of an increase in viscosity of nanofluids. According to Chen et al. [197], a well-dispersed nanofluid suspension shows lower viscosity compared with the corresponding agglomerated suspension. An increase of volume concentration beyond the dilute regime heightens the tendency of agglomeration in nanofluid systems, especially when the Van der Waals force of attraction is significant. When agglomeration occurs, it forms a porous particle with the liquid of the suspending medium filling the interstices.

This immobile additional liquid in the interstices causes an increase in the effective volume fraction, which leads to viscosity increase [132].

Shear rate

The control of the flow property of suspensions is very important in many industrial applications, such as in the manufacturing of paint, crude oil drilling, crude and petroleum product transportation, and in food and consumer products. Rheological studies of these products give insights into the type of control that needs to be applied for efficient product transportation and delivery. For instance, in the petroleum industry where hydrate formation in crude oil transportation creates a flow problem or sometimes total blockage of the flow path [198], the knowledge of the behaviour of hydrate slurry to different shear stress/shear rate among other influencing parameters will make the delivery more efficient and less expensive [199].

The rheology of numerous nanofluids containing different nanoparticles including carbon nanotubes has been studied over the past years [81, 84, 200]. Different rheological characteristics have been reported ranging from Newtonian to non-Newtonian shear thinning, shear thickening, thixotropic, etc. [81, 201]. In 2003, Tseng and Lin [83] investigated the rheology and structure of TiO_2-water nanofluid and found that within the volume fraction investigated (5-12%), the nanofluid exhibited non-Newtonian viscoplastic fluid behaviour as presented in Fig. 6 (a). As nanoparticles are added to the Newtonian base fluid up to 5%, an initial yield stress was needed to be exceeded before flow could be achieved. This feature puts the nanofluids in the viscoplastic non-Newtonian regime. When flow occurs, increase in the shearing rate from 0-1000 s^{-1} clearly shows shear thinning structure except at 5% and shear rate $\geq$ 700 s^{-1} (Fig. 6 (b)). During this shearing process, agglomerate structures formed in the nanofluid are broken down until they form an ordered arrangement without agglomeration within the limits of high shearing rates [83]. To buttress this point, similar trends and explanations have been offered in a more recent investigation by Yang et al. [202], who investigated the rheology of diamond and Al_2O_3 nanofluids relative to

the effect of agglomeration. Two Newtonian base fluids were employed, namely silicone oil (Syltherm 800) and DI-water. From their findings, the addition of as low as 0.35 and 0.24% of diamond and Al_2O_3 nanoparticles without stabiliser turn the fluid to non-Newtonian with shear thinning characteristics. Interestingly, in the stabilised Al_2O_3-DI-water nanofluids sample at 1.28% volume fraction, the nanofluid behaved as a Newtonian fluid while the non-stabilised counterpart clearly showed a shear thinning phenomenon without thixotropy. As stated earlier, the Newtonian characteristic of the stabilised sample was due to the ordered structure of the nanoparticles in suspension (i.e. devoid of agglomeration), while in the non-stabilised sample, there was agglomeration due to dominance of the Van der Waals force of attraction and at low shear rate, it showed high resistance to flow. As the shear rate increased, the agglomerates were broken down and the immobile liquids within the interstices of the porous agglomerates were released, which further reduced the viscosity alongside the ordered structure that was created at high shearing rate. In another recent paper, Aladag et al. [108] showed that shearing time also influenced the internal microstructure of nanofluids. Investigation on CNT- and Al_2O_3-water-based nanofluids at three different shearing times and shear rates up to ~ 4000 s^{-1}, showed that stabilised CNT and Al_2O_3 in water responded with shear thinning, thixotropic, and shear thickening, thixotropic, phenomena respectively. During the ramp up shear rate (low-high) there was deagglomeration and/or realignment of agglomerated nanoparticles leading to the shear thinning behaviour. The corresponding shear stress to the ramp down shear rate (high-low) was lower, which signifies the thixotropic characteristics of the nanofluids as depicted in Fig. 7(a). But in the Al_2O_3 samples, the characteristic was shear thickening with thixotropic phenomena as shown in Fig. 7(b). Based on the shearing time experiments, it was clear from Fig. 7(b) that when the shearing time was relaxed, sufficient time was provided for the rebuilding of the particle structure, which gave rise to the increased ramp down shear stress shown for samples sheared for 180 and 240 seconds respectively. Another work that showed shear thickening behaviour is the dispersion of Al_2O_3 in R141b refrigerant up to 0.15% volume fraction [201].

Size of nanoparticles

A size of 1-100 nm particles is desired for nanofluid suspensions [203]. However, particles larger than 100 nm have also been experimented with [82, 204]. Nguyen et al. [205] investigated the effect of particle size (36 and 47 nm) on the viscosity of Al_2O_3-water nanofluids and reported that the viscosity of both particles were similar at volume fraction below 4%. However, at higher volume fraction, the viscosity was clearly higher in 47 nm. He et al. [206] also observed that a bigger agglomerated size of TiO_2 had higher viscosity compared with a smaller agglomerated size. Contradictory reports [94, 207–209] have shown that smaller particle size led to an increase in viscosity. The results from these reports appear to be reasonable given the following explanation.

When nanoparticles are dispersed in fluid medium, two major interactions are possible: particle-fluid interaction and particle-particle interaction. These interactions have been termed first and second electroviscous effects respectively [128]. Another prevalent interaction is the Van der Waals force of attraction between particles. The electroviscous effect (EVE) present in the nanofluid medium determines the agglomeration and hence the degree of Brownian motion effects of the particles. For example, if the particle concentration is fixed, a reduced size of nanoparticles translates into an increased overall surface area of solid-liquid interaction and also solid-solid interaction, i.e. there will be an increase in the EVE present in the nanofluids, which, in turn, gives rise to an increase in viscosity. Similarly, if the overall surface area of solid-liquid interface is reduced, the EVE will be reduced. Thus, a reduction in viscosity had been observed experimentally (Fig. 8) due to the increased size of nanoparticles [94, 132, 207–211]. A bigger particle size giving a higher viscosity could be the result of particle agglomeration, as one of the reports clearly stated [206].

In Eq. (1), the intrinsic viscosity [η] was provided as 2.5 for uncharged hard spherical particles. However, due to the different processes of nanoparticle preparation [136, 156], the most correct opinion is that nanoparticles always carry charges and in the absence or reduced strength of EVE,

there will be pH domination of the viscosity evolution in the nanofluid, which may further the enhancement of cluster formation (i.e. agglomeration of nanoparticles). The shape of agglomerates determines the intrinsic viscosity and it has been shown to be more than 2.5 when the agglomerate is not spherical [212]. Anoop et al. [132] proposed that the intrinsic viscosity is not a shape function, rather an EVE and agglomeration function. Eq. (45) was derived for the electroviscous intrinsic viscosity and Eq. (46) for the agglomeration intrinsic viscosity:

$$[\eta]_{EV} = [\eta](1+p) \tag{45}$$

$$[\eta]_{a} = [\eta] \times f_a \tag{46}$$

where p is the electroviscous coefficient and f_a is the agglomeration factor, taken to be two because the agglomerated nanoparticles doubled the starting size nanoparticles.

Shape of nanoparticles

Virtually all reported works on the thermophysical properties of nanofluids either assumed or claimed their nanoparticles were spherical in shape except for those that worked with carbon nanotubes (CNTs) and a few other works on different nanoparticles [98, 213]. Shape factor, which is a measure of total surface area of particles, is related to the degree of solid-liquid interactions at the interface. Timofeeva et al. [98] note that as the sphericity of particles reduces, there is a corresponding increase in shape factor. Consequently, a larger surface area is presented for active solid-liquid interactions. The same authors presented a correlation to describe the viscosity of alumina-EG/water nanofluid with varying shapes. Although the proposed equation (Eq. 47) is more of a replica of Batchelor's equation (Eq. 48) [55], the authors elucidated that the coefficients A_1 and A_2 were higher than what was obtainable with Batchelor's [55] even for spherical and non-reacting particles, and these coefficients also varied with particle shapes.

$$\mu_{nf} = \mu_o \left(1 + A_1 + A_2^2\right) \tag{47}$$

$$\mu_{nf} = \mu_o \left(1 + [\eta]\phi + 6.5\phi^2\right) \tag{48}$$

The variation in viscosity as presented in [98] is the only data available with regard to different shapes of nanoparticles in the same experimental set-up and conditions. Although some researches on colloidal suspensions of shapes other than spheres had been carried out [213–215], they only considered rod-like shapes. The increase in shape factor of particles has been thought to be one of the causes of increase in nanofluid viscosity. However, the evolution of viscosity as presented by Timofeeva et al. [98] was anomalous and without a distinctive relationship with shape/shape factor of the nanoparticles.

Another factor that could cause a difference in the viscosity data of different nanoparticle shapes could lie in the aerodynamics of these shapes in the suspended medium. A streamlined shape poses less resistance to flow as compared with an irregular shape or sharp-edged shapes that resist flow because it is difficult for such shapes to fall in ordered streamlines and as such they dissipate more energy, which results in increased viscosity of the suspension. In view of the above, it is imperative that more researches be focused in this direction.

pH and electrical conductivity of suspension

pH becomes important in the engineering of nanofluids given the prospect of data available, emphasising the effect of zeta potential on the thermophysical properties of nanofluids. Zeta potential defines the electrokinetic potential of the EDL and this influences the electrostatic behaviour of nanofluids. The effect of pH on nanofluids' zeta potential and thickness of EDL was part of the investigation carried out by Rubio-Hernández et al. [212]. Manipulating the pH values has been shown to bring about viscosity decrease [98]. However, manipulation should be carefully carried out with respect to its effect on zeta potential, because an increase in the viscosity of nanofluid with changes in pH values was also reported [211]. This is probably due to the fact that the effect of pH manipulations on zeta potential values was not monitored and must have affected the stability of the suspension. It has been shown that the Van der Waals force of attraction dominates the interaction between nanoparticles when the pH of nanofluid is at the isoelectric point

(IEP). Because at IEP, the zeta potential is equal to zero and this hastens the agglomeration rate [178].

The particle surface charge Q is directly related to the zeta potential as presented in Eq. (49) and the critical zeta potential ($\zeta_{critical}$), which defines the critical surface charge, is also affected by volume concentration [129]. The effect of volume loading is such that the value of zeta potential is moved from below critical to above critical, i.e. $\zeta < \zeta_{critical} - \zeta > \zeta_{critical}$, consequently, there is a reduction in the electrical conductivity or sometimes a reduction to plateau [129].

$$Q = 4\pi\varepsilon_r\varepsilon_o a\zeta \tag{49}$$

where ε_r is the relative permittivity of the medium, ε_o is the vacuum permittivity of the medium, a is the radius of the particle, ζ is the zeta potential of the nanofluids. At this juncture, the following conclusion can be drawn:

- pH might be insignificantly affected by an increase in volume concentration [98, 212], how-ever, it greatly affects the ζ potential, which equally reduces the electrical conductivity of nanofluids;
- pH modification reduces the viscosity of nanofluids when carefully carried out such that the stability of the suspension is not compromised; and
- synergetic research is needed to be carried out on the zeta potential, pH and electrical conductivity effect on the viscosity of nanofluids.

Base fluid properties

Nanofluid viscosity amplification is a multifactorial issue. Base fluid properties such as density, thermal conductivity, viscosity and pH are definitely part of the factors that affect the overall properties of nanofluids such as stability, thermal conductivity and viscosity. As the name “base fluid” implies, it is the basis on which all enhancements are built. Many conventional heat transfer fluids have been experimented with different nanoparticles, in different mixing ratios and very common in the literature. However, researches claiming that base fluid properties influence the

viscosity enhancement have not presented any exhaustive experimental data probing the extent to which the intrinsic properties of base fluids influence the viscosity enhancement of nanofluids. Nonetheless, Syam Sundar et al. [188] investigated the viscosity of nanofluids synthesised from magnetic Fe_3O_2 and three different EG-water mixtures as the base fluids, namely EG:water – 60:40, 40:60 and 20:80. Enhancement of approximately 300% was recorded for the sample prepared from the 60:40 ratio, which was higher than that of other nanofluids. Wang et al. [193] measured the viscosity of Al_2O_3 dispersed in water and EG. In their experiment, the viscosity of Al_2O_3-water increased by 20-30% at 3% volume fraction and it was dependent on the dispersion method, while for the Al_2O_3-EG sample at 3.5%, the viscosity increase was approximately 40%. Recently, Yu et al. [106] dispersed aluminium nitride into EG and PG as base fluids and studied their thermal conductivity and rheology. The rheological study shows that the enhancement in EG is approximately 15% higher than the enhancement in PG.

These researches buttress the implication of base fluid in nanofluid viscosity. However, as conventional heat transfer fluids are the bases for nanofluid synthesis, the same nanoparticles (i.e. particles from the same metal or oxide of metal, equal volume fraction, equal average size, etc.) have exhibited different behaviours in the same base fluid medium. Therefore, it is expedient to probe into this area more deeply and possibly the unresolved cause of viscosity enhancement of nanofluids will be clarified.

Magnetorheological nanofluids (MRNF) – a smart lubricant

Nanofluids are not restricted to function as a heat transfer working fluid alone as the majority of its widely reported applications implied. For instance, its applicability has been studied in motor vehicle engine radiators [8, 127], heat pipes [121], solar applications [123], boiling and condensation systems [69, 192], circular tube heat exchangers [119], etc. In all cases cited, it has served as heat transfer agent alone. There is a high prospect of nanofluids doubling as lubricant cum heat transfer agent [216]. For example, it can be very useful in rotating shaft lubrication, journal bearings, bearing seals or even at the ball and socket joint in motor vehicles. However, all

the above-mentioned applications come with high thermal energy generation, which will lower the viscosity of any lubricant fluid, including nanofluids. Magnetic nanofluids, also called ferrofluids, magnetic fluids and/or MRNF [217, 218], are a type of nanofluids in which the suspended nanoparticles are ferromagnetic nanoparticles, ferrimagnetic nanoparticles and metallic nanoparticles that are influenced by magnetic fields [219]. These fluids have been proved to be tuneable to produce the desired thermophysical characteristics in the presence of an external magnetic field [181, 220, 221]. Issues about its stability are of great concern owing to the fact that magnetic nanoparticles (α- and γ-Fe_2O_3, Fe_3O_4, $CoFe_2O_4$, Co, Fe-C, $MnFe_2O_4$, $MgFe_2O_3$, Fe_3N, Ni, Fe, Fe-Co or Ni-Fe) are very heavy. Therefore, settling down or sedimentation due to gravitational effect is a common drawback of MRNF nanofluids. Even with relatively viscous basefluids [43], they display non-Newtonian characteristics, which can be attributed to the formation of agglomerates. This is one way to measure the stability of the magnetic nanofluids [181, 219]. To overcome the stability problem, different methods of synthesising magnetic nanoparticles have been explored, some of which are wet-grinding [222], chemical co-precipitation [223–225] and solvothermal [43] methods. Co-precipitation is the most favoured because it is rapid and the size of magnetic nanoparticles can be controlled flexibly and efficiently by parametric variation of inputs into the co-precipitation reaction [219]. In addition, the problem of non-compatibility of surfactant used in the preparation of the particles with the desired carrier fluid is eliminated. Also, particles derived from other methods, such as thermal decomposition of organometallic compounds have been shown to lose their magnetisation due to poor crystallisation and/or oxidation[226]. Correspondingly, consensus on the size of magnetic nanoparticles is that it should be ≤ 10 nm and with this, sedimentation can be overcome because sedimentation velocity is directly proportional to the square of the particle diameter (i.e. $V \alpha d^2$) [181]. However, the problem created by size ≤ 10 nm is the exhibition of magnetic saturation by individual (magnetic or metallic) particles of this size. It means even in the absence of an external magnetic field, interactions between particles will still cause instability in their respective carrier/base fluids with effects like zippering and

agglomeration. Therefore, stability is usually instituted in magnetic nanofluids and nanofluids generally, using sterical surface coating of nanoparticles with the addition of surfactant (surface modifier) or electrostatically charging (pH modification) nanoparticles in order to create a repulsive interaction between particles, thereby ensuring stability [217].

A stable MRNF is of immense significance as a lubrication fluid at extremely high working temperature. Presently, there are commercialised magnetorheological fluids (MRF) (fluids that contain magnetic microparticles) that can operate in an environment with temperature up to 200 ^{o}C [227]. However, these MRF fluids are disadvantaged just like the early colloids; they have an abrasive nature in service and they settle down quickly, hence the urgency and importance of stably and properly engineered MRNFs for lubrication application. At the switching on and off of the magnetic field, external to the site of application of these fluids (MRNFs), a renewed lubrication effect can be created and maintained by manipulating the strength and uniformity of the magnetic field, thereby creating not only an efficient lubrication (in terms of volume and power requirements) even at high temperatures, but also a durable system. Owing to this tuneable characteristic of MRNFs, it has been called smart fluid.

NUMERICAL STUDIES

Algorithm-Based Numerical Studies

Employing the recent high computational power and the knowledge of algorithm, a new window of opportunity has been opened to the nanofluid research community on the prediction models for thermal properties of these highly revered heat transfer fluids. Rudyak and Krasnolutskii [228] recently performed a computer simulation employing a standard molecular dynamics method to model the interaction between nanoparticles and the carrier fluid molecules. Based on the interaction potentials (basically a geometric function) of the particle-molecule, they simulated the viscosity of lithium-argon and aluminium-argon nanofluids.

In early works by Huseyin and Muhammet [229], Hojjat et al. [230] and Papari et al. [231], artificial neural network (ANN) had been applied for the prediction of thermal conductivity of different nanofluids with good agreement with the values obtainable in the literature. Less than a year after, Mehrabi et al. [232], using an FCM-based neuro-fuzzy inference system and genetic algorithm-polynomial neural network alongside experimental data, developed two new models for the prediction of thermal conductivity of Al_2O_3-water nanofluids.

The use of ANN is now gaining momentum in the prediction of the thermal properties of nanofluids including the viscosity of different nanofluids. This is imperative because viscosity is a known determinant parameter in the effective usage and design based on nanofluids. Yousefi et al. [233], Bahiraei et al. [234] and Hajir and Yousefi [235] have now successfully applied the neural network and genetic algorithm to the modelling of nanofluid viscosity for different nanofluids. Mehrabi et al. [236] developed four different models for the prediction of nanofluid viscosities for four different water-based nanofluids (Al_2O_3, CuO, TiO_2 and SiO_2) based on the FCM-based adaptive neuro-fuzzy inference system. The results of the respective models were compared with the experimental data points and some prominent correlations from the literature. The degree of prediction of the FCM-ANFIS models was good. Atashrouz et al. [237], using data from the literature, recently modelled the viscosity of nine nanofluids based on the group method of data handling and polynomial neural network system (hybrid GMDH-PNN). The experimental data used were on Al_2O_3-water, Al_2O_3-EG, Al_2O_3-PG, CuO-water, CuO-EG:water, SiO_2-water, TiO_2-EG, and TiO_2-water. Nine models were presented for individual nanofluids with average absolute relative deviation of 2.14%. Employing the GMDH-PNN algorithm, a model can be regarded as a set of neurons in which different pairs of the neurons in each layer are connected through a polynomial of the second order, which then produces new neurons in the following layer. This representation can be employed in modelling and predicting highly non-linear experimental data as an inputs-outputs system.

It should be mentioned that this is probably the only algorithm-based work on the prediction of the thermal conductivity and viscosity of nanofluids so far, therefore, researchers need to do more work in this regard to further enrich nanofluid research.

Algorithm-Based Selection of the Viscosity of Nanofluids

There is the possibility of creating a viscosity model database from which a selection can be made. To select nanofluid viscosity models which conform to a set of predetermined criteria, necessitates the use of a generic algorithm. Based on the diversity of the models available and used in predicting the viscosity of nanofluids, there is an emphasised need to select an appropriate model. For the selection of a viscosity model that is likely going to be used for prediction, the criteria and selection flow chart in Fig. 9 must be implemented.

The algorithm for the selection of appropriate models consists of defining arrays and sub-arrays, which can be used to represent the attributes of each model. In Fig. 10, R, S up to V are viscosity models with features and attributes given as R1, R2...R6, S1, S2...S6, and V1, V2,…V6 respectively. Additional information is held in the sub-array, represented as r1, s1 and v1 respectively. The system of arrays and sub-arrays defined for each model renders the following features, among others, in a structured form for decision-making: the empirical or theoretical nature of the model, its error margin, a mechanism for its formulation, its specificity (i.e. applicability to a range of nanofluids) and the range of parameters used in defining the models. Priority indices as shown in Fig. 10 represent the definition of selection criteria. The parameters are allocated index numbers and 0 precedes 1 in terms of priority. After the implementation of search and sort algorithm, more than one model may be presented as fitting the criteria set in their order of priority. Models selected are tested for performance as depicted in the flow chart of Fig. 9.

The actual problem lies in selecting models with a broad range of parameters. The decision-based selection algorithm can contain an infinite range of parameters in its search routine, and can be

recursively implemented. This ultimately can be used to build up a database of appropriate models and filter off redundant models.

CONCLUSIONS AND FUTURE DIRECTIONS

Conclusions

In this review, an attempt was made to throw more light on the understanding of nanofluid viscosity models and their evolution from the classical to numerical models using the findings available in the literature. The pioneering work of Einstein was developed to predict the viscosity of non-interacting and hard microsphere suspension in dilute regime. The majority of the subsequent classical works on the viscosity of suspension were carried out to further extend Einstein's work to a concentrated regime [55, 62, 68]. These efforts show the importance of the influence of increase in volume fraction on the viscosity of suspension. However, none of the classical models was developed for the estimation of nanofluid viscosity. Recently, a few new theoretical models have been developed taking into consideration some of the characteristics of nanofluids such as nanoparticle size, hydrodynamic volume fraction, particle density, aggregate diameter and capping layer thickness. The empirical models were applied to characterise the behaviour of nanofluids at different nanoparticle volume fractions, nanoparticles sizes, temperatures and shear rates. It was noted that most empirical models were developed considering a single parameter, mostly volume fraction or temperature. However, nanofluid viscosity is affected by multiple factors such as volume fraction, particle size, particle shape, shearing rate, shearing time, particle agglomeration, base fluid properties and nanolayer. Therefore, the review further looked into the factors that affect nanofluid viscosity.

Generally, experimental investigations have shown that the addition of nanoparticles to conventional heat transfer fluid leads to an increase in viscosity of the fluid. A further increase in particle volume fraction has been shown to lead to non-linear increment in the viscosity (Fig. 2 and 3). The viscosity of nanofluids decreases with an increase in temperature and it is usually described

by an exponential curve (Fig. 5). It is desirable to prepare the nanofluid with particle size ≤ 100 nm, because a bigger size in the microregime hinders practical application due to abrasion, higher rate of settlement, pressure drop in flow line and clogging of equipment. Experiments have shown that nanoparticle size is another very important factor that influences the viscosity of nanofluids. Typically, as the particle size reduces, the viscosity of suspension increases [94, 207–209]. The increase has been ascribed to an increase in particle-particle interactions due to increased Brownian motion and if the system is not sterically or electrostatically stabilised, there may be agglomeration, which increases the viscosity as many studies have shown. Other influencing factors reviewed were nanoparticle shape, shearing rate, pH and electrical conductivity, and base fluid.

The stability of nanofluids is essential for its eventual implementation for practical purposes. Experimental results available have shown that the methods of nanofluid preparation especially from the two-step method go a long way in dictating the stability of nanofluid. Fedele et al. [157] showed that the ultrasonication method of nanoparticles dispersion was more effective than ball milling when they prepared DI-water-based nanofluids of CuO, TiO_2 and SWCNHs. The addition of surfactant (dispersant or surface modifier) or pH modification was also shown to be effective [157, 180]. However, there have been reports that surfactant and pH sometimes lead to an unnecessary increase in viscosity of nanofluids when not properly modified [82, 211]. This review also showed that the present methods of investigating the stability of nanofluids are deficient because they do not represent what is obtainable in the practical situations that nanofluids might be subjected to.

Lastly, the emerging numerical methods available for the prediction of nanofluids viscosity were also presented. Molecular dynamics simulation and the use of artificial intelligence (artificial neural networks) are fast gaining ground due to their ability to model the non-linear nature of viscosity data. The ANN-based models have shown good predictions with reduced % AARD and

can take a wide range of influencing factors into consideration compared with most empirical models that are built around a single parameter such as temperature or volume fraction.

Regarding the composite of nanofluids, which can consist of different fluid bases and different nanoparticles, different accurate correlations for different nanofluids for a specific range of volume fraction, nanoparticle size and temperature (with or without surfactant) need to be developed.

Future direction

The review of Wong and De Leon [238] on the current and future trends of nanofluids dealt extensively with the present potentials obtainable from the use of nanofluids. Others that have reviewed the current areas of applications of nanofluids include Yu and Xie [239] and Wang and Mujumdar [6]. The following are the key areas common to all the above-mentioned reviews:

- application of nanofluids in industrial cooling such as in heat exchangers, including nuclear reactor cooling;
- use of nanofluid as motor vehicle coolants such as in engine oil, transmission fluid, grease and radiator coolant;
- application of nanofluids in electronics cooling;
- nanofluids as fuel enhancer to boost energy recovery and reduce greenhouse and poisonous gas emissions; application in space and defence industry; and
- use of nanofluid for biomedical applications such as nanodrug delivery, antibacterial activities and in targeted cancer therapeutics.

All the above bullet points have been appropriately dealt with in more elaborate manner [238–240]. However, there are still few areas that need attention. Firstly, the enhanced properties of nanofluids can be employed in boosting energy storage and recovery in solar ponds. A solar pond consists of a body of fluid used in the collection and storage of thermal energy. Research has shown the possibility of using saturated saltwater for heat and energy generation [241]. With the invention of nanofluid, it is believed that heat transfer mechanism of a saltwater solar pond vis-à-

vis absorption and storage can be enhanced with the use of nanofluid. Recently, Al-Nimr and Al-Dafaie [242] numerically investigated the use of Ag-water nanofluid and mineral oil in a two-layer nanofluid solar pond. They found that high absorption coefficient is required for better performance and this was observed to be directly related to an increase in volume fraction. Therefore, at high nanoparticle concentration, the nanofluid solar pond was found to be more effective that the conventional saltwater solar pond. In this regard, there is the need for experimental validation and more robust numerical research to further unlock nanofluid potential for use in solar ponds. Secondly, nanofluid stability is an important issue as already highlighted in this review. The effect of pH on stability cannot be underestimated because through pH modification, nanofluid suspension can be electrostatically stabilised [179, 180]. Studies have shown that as the pH of nanofluids moves further away from the IEP, the higher the absolute value of zeta potential, which is the measure of stability. It should be noted that most of these studies were carried out at room temperature. Until very recently, there has been no study on the effect of temperature on the pH of nanofluids [189, 243]. These studies [189, 243] have shown that temperature has a considerable effect on the pH of nanofluids. Therefore, it is expedient to intensify research efforts in this regard with the hope of producing nanofluid at a pH and temperature where zeta potential is in the stable region, such that if the nanofluid is kept at this temperature for a period, its stability can be studied. Lastly, the need to study sonication energy and nanofluid stability with respect to viscosity enhancement is of paramount importance. In many experiments, as shown in this review, researchers just chose an arbitrary number of hours for their ultrasonication. This method is not standard as is the reporting as well. Further experimental investigation should be carried out to study the impact of ultrasonication on the viscosity and stability of nanofluids. Above all, the experimental values on ultrasonication should be reported on energy/volume (energy density) of nanofluids prepared to enhance repeatability of experiment by other researchers.

ACKNOWLEDGEMENTS

The funding obtained from the National Research Foundation of South Africa (NRF), Stellenbosch University/University of Pretoria Solar Hub, CSIR, EEDSM Hub, NAC and IRT SEED is acknowledged and duly appreciated.

NOMENCLATURE

a	particle radius
a_a	effective radius of aggregate
a_i	empirical constants
A	empirical parameter
b_I	characteristics of electrolyte
B	empirical parameter
C_1	correction factor
C	empirical constant
CL	Chen and Law model
CNT	carbon nanotube
d_p	nanoparticle diameter
d_f	base fluid molecular diameter
d_i	diameter of the i^{th} particle size
D_a	aggregate diameter
D_{ai}	i^{th} aggregate diameter
D_E	dielectric constant
D_x	average particle diameter in
DI	deionized
e	charge
E	empirical constant

E_a activation energy

EDL electrical double layer

EVE electroviscous effect

f_a agglomeration factor

h thickness of nanolayer

h_s minimum separation distance between two spheres

HPH high pressure homogenization

k specific conductivity

k_b Stephan-Boltzmann constant

k_H Hugging's coefficient

m system property constant

MRF magnetorheological fluid

MRNF magnetorheological nanofluid

MWCNT multi-wall carbon nanotube

N_i number of particles with i^{th} size diameter

p electroviscous coefficient

$\bar{p}$ average aspect ratio

PSD particle size distribution

P_i packing fraction of each class size i

Q particle surface charge

r capping layer thickness

R adjustable parameter,

R_g universal gas constant

SWCNH single-wall carbon nanohorn

SWCNT single-wall carbon nanotube

t_o initial time after preparation

t_3 final time at phase separation

T suspension temperature

T_o reference temperature

v_j binary packing coefficient

V sedimentation velocity

V_B Brownian velocity

z number of different class of particle size in suspension

Greek Symbols

α empirical constant

β diffusion coefficient

γ empirical constant

$\dot{\gamma}$ shear rate

γ_{ij} binary packing fraction

δ particle centre-centre distance

ε_o permittivity of the vacuum

ε_r relative permittivity of the medium

η intrinsic viscosity

ζ zeta potential

η_r relative viscosity

θ temperature in degree Celsius

λ empirical constant

μ_e electrophoretic mobility

μ_{eff} effective viscosity

μ_i viscosity corresponding to i^{th} class particle size distribution

μ_{nf} nanofluid viscosity

μ_o suspending medium viscosity

μ_s specific viscosity

μ_∞ intrinsic viscosity at infinite shear rate

$\mu_{\infty,T}$ viscosity at infinite temperature

μ' viscosity of fluid droplet

$\pi_1 - \pi_4$ dimensionless parameters

ρ_f base fluid density

ρ_p nanoparticle density

σ empirical constant

τ shear stress

τ_o yield stress

υ crowding factor

Φ packing geometry of inorganic materials

ϕ particle volume fraction

ϕ_a aggregate volume fraction

ϕ_{eff} effective volume fraction

ϕ_h hydrodynamic volume fraction

ϕ_i volume fraction corresponding to i^{th} class particle size distribution

ϕ_m maximum particle volume fraction

ϕ_{ma} packing fraction of aggregates

ϕ_z ultimate packing fraction

φ nanoparticle mass fraction

φ_i mass fraction of the aggregate *i*

ψ empirical constant

ω empirical constant

Subscripts

a aggregate

b Boltzmann

B Brownian

eff effective

EV electroviscous

f fluid

h hydrodynamic

i i^{th} class

j j^{th} class

m maximum

nf nanofluid

o reference

p particle

r relative

s separation

Superscripts

mono monomodal particle distribution

n empirical constant

x particle size distribution average

z number of modal suspensions (mono, bi or multi)

REFERENCES

[1] Maxwell, J.C., *Electricity and Magnetism*, Oxford, Clarendon, 1873.

[2] Masoumi, N., Sohrabi, N., and Behzadmehr, A., A new model for calculating the effective viscosity of nanofluids, *Journal of Physics D: Applied Physics*, vol. 42, no. 5, pp. 0555011–0555016, 2009.

[3] Choi, S.U.S., Enhancing thermal conductivity of fluid with nanoparticles, ASME. pp. 99–109. , New York, 1995.

[4] Lee, S., Choi, U.S., and Li, S., Measuring thermal conductivity of fluids containing oxide nanoparticles, *Journal of Heat Transfer*, vol. 121, pp. 280–289, 1999.

[5] Murshed, S.M.S., Leong, K.C., and Yang, C., Thermophysical and electrokinetci properties of nanofluids - A critical review, *Applied Thermal Engineering*, vol. 28, pp. 2109–2125, 2008.

[6] Xiang-Qi, W., and Arun, S.M., A review on nanofluids - part II: experiments and applications, *Brazilian Journal of Chemical Engineering*, vol. 24, no. 04, pp. 631–648, 2008.

[7] Vajjha, R.S., Das, D.K., and Namburu, P.K., Numerical study of fluid dynamic and heat transfer performance of Al_2O_3 and CuO nanofluids in the flat tubes of a radiator, *International Journal of Heat and Fluid Flow*, vol. 31, no. 4, pp. 613–621, 2010.

[8] Peyghambarzadeh, S.M., Hashemabadi, S.H., Jamnani, M.S., and Hoseini, S.M., Improving the cooling performance of automobile radiator with Al_2O_3/water nanofluid, *Applied Thermal Engineering*, vol. 31, no. 10, pp. 1833–1838, 2011.

[9] Nguyen, C.T., Roy, G., Gauthier, C., and Galanis, N., Heat transfer enhancement using Al_2O_3-water nanofluid for an electronic liquid cooling system, *Applied Thermal Engineering*, vol. 27, pp. 1501–1506, 2007.

[10] Tsai, C.Y., Chien, H.T., Ding, P.P., Chan, B., Luh, T.Y., and Chen, P.H., Effect of structural character of gold nanoparticles in nanofluid on heat pipe thermal perfomance, *Material Letters*, vol. 58, no. 9, pp. 1461–1465, 2004.

[11] Ma, H.B., Wilson, C., Borgmeyer, B., Park, K., and Yu, Q., Effect of nanofluid on the heat transport capability in an oscilating heat pipe, *Applied Physics Letters*, vol. 88, no. 143116, pp. 1–3, 2006.

[12] Nguyen, C.T., Roy, G., Lajoie, P.R., and Maiga, S.E.B., Nanofluids Heat Transfer Performance for Cooling of High Heat Output Microprocessor, Proc. of 3rd IASME/WSEAS Int. Conf. on Heat Transfer, Thermal Engineering and Environment. pp. 160–165. , Corfu, Greece, 2005.

[13] Jain, P., El-Sayed, I., and El-Sayed, M., Au nanoparticles target cancer, *nano today*, vol. 2, no. 1, pp. 18–29, 2007.

[14] Sun, X., Liu, Z., Welsher, K., Robinson, J.T., Goodwin, A., Zaric, S., and Dai, H., Nano-Graphene Oxide for Cellular Imaging and Drug Delivery., *Nano research*, vol. 1, no. 3, pp. 203–212, 2008.

[15] Pankhurst, Q. a, Connolly, J., Jones, S.K., and Dobson, J., Applications of magnetic nanoparticles in biomedicine, *Journal of Physics D: Applied Physics*, vol. 36, no. 13, pp. R167–R181, 2003.

[16] Gupta, A.K., and Gupta, M., Synthesis and surface engineering of iron oxide nanoparticles for biomedical applications., *Biomaterials*, vol. 26, no. 18, pp. 3995–4021, 2005.

[17] Lee, J.-H., Hwang, K.S., Jang, S.P., Lee, B.H., Kim, J.H., Choi, S.U.S.S., and Choi, C.J., Effective viscosities and thermal conductivities of aqueous nanofluids containing low volume concentrations of Al_2O_3 nanoparticles, *International Journal of Heat and Mass Transfer*, vol. 51, no. 11-12, pp. 2651–2656, 2008.

[18] Yu, W., Xie, H., Chen, L., and Li, Y., Investigation of thermal conductivity and viscosity of ethylene glycol based ZnO nanofluid, *Thermochimica Acta*, vol. 491, no. 1-2, pp. 92–96, 2009.

[19] Eastman, J. a. A., Phillpot, S.R.R., Choi, S.U.S.U.S., and Keblinski, P., Thermal Transport in Nanofluids, *Annual Review of Materials Research*, vol. 34, no. 1, pp. 219–246, 2004.

[20] Maïga, S.E., Palm, S.J., Nguyen, C.T., Roy, G., and Galanis, N., Heat transfer enhancement by using nanofluids in forced convection flows, *International Journal fo Heat and Fluid Flow*, vol. 26, pp. 530–546, 2005.

[21] Heyhat, M.M.M., Kowsary, F., Rashidi, A.M.M., Memenpour, M.H., Amrollahi, A., and Momenpour, M.H., Exeprimental investigation of laminar convective heat transfer and pressure drop of water-based Al_2O_3 nanofluids in fuly developed flow regime, *Experimental Thermal and Fluid Science*, vol. 44, pp. 483–489, 2013.

[22] Quaresma, J.N.N., Macêdo, E.N., da Fonseca, H.M., Orlande, H.R.B., Cotta, R.M., Macedo, E.N., and Fonseca, H.M.D., An Analysis of Heat Conduction Models for Nanofluids, *Heat Transfer Engineering*, vol. 31, no. 14, pp. 1125–1136, 2010.

[23] Wang, J.J., Zheng, R.T., Gao, J.W., and Chen, G., Heat conduction mechanisms in nanofluids and suspensions, *Nano Today*, vol. 7, no. 2, pp. 124–136, 2012.

[24] Wen, D., Lin, G., Vafaei, S., and Zhang, K., Review of nanofluids for heat transfer applications, *Particuology*, vol. 7, no. 2, pp. 141–150, 2009.

[25] Philip, J., and Shima, P.D., Thermal properties of nanofluids, *Advances in Colloid and Interface Science*, vol. 183, pp. 30–45, 2012.

[26] Buschmann, M.H., Thermal conductivity and heat transfer of ceramic nanofluids, *International Journal of Thermal Sciences*, vol. 62, no. 0, pp. 19–28, 2012.

[27] Mallick, S.S., Mishra, A., and Kundan, L., An investigation into modelling thermal conductivity for alumina-water nanofluids, *Powder Technology*, vol. 233, pp. 234–244, 2013.

[28] Fan, J., and Wang, L., Heat conduction in nanofluids: Structure-property correlation, *International Journal of Heat and Mass Transfer*, vol. 54, no. 19, pp. 4349–4359, 2011.

[29] Saleh, R., Putra, N., Prakoso, S.P., and Septiadi, W.N., Experimental investigation of thermal conductivity and heat pipe thermal performance of ZnO nanofluids, *International Journal of Thermal Sciences*, vol. 63, no. 0, pp. 125–132, 2013.

[30] Altan, C.L., Elkatmis, A., Yuksel, M., Aslan, N., and Bucak, S., Enhancement of thermal conductivity upon application of magnetic field to Fe_3O_4 nanofluids, *Journal of Applied Physics*, vol. 110, no. 093917, pp. 1–8, 2011.

[31] Gupta, S.S., Siva, M. V, Krishnan, S., Sreeprasad, T.S., Singh, P.K., Pradeep, T., and Das, S.K., Thermal conductivity enhancement of nanofluids containing graphene nanosheets, *Journal of Heat Transfer*, vol. 110, no. 084302, pp. 1–7, 2011.

[32] Chandrasekar, M., Suresh, S., and Bose, A.C., Experimental investigations and theoretical determination of thermal conductivity and viscosity of Al_2O_3/water nanofluid, *Experimental Thermal and Fluid Science*, vol. 34, no. 2, pp. 210–216, 2010.

[33] Hosseini, S., Moghadassi, A., and Henneke, D.E., A new dimensionless group model for determining the viscosity of nanofluids, *J. Therm Anal calorim*, vol. 100, pp. 873–877, 2010.

[34] Namburu, P.K., Kulkarni, D.P., Misra, D., and Das, D.K., Viscosity of copper oxide nanoparticles dispersed in ethylene glycol and water mixture, *Experimental Thermal and Fluid Science*, vol. 32, pp. 397–402, 2007.

[35] Rashin, M.N., and Hemalatha, J., Viscosity studies on novel copper oxide – coconut oil nanofluid, *Experimental Thermal and Fluid Science*, vol. 48, pp. 67–72, 2013.

[36] Mahbubul, I.M., Saidur, R., and Amalina, M.A., Latest developments on the viscosity of nanofluids, *International Journal of Heat and Mass Transfer*, vol. 55, no. 4, pp. 874–885, 2012.

[37] Sundar, L.S., Sharma, K.V., Naik, M.T., and Singh, M.K., Empirical and theoretical correlations on viscosity of nanofluids: A review, *Renewable and Sustainable Energy Reviews*, vol. 25, pp. 670–686, 2013.

[38] Das, S.K., Choi, S.U.S., and Patel, H.E., Heat transfer in nanofluids - A review, *Heat Transfer Engineering*, vol. 27, no. 10, pp. 3–19, 2006.

[39] Okhio, C., Hodges, D., and Black, J., Review of Literature on Nanofluid Flow and Heat Transfer Properties, *Cyber Journals: Multidisciplinary Journals in Science and Technology, JOurnal of Selected Areas in Nanotechnology (JSAN)*, pp. 1–8, 2010.

[40] Wang, X.-Q., and Mujumdar, A.S., Heat transfer characteristics of nanofluids: a review, *International Journal of Thermal Sciences*, vol. 46, no. 1, pp. 1–19, 2007.

[41] Wang, X., and Mujumdar, A., A review on nanofluids-part I: theoretical and numerical investigations, *Brazilian Journal of Chemical Engineering*, vol. 25, no. 04, pp. 613–630, 2008.

[42] Moosavi, M., Goharshadi, E.K., and Youssefi, A., Fabrication, characterization and measurement of some physicochemical properties of ZnO nanofluids, *International journal of Heat and Fluid Flow*, vol. 31, no. 4, pp. 599–605, 2010.

[43] Abareshi, M., Sajjadi, S.H., Zebarjad, S.M., and Goharshadi, E.K., Fabrication, characterization, and measurement of viscosity of α-Fe_2O_3-glycerol nanofluids, *Journal of Molecular Liquids*, vol. 163, no. 1, pp. 27–32, 2011.

[44] Kole, M., and Dey, T.K., Effect of aggregation on the viscosity of copper oxide-gear oil nanofluids, *International Journal of Thermal Sciences*, vol. 50, no. 9, pp. 1741–1747, 2011.

[45] Avsec, J., and Oblak, M., The calculation of thermal conductivity, viscosity and thermodynamic properties for nanofluids on the basis of statistical nanomechanics, *International Journal of Heat and Mass Transfer*, vol. 50, no. 21-22, pp. 4331–4341, 2007.

[46] Meyer, J.P., Nwosu, P., Sharifpur, M., and Ntumba, T., Parametric analysis of effective viscosity models for nanofluids, *Proceedings of the ASME 2012 International Mechanical Engineering Congress & Exposition*. pp. 1–9. , Houston, TX, 2012.

[47] Einstein, A., A New Determination of Molecular Dimensions, *Annalen der Physik*, vol. 4, no. 19, pp. 37–62, 1906.

[48] Smoluchowski, M. V, Theoretishche Bemerkungen uber die Viskositat der Kolloide, *Kolloidzschr*, vol. 80, pp. 190–195, 1916.

[49] Jeffery, G.B., The Motion of Ellipsoidal Particles Immersed in a Viscous Fluid, *Proceedings of the Royal Society A: Mathematical, Physical and Engineering Sciences*, vol. 102, no. 715, pp. 161–179, 1922.

[50] Taylor, G.I., The viscosity of a fluid containign small drops of another fluid, *Proc. Roy. Soc.*, vol. 138, no. 834, pp. 41–48, 1932.

[51] Brinkman, H.C., The viscosity of concentrated suspensions and solutions, *Journal of Chemical Physics*, vol. 20, no. 4, pp. 571, 1952.

[52] Vand, V., Viscosity of solutions and suspensions. I. Theory, *The Journal of Physical Chemistry*, pp. 277–299, 1948.

[53] Mooney, M., The viscosity of a concentrated suspension of spherical particles, *Journal of Colloid Science*, no. 113, pp. 3–4, 1951.

[54] Roscoe, R., The viscosity of suspensions of rigid spheres, *Journal of Applied Physics*, vol. 267, pp. 3–6, 1952.

[55] Batchelor, G., The effect of Brownian motion on the bulk stress in the suspension of sphrerical particles, *Journal of Fluid Mechanics*, vol. 83, no. 01, pp. 97–117, 1977.

[56] Krieger, I., and Dougherty, T., A mechanicsm for non-Newtonian flow in suspensions of rigid spheres, *Trans. Soc. Rheology*, vol. 3, pp. 137–152, 1959.

[57] Lundgren, T.S., Slow flow through stationary random beds and suspensions of spheres, *Journal of Fluid Mechanics*, vol. 51, no. 02, pp. 273–299, 1972.

[58] Graham, A.L., On the viscosity of suspensions of solid spheres, *Applied Scientific Research*, vol. 37, no. june, pp. 275–286, 1981.

[59] Saitô, N., Concentration dependence of the viscosity of high polymer solution, *J. Phys. Soc. Jpn*, vol. 5, pp. 4–8, 1950.

[60] Hatschek, E., The general theory of viscosity of two phase systems, *Trans. Faraday Soc.*, vol. 9, no. 2, pp. 80–92, 1913.

[61] Thomas, C.U., and Muthukumar, M., Three-body hydrodynamic effects on viscosity of suspensions of spheres, *The Journal of Chemical Physics*, vol. 94, no. 7, pp. 5180, 1991.

[62] Frankel, N., and Acrivos, A., On the viscosity of a concentrated suspension of solid spheres, *Chemical Engineering Science*, vol. 22, pp. 847–853, 1967.

[63] Booth, F., The electroviscous effect for suspensions of solid spherical particles, *Proceedings of the Royal Society A: Mathematical, Physical and Engineering Sciences*, vol. 203, no. 1075, pp. 533–551, 1950.

[64] Bull, H., The electroviscous effect in egg albumin solutions, *Trans. Faraday Soc.*, no. 80, pp. 80–84, 1940.

[65] Ward, S., and Whitmore, R., Studies of the viscosity and sedimentation of suspensions Part 1.-The viscosity of suspension of spherical particles, *British Journal of Applied Physics*, vol. 286, pp. 1–6, 1950.

[66] Williams, P.S., Flow of concentrated suspensions, *Journal of Applied Chemistry*, vol. 3, no. 3, pp. 120–128, 1953.

[67] Maron, S., and Fok, S., Effect of concentration on flow behavior of glass sphere suspensions, *Journal of Colloid Science*, pp. 540–542, 1953.

[68] Chen, H., Ding, Y., and Tan, C., Rheological behaviour of nanofluids, *New Journal of Physics*, vol. 9, no. 10, pp. 367–391, 2007.

[69] Kole, M., and Dey, T.K., Thermophysical and pool boiling characteristics of ZnO-ethylene glycol nanofluids, *International Journal of Thermal Sciences*, vol. 62, pp. 61–70, 2012.

[70] Farris, R., Prediction of the viscosity of multimodal suspension from unimodal viscosity data, *Trans. Soc. Rheol*, vol. 12, pp. 281–301, 1968.

[71] Chong, J., Christiansen, E., and Baer, A., Rheology of concentrated suspensions, *Journal of applied polymer science*, vol. 15, no. 1971, pp. 2007–2021, 1971.

[72] Storms, R.F., Ramarao, B.V., and Weiland, R.H., Low shear rate viscosity of bimodally dispersed suspensions, *Powder Technology*, vol. 63, no. 3, pp. 247–259, 1990.

[73] Dames, B., Morrison, B.R., and Willenbacher, N., An empirical model predicting the viscosity of highly concentrated, bimodal dispersions with colloidal interactions, *Rheologica Acta*, vol. 40, no. 5, pp. 434–440, 2001.

[74] Muralidharan, G., and Runkana, V., Rheological Modeling of Spherical Polymeric Gels and Dispersions Incorporating the Influence of Particle Size Distribution and Surface Forces, *Industrial & Engineering Chemistry Research*, vol. 48, no. 19, pp. 8805–8811, 2009.

[75] Servais, C., Jones, R., and Roberts, I., The influence of particle size distribution on the processing of food, *Journal of Food Engineering*, vol. 51, pp. 201–208, 2002.

[76] Kole, M., and Dey, T.K., Viscosity of alumina nanoparticles dispersed in car engine coolant, *Experimental Thermal and Fluid Science*, vol. 34, no. 6, pp. 677–683, 2010.

[77] Prasher, R., Bhattacharya, P., and Phelan, P.E., Brownian-Motion-Based Convective-Conductive Model for the Effective Thermal Conductivity of Nanofluids, *Journal of Heat Transfer*, vol. 128, no. 6, pp. 588–595, 2006.

[78] Graf, W.H., *Hydraulics of Sediment Transport*, McGraw-Hill, New York, 1971.

[79] Batchelor, G.K., and Green, J.T., The hydrodynamic interaction of two small freely-moving spheres in a linear flow field, *Journal of Fluid Mechanics*, vol. 56, no. 3, pp. 401–427, 1972.

[80] Cheng, N., and Law, A., Exponential formula for computing effective viscosity, *Powder technology*, vol. 129, pp. 156–160, 2003.

[81] Chen, H., Ding, Y., He, Y., and Tan, C., Rheological behaviour of ethylene glycol based titania nanofluids, *Chemical Physics Letters*, vol. 444, pp. 333–337, 2007.

[82] Tseng, W.J., and Chen, C., Effect of polymeric dispersant on rheological behavior of nickel-terpineol suspensions, *Materials Science and Engineering: A*, vol. 347, no. 1, pp. 145–153, 2003.

[83] Tseng, W.J., and Lin, K., Rheology and colloidal structure of aqueous TiO_2 nanoparticle suspensions, *Materials Science and Engineering: A*, vol. 355, pp. 186–192, 2003.

[84] Chen, H., Ding, Y., Lapkin, A., and Fan, X., Rheological behaviour of ethylene glycol-titanate nanotube nanofluids, *Journal of Nanoparticle Research*, vol. 11, pp. 1513–1520, 2009.

[85] Horri, B.A., Ranganathan, P., Selomulya, C., and Wang, H., A new empirical viscosity model for ceramic suspensions, *Chemical Engineering Science*, vol. 66, no. 12, pp. 2798–2806, 2011.

[86] Sahoo, B.C., Vajjha, R.S., Ganguli, R., Chukwu, G.A., and Das, D.K., Determination of Rheological Behaviour of Aluminium Oxide Nanofluid and Development of New Viscosity Correlations, *Petroleum Science and Technology*, vol. 27, pp. 1757–1770, 2009.

[87] Nguyen, C.T., Desgranges, F., Galanis, N., Roy, G., Maré, T., Boucher, S., Angue Mintsa, H., Maré, T., and Mintsa, H.A., Viscosity data for Al_2O_3 - water nanofluid - hysteresis: is heat transfer enhancement using nanofluids reliable?, *International Journal of Thermal Sciences*, vol. 47, no. 2, pp. 103–111, 2008.

[88] Hernández Battez, A., Viesca, J.L., González, R., García, A., Reddyhoff, T., and Higuera-Garrido, a., Effect of Shear Rate, Temperature, and Particle Concentration on the Rheological Properties of ZnO and ZrO_2 Nanofluids, *Tribology Transactions*, vol. 57, no. 3, pp. 489–495, 2014.

[89] Vakili-Nezhaad, G., and Dorany, A., Effect of Single-Walled Carbon Nanotube on the Viscosity of Lubricants, *Energy Procedia*, vol. 14, no. 1998, pp. 512–517, 2012.

[90] Garg, J., Poudel, B., Chiesa, M., Gordon, J.B., Ma, J.J., Wang, J.B., Ren, Z.F., Kang, Y.T., Ohtani, H., Nanda, J., McKinley, G.H., and Chen, G., Enhanced thermal conductivity and

viscosity of copper nanoparticles in ethylene glycol nanofluid, *Journal of Applied Physics*, vol. 103, no. 7, pp. 074301, 2008.

[91] Godson, L., Raja, B., Lal, D.M., and Wongwises, S., Experimental Investigation on the Thermal Conductivity and Viscosity of Silver-Deionized Water Nanofluid, *Experimental Heat Transfer*, vol. 23, no. 4, pp. 317–332, 2010.

[92] Duangthongsuk, W., and Wongwises, S., Measurement of temperature-dependent thermal conductivity and viscosity of TiO_2-water nanofluids, *Experimental Thermal and Fluid Science*, vol. 33, no. 4, pp. 706–714, 2009.

[93] Colla, L., Fedele, L., Scattolini, M., and Bobbo, S., Water-Based Fe2O3 Nanofluid Characterization: Thermal Conductivity and Viscosity Measurements and Correlation, *Advances in Mechanical Engineering*, vol. 2012, pp. 1–8, 2012.

[94] Chevalier, J., Tillement, O., and Ayela, F., Rheological properties of nanofluids flowing through microchannels, *Applied Physics Letters*, vol. 91, no. 233103, pp. 1–3, 2007.

[95] Suganthi, K.S., and Rajan, K.S., Temperature induced changes in ZnO–water nanofluid: Zeta potential, size distribution and viscosity profiles, *International Journal of Heat and Mass Transfer*, vol. 55, no. 25-26, pp. 7969–7980, 2012.

[96] Suganthi, K., Anusha, N., and Rajan, K., Low viscous ZnO–propylene glycol nanofluid: a potential coolant candidate, *Journal of nanoparticle research*, vol. 15, no. 1986, pp. 1986–1–6, 2013.

[97] Singh, D., Timofeeva, E., Yu, W., Routbort, J., France, D., Smith, D., and Lopez-Cepero, J.M., An investigation of silicon carbide-water nanofluid for heat transfer applications, *Journal of Applied Physics*, vol. 105, no. 6, pp. 064306, 2009.

[98] Timofeeva, E. V., Routbort, J.L., and Singh, D., Particle shape effects on thermophysical properties of alumina nanofluids, *Journal of Applied Physics*, vol. 106, no. 1, pp. 014304–1 – 10, 2009.

[99] Takeuchi, A., Kato, H., and Inoue, A., Vogel--Fulcher--Tammann plot for viscosity scaled with temperature interval between actual and ideal glass transitions for metallic glasses in liquid and supercooled liquid states, *Intermetallics*, vol. 18, pp. 406–411, 2010.

[100] Żyła, G., Witek, A., and Cholewa, M., Viscosity of diethylene glycol-based Y_2O_3 nanofluids, *Journal of Experimental Nanoscience*, pp. 1–8, 2013.

[101] Kulkarni, D., Das, D., and Chukwu, G.A., Temperature dependent rheological property of copper oxide nanoparticles suspension (nanofluid), *J. Nanosci. Nanotechnol.*, vol. 6, no. 4, pp. 679–690, 2009.

[102] Yiamsawas, T., Dalkilic, A.S., Mahian, O., and Wongwises, S., Measurement and Correlation of the Viscosity of Water-Based Al_2O_3 and TiO_2 Nanofluids in High Temperatures and Comparisons with Literature Reports, *Journal of Dispersion Science and Technology*, vol. 34, no. 12, pp. 1697–1703, 2013.

[103] Hemmat Esfe, M., and Saedodin, S., An experimental investigation and new correlation of viscosity of ZnO–EG nanofluid at various temperatures and different solid volume fractions, *Experimental Thermal and Fluid Science*, vol. 55, pp. 1–5, 2014.

[104] Azmi, W.H., Sharma, K. V, Mamat, R., Alias, a B.S., and Misnon, I.I., Correlations for thermal conductivity and viscosity of water based nanofluids, *IOP Conference Series: Materials Science and Engineering*, vol. 36, pp. 012029, 2012.

[105] Khanafer, K., and Vafai, K., A critical synthesis of thermophysical characteristics of nanofluids, *International Journal of Heat and Mass Transfer*, vol. 54, no. 19-20, pp. 4410–4428, 2011.

[106] Yu, W., Xie, H., Li, Y., and Chen, L., Experimental investigation on thermal conductivity and viscosity of aluminum nitride nanofluid, *Particuology*, vol. 9, no. 2, pp. 187–191, 2011.

[107] Halelfadl, S., Estellé, P., Aladag, B., Doner, N., and Maré, T., Viscosity of carbon nanotubes water-based nanofluids: Influence of concentration and temperature, *International Journal of Thermal Sciences*, vol. 71, pp. 111–117, 2013.

[108] Aladag, B., Halelfadl, S., Doner, N., Maré, T., Duret, S., Estellé, P., and Haleifadl, S., Experimental investigations of the viscosity of nanofluids at low temperatures, *Applied energy*, vol. 97, pp. 876–880, 2012.

[109] Syam Sundar, L., Singh, M.K., and Sousa, A.C.M., Investigation of thermal conductivity and viscosity of Fe3O4 nanofluid for heat transfer applications, *International Communications in Heat and Mass Transfer*, vol. 44, pp. 7–14, 2013.

[110] Phuoc, T.S.X., and Massoudi, M., Experimental observations of the effects of shear rates and particle concentration on the viscosity of Fe_2O_3-deionized water nanofluids, *Internationl Journal of Thermal Sciences*, vol. 48, no. 7, pp. 1294–1301, 2009.

[111] Corcione, M., Empirical correlating equations for predicting the effective thtermal conductivity and dynamic viscosity of nanofluids, *Energy Conversion and Management*, vol. 52, no. 1, pp. 789–793, 2011.

[112] Sekhar, Y.R., and Sharma, K. V., Study of viscosity and specific heat capacity characteristics of water-based Al_2O_3 nanofluids at low particle concentrations, *Journal of Experimental Nanoscience*, no. june 2014, pp. 1–17, 2013.

[113] Kitano, T., Kataoka, T., and Shirota, T., An empirical equation of the relative viscosity of polymer melts filled with various inorganic fillers, *Rheol. Acta*, vol. 20, pp. 207–209, 1981.

[114] Bobbo, S., Fedele, L., Benetti, A., Colla, L., Fabrizio, M., Pagura, C., and Barison, S., Viscosity of water based SWCNH and TiO2 nanofluids, *Experimental Thermal and Fluid Science*, vol. 36, pp. 65–71, 2012.

[115] Paul, G., Chopkar, M., Manna, I., and Das, P.K., Techniques for measuring the thermal conductivity of nanofluids: A review, *Renewable and Sustainable Energy Reviews*, vol. 14, no. 7, pp. 1913–1924, 2010.

[116] Sundar, L.S., Farooky, M.H., Sarada, S.N., and Singh, M.K., Experimental thermal conductivity of ethylene glycol and water mixture based low volume concentration of Al_2O_3

and CuO nanofluids, *International Communications in Heat and Mass Transfer*, vol. 41, no. 0, pp. 41–46, 2013.

[117] Vajjha, R.S., and Das, D.K., Experimental determination of thermal conductivity of three nanofluids and development of new correlations, *International Journal of Heat and Mass Transfer*, vol. 52, pp. 4675–4682, 2009.

[118] Mansour, R.B., Galanis, N., and Nguyen, C.T., Experimental study of mixed convection with water–Al_2O_3 nanofluid in inclined tube with uniform wall heat flux, *International Journal of Thermal Sciences*, vol. 50, no. 3, pp. 403–410, 2011.

[119] Fotukian, S.M., and Esfahany, M.N., Experimental study of turbulent convective heat transfer and pressure drop of dilute CuO/water nanofluid inside a circular tube, *International Communications in Heat and Mass Transfer*, vol. 37, no. 2, pp. 214–219, 2010.

[120] Liu, Z.-H., and Li, Y.-Y., A new frontier of nanofluid research – Application of nanofluids in heat pipes, *International Journal of Heat and Mass Transfer*, vol. 55, no. 23-24, pp. 6786–6797, 2012.

[121] Wang, P.-Y., Chen, X.-J., Liu, Z.-H., and Liu, Y.-P., Application of nanofluid in an inclined mesh wicked heat pipes, *Thermochimica Acta*, vol. 539, pp. 100–108, 2012.

[122] Hajian, R., Layeghi, M., and Sani, K.A., Experimental study of nanofluid effects on the thermal performance with response time of heat pipe, *Energy Conversion and Management*, vol. 56, no. 0, pp. 63–68, 2012.

[123] Saidur, R., Meng, T.C., Said, Z., Hasanuzzaman, M., and Kamyar, A., Evaluation of the effect of nanofluid-based absorbers on direct solar collector, *International Journal of Heat and Mass Transfer*, vol. 55, pp. 5899–5907, 2012.

[124] Yousefi, T., Shojaeizadeh, E., Veysi, F., and Zinadini, S., An experimental investigation on the effect of pH variation of MWCNT-H_2O nanofluid on the efficiency of a flat-plate solar collector, *Solar Energy*, vol. 86, no. 2, pp. 771–779, 2012.

[125] Yousefi, T., Veisy, F., Shojaeizadeh, E., Zinadini, S., and Veysi, F., An experimental investigation on the effect of MWCNT-H_2O nanofluid on the efficiency of flat-plate solar collectors, *Experimental Thermal and Fluid Science*, vol. 39, no. 0, pp. 207–212, 2012.

[126] Yousefi, T., Veysi, F., Shojaeizadeh, E., and Zinadini, S., An experimental investigation on the effect of Al_2O_3-H_2O nanofluid on the efficiency of flat-plate solar collectors, *Renewable Energy*, vol. 39, no. 1, pp. 293–298, 2012.

[127] Nieh, H.-M., Teng, T.-P., and Yu, C.-C., Enhanced heat dissipation of a radiator using oxide nano-coolant, *International Journal of Thermal Sciences*, vol. 77, pp. 252–261, 2014.

[128] Murshed, S.M.S., Leong, K.C., and Yang, C., Determination of the effective thermal diffusivity of nanofluids by the double hot-wire technique, *Journal of Physics D: Applied Physics*, vol. 39, no. 24, pp. 5316–5322, 2006.

[129] White, S.B., Shih, A.J., and Pipe, K.P., Investigation of the electrical conductivity of propylene glycol-based ZnO nanofluids, *Nanoscale Research Letters*, vol. 6, pp. 346–350, 2011.

[130] Rella, R., Spadavecchia, J., Menera, M.G., Capone, S., and Taurino, A., Acetone and ethanol solid-state gas sensor based on TiO_2 nanoparticles thin film deposited by matrix assisted pulsed laser evaporation, *Sensors and Actuators B*, vol. 127, pp. 426–431, 2007.

[131] Madaria, A.R., Kumar, A., Ishikawa, F.N., and Zhou, C., Uniform, highly conductive, and patterned transparent films of a percolating silver nanowire network on rigid and flexible substrates using a dry transfer technique, *Nano Research*, vol. 3, no. 8, pp. 564–573, 2010.

[132] Anoop, K.B., Kabelac, S., Sundararajan, T., and Das, S.K., Rheological and flow characteristics of nanofluids: Influence of electroviscous effects and particle agglomeration, *Journal of Applied Physics*, vol. 106, no. 3, pp. 034909 1–7, 2009.

[133] Janot, R., and Guérard, D., One-step synthesis of maghemite nanometric powers by ball milling, *Journal of Alloys and Compounds*, vol. 333, pp. 302–307, 2002.

[134] Chin, P.P., Ding, J., Yi, J.B., and Liu, B.H., Synthesis of FeS2 and FeS nanoparticles by high-energy mechanical milling and mechanochemical processing, *Journal of Alloys and Compound*, vol. 390, pp. 255–260, 2005.

[135] Lam, C., Zhang, Y.F., Tang, Y.H., Lee, C.S., Bello, I., and Lee, S.T., Large-scale synthesis of ultrafine Si nanoparticles by ball milling, *Journal of Crystal Growth*, vol. 220, pp. 466–470, 2000.

[136] Franzel, L., Bertino, M.F., Huba, Z.J., and Carpenter, E.E., Synthesis of magnetic nanoparticles by paulsed laser ablation, *Applied Surface Science*, vol. 261, pp. 332–336, 2012.

[137] Cristoforetti, G., Pitzalis, E., Spiniello, R., Ishak, R., Giammanco, F., Muniz-Miranda, M., and Caprali, S., Physic-chemical properties of Pd nanoparticles produced by Pulsed Laser Ablation in different organic solvents, *Applied Surface Science*, vol. 258, pp. 3289–3297, 2012.

[138] Mutisya, S., Franzel, L., Barnstein, B.O., Faber, T.W., Ryann, J.J., and Bertino, M.F., Comparison of in situ and ex situ bioconjugate of Au nanoparticles generated by laser ablation, *Applied Surface Science*, vol. 264, pp. 27–30, 2013.

[139] Manera, M.G., Taurino, A., Catalano, M., Rella, R., Caricato, A.P., and Buonsanti, R., Enhancement of the optically activated NO_2 gas sensing response of brookite Ti_2 nanorods/nanoparticles thin films deposited by matrix-assisted pulsed-laser evaporation, *Sensors and Actuator B: Chemical*, vol. 161, pp. 869–879, 2012.

[140] Singh, V., and Chauhan, P., Structural and optical characterization of CdS nanoparticles prepared by chemical precipitation, *Journal of Physics and Chemistry of Solids*, vol. 70, pp. 1074–1079, 2009.

[141] Chen, J.-F., Wang, Y.-H., Guo, F., Wang, X.-M., and Zheng, C., Synthesis of Nanoparticles with Novel Technology: High-Gravity Reactive Precipitation, *Industrial & Engineering Chemistry Research*, vol. 39, no. 4, pp. 948–954, 2000.

[142] Hsu, W.-C., Chen, S.., Kuo, P.., Lie, C.., and Tsai, W.., Preparation of NiCuZn ferrite nanoparticles from chemical co-precipitation method and the magnetic properties after sintering, *Materials Science and Engineering: B*, vol. 111, no. 2-3, pp. 142–149, 2004.

[143] Zhu, J., Liu, S., Palchik, O., Koltypin, Y., and Gedanken, A., Shape-controlled synthesis of silver nanoparticles by pulse sonoelectrochemical methods, *Langmuir*, no. 23, pp. 6396–6399, 2000.

[144] Mastai, Y., Polsky, R., Koltypin, Y., Gedanken, A., and Hodes, G., Pulsed sonoelectrochemical synthesis of cadmium selenide nanoparticles, *J. Am. Chem. Soc.*, vol. 121, pp. 10047–10052, 1999.

[145] Zhu, J., Aruna, S.T., Koltypin, Y., and Gedanken, A., A Novel Method for the preparation of Lead Selenide: Pulse Sonoelectrochemical Synthesis of Lead Selenide Nanoparticles, *Chem. Mater.*, vol. 12, pp. 143–147, 2000.

[146] Zin, V., Pollet, B.G., and Dabalà, M., Sonoelectrochemical (20kHz) production of platinum nanoparticles from aqueous solutions, *Electrochimica Acta*, vol. 54, no. 28, pp. 7201–7206, 2009.

[147] Lei, H., Tang, Y.-J., Wei, J.-J., Li, J., Li, X.-B., and Shi, H.-L., Synthesis of tungsten nanoparticles by sonoelectrochemistry., *Ultrasonics sonochemistry*, vol. 14, no. 1, pp. 81–3, 2007.

[148] Sáez, V., and Mason, T.J., Sonoelectrochemical Synthesis of Nanoparticles, *molecules*, vol. 14, pp. 4284–4299, 2009.

[149] Mueller, R., Mädler, L., and Pratsinis, S.E., Nanoparticle synthesis at high production rates by flame pyrolysis, *Chemical Engineering Science*, vol. 58, pp. 1969–1976, 2003.

[150] Sahm, T., Mädler, L., Gurlo, A., Barsan, N., Pratsinis, S.E., and Weimar, U., Flame spray synthesis of tin dioxide nanoparticles for gas sensing, *Sensors and Actuators B*, vol. 98, pp. 148–153, 2004.

[151] Kong, J., Cassell, A., and Dai, H., Chemical vapor deposition of methane for single-walled carbon nanotubes, *Chemical Physics Letters*, no. august, pp. 567–574, 1998.

[152] Colomer, J.-F., Stephan, C., Lefrant, S., Tendeloo, G. V, Willems, I., Kónya, Z., Fonseca, A., Laurent, C., and Nagy, J.B., Large-scale synthesis of single-wall carbon nanotubes by catalytic chemical vapor deposition (CCVD) method, *Chemical Physics Letters*, vol. 317, pp. 83–89, 2000.

[153] Nakaso, K., Han, B., Ahn, K.H., Choi, M., and Okuyama, K., Synthesis of non-agglomerated nanoparticles by an electrospray assisted chemical vapour depostion (ES-CVD) method, *Aerosol Science*, vol. 34, pp. 869–881, 2003.

[154] Sahoo, P.K., Kamal, S.S.K., Premkumar, M., Kumar, T.J., Sreedhar, B., Singh, A.K., Srivastava, S.K., and Sekhar, K.C., Synthesis of tungsten nanoparticles by solvothermal decomposition of tungsten hexacarbonyl, *Int. Journal of Refractory Metals and Hard Materials*, vol. 27, pp. 567–574, 2009.

[155] Rao, J.P., and Geckeler, K.E., Polymer nanoparticles: Preparation techniwues and size-control parameters, *Progress in Polymer Science*, vol. 36, pp. 887–913, 2011.

[156] Koch, C.C., The synthesis and structure of nanocrystalline materials produced by mechanical attrition: A review, *NanoStructured Materials*, vol. 2, pp. 109–129, 1993.

[157] Fedele, L., Colla, L., Bobbo, S., Barison, S., and Agresti, F., Experimental stability analysis of different water-based nanofluids., *Nanoscale research letters*, vol. 6, no. 1, pp. 300, 2011.

[158] Zamzamian, A., Oskouie, S.N., Doosthoseini, A., Joneidi, A., and Pazouki, M., Experimental investigation of forced convective heat transfer coefficient in nanofluids of Al_2O_3/EG and CuO/EG in a double pipe and plate heat exchangers under turbulent flow, *Experimental Thermal and Fluid Science*, vol. 35, no. 3, pp. 495–502, 2011.

[159] Singh, A.K., and Raykar, V.S., Microwave synthesis of silver nanofluids with polyvinylpyrrolidone (PVP) and their transport properties, *Colloid and Polymer Science*, vol. 286, no. 14-15, pp. 1667–1673, 2008.

[160] Kim, D., Hwang, Y., Cheong, S.I., Lee, J.K., Hong, D., Moon, S., Lee, J.E., and Kim, S.H., Production and characterization of carbon nano colloid via one-step electrochemical method, *Journal of Nanoparticle Research*, vol. 10, no. 7, pp. 1121–1128, 2008.

[161] Singaravelu, G., Arockiamary, J., Ganesh, K., and Govindaraju, K., A novel extracellular synthesis of monodispersed gold nanoparticles using marine alga, Sargassum wightii grevile, *Colloids and Surface B: Biointerfaces*, vol. 28, pp. 313–318, 2003.

[162] Ahmad, A., Mukherjee, P., Senapati, S., Mandal, D., Khan, M.I., Kumar, R., and Sastry, M., Extracellular biosynthesis of silver nanoparticles using the fungus *Fusarium osysporum*, *Colloids and Surfaces B: Biointerfaces*, vol. 28, pp. 313–318, 2007.

[163] Bhainsa, K.C., and D\rqSouza, S.F., Extracellular biosynthesis of silver nanoparticles using the fungus *Aspergillus fumigatus*, *Colloids Surfaces B: Biointerfaces*, vol. 47, pp. 160–164, 2006.

[164] Elumalai, E.K., Prasad, T.N.V.K. V, Hemachandran, J., and Therasa, S. V, Extracellular synthesis of silver nanoparticles using leaves of Euphorbia hirta and their antibacterial activities, *Jorunal of Pharmaceutical Sciences and Research*, vol. 2, no. 9, pp. 549–554, 2010.

[165] Krishnaraj, C., Jagan, E.G., Rajasekar, S., Selvakumar, P., Kalaichelvan, P.T., and Mohan, N., Synthesis of silver nanoparticles using *Acalypha indica* leaf extracts and its antibacterial activity against water borne pathogens, *Colloids and Surface B: Biointerfaces*, vol. 76, pp. 50–56, 2010.

[166] Huang, J., Li, Q., Sun, D., Lu, Y., Su, Y., Yang, X., Wang, H., Wang, Y., Shao, W., He, N., Hong, J., and Chen, C., Biosynthesis of silver and gold nanoparticles by novel sundried Cinnamomum camphora leaf, *Nanotechnology*, vol. 18, no. 10, pp. 105104, 2007.

[167] Narayanan, K.B., and Sakthivel, N., Coriander leaf mediated biosynthesis of gold nanoparticles, *Materials Letters*, vol. 62, no. 30, pp. 4588–4590, 2008.

[168] Song, J.Y., Jang, H., and Kim, B.S., Biological synthesis of gold nanoparticles using *Magnolia kobus* and *Diopyros kaki* leaf extracts, *Process Biochemistry*, vol. 44, pp. 1133–1138, 2009.

[169] Shivaji, S., Madhu, S., and Singh, S., Extracellular synthesis of antibacterial silver nanoparticle using psychrophilic bacteria, *Process Biochemistry*, vol. 46, pp. 1800–1807, 2011.

[170] He, S., Guo, Z., Zhang, Y., Zhang, S., Wang, J., and Gu, N., Biosynthesis of gold nanoparticles using the bacteria *Rhodopseudomonas capsulata*, *Materials Letters*, vol. 61, pp. 3984–3987, 2007.

[171] Husseiny, M.I., El-Aziz, M.A., Badr, Y., and Mahmoud, M.A., Biosynthesis of gold nanoparticles using *Pseudomonas aeruginosa*, *Spectrochimica Acta Part A*, vol. 67, pp. 1003–1006, 2007.

[172] Agnihotri, M., Joshi, S., Kumar, A.R., Zinjarde, S., and Kulkarni, S., Biosynthesis of gold nanoparticles by the tropical marine yeast *Yarrowia lipolytica* NCIM 3589, *Materials Letters*, vol. 63, pp. 1231–1234, 2009.

[173] Apte, M., Girme, G., Nair, R., Bankar, A., Kumar, A.R., and Zinjarde, S., Melanin mediated synthesis of gold nanoparticles by *Yarrowia lipolytica*, *Materials Letters*, vol. 95, pp. 149–152, 2013.

[174] Krumov, N., Oder, S., Perner-Nochta, I., Angelov, A., and Posten, C., Accumulation of CdS nanoparticles by yeast in a fed-batch bioprocess, *Journal of Biotechnology*, vol. 132, pp. 481–486, 2007.

[175] Jha, A.K., and Prasad, K., A green low-cost biosynthesis of Sb_2O_3 nanoparticles, *Biochemical Engineering Journal*, vol. 43, no. 3, pp. 303–306, 2009.

[176] Inbakandan, D., Sivaleela, G., Magesh Peter, D., Kiurbagaran, R., Venkatesan, R., and Ajmal Khan, S., Marine sponge extract assisted biosynthesis of silver nanoparticles, *Materials Letters*, vol. 87, no. null, pp. 66–68, 2012.

[177] Thakkar, K.N., Mhatre, S.S., and Parikh, R.Y., Biological synthesis of metallic nanoparticles, *Nanomedicine: Nanotechnology, Biology, and Medicine*, vol. 6, pp. 257–262, 2010.

[178] Prasher, R., Phelan, P.E., and Bhattacharya, P., Effect of aggregation kinetics on the thermal conductivity of nanoscale colloidal solutions (nanofluid)., *Nano letters*, vol. 6, no. 7, pp. 1529–34, 2006.

[179] Samal, S., Satpati, B., and Chaira, D., Production and dispersion stability of ultrafine Al–Cu alloy powder in base fluid, *Journal of Alloys and Compounds*, vol. 504, pp. S389–S394, 2010.

[180] Wang, X., Li, X., and Yang, S., Influence of pH and SDBS on the stability and thermal conductivity of nanofluids, *Energy & Fuels*, vol. 23, no. 16, pp. 2684–2689, 2009.

[181] Shima, P.D., Philip, J., and Raj, B., Magnetically controllable nanofluid with tunable thermal conductivity and viscosity, *Applied Physics Letters*, vol. 95, no. 13, pp. 133112, 2009.

[182] Lee, S.W., Park, S.D., Kang, S., Bang, I.C., and Kim, J.H., Investigation of viscosity and thermal conductivity of SiC nanofluids for heat transfer applications, *International Journal of Heat and Mass Transfer*, vol. 54, no. 1-3, pp. 433–438, 2011.

[183] Phuoc, T.X., Massoudi, M., and Chen, R.-H., Viscosity and thermal conductivity of nanofluids containing multi-walled carbon nanotubes stabilized by chitosan, *International Journal of Thermal Sciences*, vol. 50, no. 1, pp. 12–18, 2011.

[184] Utomo, A.T., Poth, H., Robbins, P.T., and Pacek, A.W., Experimental and theoretical studies of thermal conductivity, viscosity and heat transfer coefficient of titania and alumina nanofluids, *International Journal of Heat and Mass Transfer*, vol. 55, no. 25-26, pp. 7772–7781, 2012.

[185] Kumaresan, V., and Velraj, R., Experimental investigation of the thermo-physical properties of water–ethylene glycol mixture based CNT nanofluids, *Thermochimica Acta*, vol. 545, pp. 180–186, 2012.

[186] Chen, H., Ding, Y., and Lapkin, A., Rheological behaviour of nanofluids containing tube / rod-like nanoparticles, *Powder Technology*, vol. 194, pp. 132–141, 2009.

[187] Yang, J.-C., Li, F.-C., Zhou, W.-W., He, Y.-R., and Jiang, B.-C., Experimental investigation on the thermal conductivity and shear viscosity of viscoelastic-fluid-based nanofluids, *International Journal of Heat and Mass Transfer*, vol. 55, no. 11-12, pp. 3160–3166, 2012.

[188] Syam Sundar, L., Venkata Ramana, E., Singh, M.K., and De Sousa, a. C.M., Viscosity of low volume concentrations of magnetic Fe3O4 nanoparticles dispersed in ethylene glycol and water mixture, *Chemical Physics Letters*, vol. 554, pp. 236–242, 2012.

[189] Adio, S.A., Sharifpur, M., and Meyer, J.P., Investigation into Effective Viscosity and Electrical Conductivity of γ-Al_2O_3-Glycerol Nanofluids in Einstein Concentration Regime, UKHTC 2013. pp. 1–13 2013.

[190] Murshed, S.M.S., Leong, K.C., and Yang, C., Investigations of thermal conductivity and viscosity of nanofluids, *International Journal of Thermal Sciences*, vol. 47, no. 5, pp. 560–568, 2008.

[191] Prasher, R., Song, D., and Wang, J., Measurements of nanofluid viscosity and its implication for thermal application, *Applied Physics Letters*, vol. 89, pp. 133108–1–3, 2006.

[192] Das, S.K., Putra, N., and Roetzel, W., Pool boiling characteristics of nano-fluids, *International Journal of Heat and Mass Transfer*, vol. 46, no. 5, pp. 851–862, 2003.

[193] Wang, X., Xu, X., and Choi, S.U.., Thermal Conductivity of Nanoparticle - Fluid Mixture, *Journal of Thermophysics and Heat Transfer*, vol. 13, no. 4, pp. 474–480, 1999.

[194] Hosseini, M., and Ghader, S., A model for temperature and particle volume fraction effect on nanofluid viscosity, *Journal of Molecular Liquids*, vol. 153, pp. 139–145, 2010.

[195] Suresh, S., Venkitaraj, K.P., Selvakumar, P., and Chandrasekar, M., Synthesis of Al_2O_3-Cu/water hybrid nanofluids using two step method and its thermo physical properties, *Colloids and Surfaces A: Physicochem. Eng. Aspects*, vol. 388, pp. 41–48, 2011.

[196] Larson, R.G., *The structure and rheology of complex fluids*, Oxford University Press, Inc., New York, 1999.

[197] Chen, H., Witharana, S., Jin, Y., Kim, C., and Ding, Y., Predicting thermal conductivity of liquid suspensions of nanoparticles (nanofluids) based on rheology, *Particuology*, vol. 7, no. 2, pp. 151–157, 2009.

[198] Moradpour, H., Chapoy, A., and Tohidi, B., Bimodal model for predicting the emulsion-hydrate mixture viscosity in high water cut systems, *Fuel*, vol. 90, no. 11, pp. 3343–3351, 2011.

[199] Rensing, P.J., Liberatore, M.W., Sum, A.K., Koh, C. a., and Dendy Sloan, E., Viscosity and yield stresses of ice slurries formed in water-in-oil emulsions, *Journal of Non-Newtonian Fluid Mechanics*, vol. 166, no. 14-15, pp. 859–866, 2011.

[200] Singh, N., Chand, G., and Kanagaraj, S., Investigation of Thermal Conductivity and Viscosity of Carbon Nanotubes –, *Heat Transfer Engineering*, vol. 33, no. 9, pp. 821–827, 2012.

[201] Mahbubul, I.M., Khaleduzzaman, S.S., Saidur, R., and Amalina, M. a., Rheological behavior of Al_2O_3/R141b nanorefrigerant, *International Journal of Heat and Mass Transfer*, vol. 73, pp. 118–123, 2014.

[202] Yang, Y., Oztekin, A., Neti, S., and Mohapatra, S., Particle agglomeration and properties of nanofluids, *Journal of Nanoparticle Research*, vol. 14, no. 5, pp. 852, 2012.

[203] Keblinski, P., Prasher, R., and Eapen, J., Thermal conductance of nanofluids: is the controversy over?, *J. Nanopart Res.*, vol. 10, pp. 1089–1097, 2008.

[204] Tseng, W.J., and Lin, C.L., Effect of dispersant on rheological behaviour of $BaTiO_3$ poweders in ethano-isopropanol mixtures, *Mater. Chem. Phys.*, vol. 80, pp. 232–238, 2003.

[205] Nguyen, C.T., Desgranges, F., Roy, G., Galanis, N., Maré, T., Boucher, S., and Angue Mintsa, H., Temperature and particle-size dependent viscosity data for water-based nanofluids – Hysteresis phenomenon, *International Journal of Heat and Fluid Flow*, vol. 28, no. 6, pp. 1492–1506, 2007.

[206] He, Y., Jin, Y., Chen, H., Ding, Y., Cang, D., and Lu, H., Heat transfer and flow behaviour of aqueous suspensions of TiO_2 nanoparticles (nanofluids) flowing upward through a vertical pipe, *International Journal of Heat and Mass Transfer*, vol. 50, no. 11-12, pp. 2272–2281, 2007.

[207] Namburu, P., and Kulkarni, D., Experimental investigation of viscosity and specific heat of silicon dioxide nanofluids, *Micro & Nano Letters*, vol. 2, no. 3, pp. 67–71, 2007.

[208] Pastoriza-Gallego, M.J., Casanova, C., Legido, J.L., and Piñeiro, M.M., CuO in water nanofluid: Influence of particle size and polydispersity on volumetric behaviour and viscosity, *Fluid Phase Equilibria*, vol. 300, no. 1-2, pp. 188–196, 2011.

[209] Anoop, K.B., Sundararajan, T., and Das, S.K., Effect of particle size on the convective heat transfer in nanofluid in the developing region, *International Journal of Heat and Mass Transfer*, vol. 52, no. 9-10, pp. 2189–2195, 2009.

[210] Timofeeva, E. V, Smith, D.S., Yu, W., France, D.M., Singh, D., and Routbort, J.L., Particle size and interfacial effects on thermo-physical and heat transfer characteristics of water-based alpha-SiC nanofluids., *Nanotechnology*, vol. 21, no. 21, pp. 215703, 2010.

[211] Jia-Fei, Z., and Zhong-Yang, L., Dependence of nanofluid viscosity on particle size and pH value, *Chinese Physics Lett.*, vol. 26, no. 6, pp. 10–13, 2009.

[212] Rubio-Hernández, F.J., Ayúcar-Rubio, M.F., Vlaázquez-Navarro, J.F., and Galindo-Rosales, F.J., Intrinsic viscosity of SiO_2, $Al_2O_3$and TiO_2 aqueous suspensions, *Journal of Colloid and Interface Science*, vol. 298, pp. 967–972, 2006.

[213] Boluk, Y., Lahiji, R., Zhao, L., and McDermott, M.T., Suspension viscosities and shape parameters of cellulose nanocrystals (CNC), *Colloids and Surfaces A: Physicochem. Eng. Aspects*, vol. 337, pp. 297–303, 2011.

[214] Wierenga, A.M., and Philipse, A.P., Low-shear viscosities of (semi-)dilute, aqueous dispersions of charged boehmite rods: dynamic scaling of double layer effects, *Langmuir*, vol. 13, pp. 4574–4582, 1997.

[215] Wierenga, A.M., and Philipse, A.P., Low-shear viscosities of dilute dispersions of colloidal rodlike silica particles in cyclohexane, *Journal of Colloid and Interface Science*, vol. 180, pp. 360–370, 1996.

[216] Hwang, Y., Park, H.S., Lee, J.K., and Jung, W.H., Thermal conductivity and lubrication characteristics of nanofluids, *Current Applied Physics*, vol. 6, pp. e67–e71, 2006.

[217] Vékás, L., Bica, D., and Avdeev, M., Magnetic nanoparticles and concentrated magnetic nanofluids: synthesis, properties and some applications, *China Particuology*, vol. 5, pp. 43–49, 2007.

[218] Sharifpur, M., Meyer, J.P., and Africa, S., Opportunities in Nanofluid Composites, The 3rd International Coference on Composites: Characterization, Fabrication and Application (CCFA-3). pp. 9–10. , Tehran, Iran, 2012.

[219] Charles, S., The preparation of magnetic fluids, *Ferrofluids*, pp. 3–18, 2003.

[220] Shima, P., and Philip, J., Tuning of thermal conductivity and rheology of nanofluids using an external stimulus, *The Journal of Physical Chemistry C*, pp. 20097–20104, 2011.

[221] Andablo-Reyes, E., Hidalgo-Álvarez, R., and Vicente, J., Controlling friction using magnetic nanofluids, *Soft Matter*, vol. 7, pp. 880–883, 2011.

[222] S S Papell, Low viscosity magnetic fluid obtained by the colloidal suspension of magnetic particles, 1965.

[223] Vekas, L., Magnetic nanofluids properties and some applications, *Romanian Journal of Physics*, vol. 49, pp. 707–721, 2004.

[224] Vekas, L., Bica, D., and Marinica, O., Magnetic nanofluids stabilized with various chain length surfactants, *Romanian Reports in Physics*, vol. 58, no. 3, pp. 257–267, 2006.

[225] Shima, P., Philip, J., and Raj, B., Synthesis of aqueous and nonaqueous iron oxide nanofluids and study of temperature dependence on thermal conductivity and viscosity, *The Journal of Physical Chemistry C*, pp. 18825–18833, 2010.

[226] Wonterghem, J., Mørup, S., Charles, S., Wells, S., and Villadsen, J., Formation of a metallic glass by thermal decomposition of $Fe(CO)_5$, *Physical review Letters*, vol. 55, no. 4, 1985.

[227] Jolly, M., Bender, J.W., and Carlson, D.J., Properties and applications of commercial magnetorheological fluids, SPIE 5th Annual Int. Symposium on Smart Structures and Matherials. pp. 1–14. , San Diego, CA, 1998.

[228] Rudyak, V.Y., and Krasnolutskii, S.L., Dependence of the viscosity of nanofluids on nanoparticle size and material, *Physics Letters A*, vol. 378, no. 26-27, pp. 1845–1849, 2014.

[229] Huseyin, K., and Muhammet, K., Prediction of thermal conductivity of ethylene glycol - water solutions by using artificial neural networks, *Applied Energy*, vol. 86, pp. 2244–2248, 2009.

[230] Hojjat, M., Etemad, S.G., Bagheri, R., and Thibault, J., Thermal conductivity of non-Newtonian nanofluids: Experimental data and modeling using neural network, *International Journal of Heat and Mass Transfer*, vol. 54, pp. 1017–1023, 2011.

[231] Papari, M.M., Yousefi, F., Moghadasi, J., Karimi, J., and Campo, A., Modeling thermal conductivity augmentation of nanofluids using diffusion neural networks, *International Journal of Thermal Sciences*, vol. 50, pp. 44–52, 2011.

[232] Mehrabi, M., Sharifpur, M., and Meyer, J.P., Application of the FCM-based neuro-fuzzy inference system and genetic algorithm-polynomial neural network approaches to modelling the thermal conductivity of alumina--water nanofluids, *International Communications in Heat and Mass Transfer*, vol. 39, pp. 971–997, 2012.

[233] Yousefi, F., Karimi, H., and Papari, M.M., Modeling viscosity of nanofluids using diffusional neural networks, *Journal of Molecular Liquids*, vol. 175, pp. 85–90, 2012.

[234] Bahiraei, M., Hosseinalipour, S., Zabihi, K., and Taheran, E., Using Neural Network for Determination of Viscosity in Water-TiO_2 Nanofluids, *Advances in Mechanical Engineering*, vol. 742680, no. 1-10, 2012.

[235] Karimi, H., and Yousefi, F., Application of artificial neural network–genetic algorithm (ANN–GA) to correlation of density in nanofluids, *Fluid Phase Equilibria*, vol. 336, pp. 79–83, 2012.

[236] Mehrabi, M., Sharifpur, M., and Meyer, J.P., Viscosity of nanofluids based on an artificial intelligence model, *International Communications in Heat and Mass Transfer*, vol. 43, pp. 6–11, 2013.

[237] Atashrouz, S., Pazuki, G., and Alimoradi, Y., Estimation of the viscosity of nine nanofluids using a hybrid GMDH-type neural network system, *Fluid Phase Equilibria*, vol. 372, pp. 43–48, 2014.

[238] Wong, K. V., and De Leon, O., Applications of Nanofluids: Current and Future, *Advances in Mechanical Engineering*, vol. 2010, pp. 1–11, 2010.

[239] Yu, W., and Xie, H., A Review on Nanofluids: Preparation, Stability Mechanisms, and Applications, *Journal of Nanomaterials*, vol. 2012, pp. 1–17, 2012.

[240] Huminic, G., and Huminic, A., Application of nanofluids in heat exchangers: A review, *Renewable and Sustainable Energy Reviews*, vol. 16, no. 8, pp. 5625–5638, 2012.

[241] Weinberger, H., The Physics of the Solar Pond, vol. 8, no. 2, pp. 45–56, 1963.

[242] Al-Nimr, M. a., and Al-Dafaie, A.M.A., Using nanofluids in enhancing the performance of a novel two-layer solar pond, *Energy*, vol. 68, pp. 318–326, 2014.

[243] Konakanchi, H., Vajjha, R.S., Chukwu, G., and Das, D.K., Measurements of pH of Three Nanofluids and Development of New Correlations, *Heat Transfer Engineering*, no. june, pp. 81–90, 2014.

Table 1 Summarised list of the available classical models

Investigators	Classical Models	Remarks
Einstein [47]	$\mu_{eff} = \mu_o(1+2.5\phi)$	Established on extremely dilute suspension of rigid solid spheres and non-interacting medium. Volume fraction of $\phi \leq 0.02$. From the model, it is clear that viscosity is a linear function of volume fraction.
Taylor [50]	$\mu_{eff} = \mu_o\left\{1+2.5\phi\left(\frac{\mu'+\frac{2}{3}\mu_o}{\mu'+\mu_o}\right)\right\}$	An extension of model [47], for liquid containing drops of another liquid in suspension. The liquid drops have been assumed spherical and, for sphericity to be maintained, there must be high surface tension. Therefore, this model is only valid when the condition above is met.
Brinkman [51]	$\mu_{eff} = \mu_o(1-\phi)^{-2.5}$	This is an extension of [47] and for a volume fraction, $\phi \leq 0.04$.
Vand [52]	$\mu_{eff} = \mu_o\left(1+2.5\phi+7.348\phi^2+...\right)$	
Mooney [53]	$\mu_{eff} = \mu_o \exp\left(\frac{2.5\phi}{1-\upsilon\phi}\right)$	Formulated on the premise of [47] and the model is limited to rigid spherical particles. This is a semi-empirical model as the interaction data, υ (crowding factor) was left to be obtained by empirical means. Accounts for suspensions containing a wide spectrum of continuous size distribution, i.e. for monodispersed suspension of finite concentration, The crowding factor υ will be different for particulate suspension of two different diameters, see [53].
Roscoe [54]	$\mu_{eff} = \mu_o(1-1.35\phi)^{-2.5}$	This model equation was developed for spheres of equal size and high concentration. For spheres of very diverse sizes, the viscosity is to be predicted with $\mu_{nf} = \mu_o(1-\phi)^{-2.5}$, this equation is valid for all concentration and as the vol. concentration is tending towards zero, it reduces to model [30].
Batchelor [55]	$\mu_{eff} = \mu_o\left(1+2.5\phi+6.5\phi^2\right)$	Effect of interactions between particles was considered in the development of this model. Within the limits of a very low particle volume concentration, this model approaches model [47].

Table 1 Continued

Investigators	Classical Models	Remarks
Krieger and Dougherty [56]	$\mu_{eff} = \mu_o \left(1 - \frac{\phi}{\phi_m}\right)^{-[\eta]\phi_m}$	Covers virtually the whole spectrum of nanoparticles. ϕ_m is the maximum concentration at which flow can occur, and its value for high shear rate is 0.605. η is the intrinsic viscosity with a typical value of 2.5.
Lundgren [57]	$\mu_{eff} = \mu_o \left(1 + 2.5\phi + \frac{25}{4}\phi^2 + f\left(\phi^3\right)\right)$	This model was proposed considering Brownian motion of isotropic suspension of rigid spherical particles. The resulting bulk stress on the particles was taken into account. Within the limits of a very low particle volume concentration, this model approaches model [47].
Graham [58]	$\mu_{eff} = \mu_o \left\{1 + 2.5\phi + 4.5 \times \left[\frac{1}{\left(h_s/d_p\right)\left(2 + \left(h_s/d_p\right)\right)\left(1 + \left(h_s/d_p\right)^2\right)}\right]\right\}$	This model approaches [47] and [62] as the lower and upper limit of solid volume fraction tends to zero and infinity respectively. Cell-based theory was used where spheres were arranged in equidistance to a central sphere. The diameters of the spheres were assumed uniform and zero inertial, Brownian motion, Van der Waals, and electroviscous forces were considered.
Saito [59]	$\mu_{eff} = \mu_o \left(2.5\phi + 14.1\phi^2\right)$	
Hatchek [60]	$\mu_{eff} = \mu_o \left(1 + 4.5\phi\right)$	It is applicable for up to 40% solid concentration.
Thomas and Muthukumar [61]	$\mu_{eff} = \mu_o \left(1 + 2.5\phi + 4.83\phi^2 + 6.4\phi^3\right)$	
Frankel and Acrivos [62]	$\mu_{eff} = \mu_o \frac{9}{8}\left[\frac{\left(\phi/\phi_m\right)^{\frac{1}{3}}}{1 - \left(\phi/\phi_m\right)^{\frac{1}{3}}}\right]$	Developed using asymptotic technique to describe the viscosity of suspension within the concentrated limit where maximum volume fraction is obtainable. Assume uniform solid sphere to complement Einstein's work from dilute to concentrated regime.

Table 2 New theoretical models

Investigators	New Models	Remarks
Masoumi et al. [2]	$\mu_{nf} = \mu_o + \frac{\rho_p V_B d_p^2}{72C\delta}$ $\delta = \sqrt[3]{\frac{\pi}{6\phi}} d_p$	Developed based on Brownian motion, considering five parameters (volumetric fraction, temperature, particle diameter, nanoparticle density and base fluid physical properties). Calculated a correction factor to take care of simplification assumptions. Tested the models with nanofluids with single- and two-base fluids.
Hosseini et al. [33]	$\mu_{nf} = \mu_o . \exp\left[m + \alpha\left(\frac{T}{T_0}\right) + \omega(\phi_h) + \gamma\left(\frac{d_p}{1+r}\right)\right]$	This model was formulated using dimensionless groups considering the viscosity of the base fluid, hydrodynamic volume fraction of nanoparticles, diameter of nanoparticles, thickness of capping layer of the nanoparticles and temperature as π_1, π_2, π_3 and π_4 respectively. The dimensionless group is defined as $\pi_1 = \frac{\mu_{nf}}{\mu_{bf}}$, $\pi_2 = \phi_h$, $\pi_3 = \frac{d}{1+r}$, and $\pi_4 = \frac{T}{T_0}$, m is a system property constant, α, ω, γ are empirical constants obtainable from the experimental data.
Chen et al. [68]	$\mu_{nf} = \mu_o \left(1 - \frac{\phi_a}{\phi_m}\right)^{-[\eta]\varphi_m}$	Modified [56], considering the effect of agglomeration, therefore proposed ϕ_a as the effective volume fraction of agglomerates. The power in the model $\left(-[\eta]\varphi_m\right)$ was evaluated to be -1.5125, $\phi_a = \phi(a_a / a)^{3-D}$ where D is the fractal index and the duo of a_a and a are the radii of the agglomerates and primary particles.

Table 3 Summary of available empirical models

Investigators	Empirical Models	Concentration (%)	Size (nm)	Temperature (°C)	Remarks
Heyhat et al. [21]	$\mu_{nf} = \mu_o(T)\,Exp\left(\frac{5.989\phi}{0.278-\phi}\right)$	0.1-2	40	20-60	◦ Al_2O_3-water nanofluid. ◦ Correlation coefficient of 0.99. ◦ Valid for the temperature range investigated.
Chandreasekar et al. [32]	$\mu_{nf} = \mu_o\left(1+A\left(\frac{\phi}{1-\phi}\right)^n\right)$	0.33-5	43	25	◦ Al_2O_3-water nanofluid. ◦ Model was developed based on mean free path between nanoparticles. ◦ *A*and *n* were taken as 5 200 and 2.8 respectively.
Namburu et al. [34]	$Log(\mu_{nf}) = Ae^{-BT}$ $A = 1.8375\phi^2 - 29.643\phi + 165.56$ $R^2 = 0.9873$ $B = 4\times10^{-6}\phi^2 - 1\times10^{-3}\phi + 1.86\times10^{-2}$ $R^2 = 0.988$	1-6.12	29	-35-50	◦ CuO-EG/water (60:40) nanofluid. ◦ Newtonian nanofluid. ◦ *T* is the absolute temperature in Kelvin. ◦ *A* and *B* are empirical curve fit parameters and in this case are functions of ϕ, with $R^2 = 0.99$.
Abareshi et al. [43]	$\mu_{nf}(T) = \mu_o(T)\,Ae^{\left(\frac{B}{T+T_o}\right)}$	0.125-0.75	25-50	30-70	◦ α – F_e2O_3-glycerol nanofluid. ◦ Non-Newtonian shear thinning nanofluid. ◦ Based on Vogel-Fulcher-Tammann (VTF) equation. ◦ μ_{nf} was obtained at shear rate of 40 s^{-1} ◦ *A* and T_o are fitting parameters of the shear viscosity. ◦ *B* is related to the free activation energy of the fluid (empirically obtainable).
Kole and Dey [44]	$\mu_{nf} = \mu_o\left(1-\frac{\phi}{0.5}\left(\frac{a_a}{a}\right)^{1.3}\right)^{-1.25}$ $In(\mu_{nf}) = A + \frac{1000B}{(T+C)}$	0.5-2.5	40	5-80	◦ CuO-gear oil nanofluid. ◦ Newtonian nanofluid (ϕ = 0.5%). ◦ Non-Newtonian shear thinning ($0.5 \leq \phi \leq 2.5$ %). ◦ *T* is the absolute temperature in Kelvin. ◦ Aggregated size is 200-360 nm. ◦ *A*, *B* and *C* are empirical curve fit parameters with deviation ~ 1.4%. ◦ μ_{nf} was obtained at 30 °C.

Table 3 Continued

Investigators	Empirical Models	Concentration (%)	Size (nm)	Temperature (°C)	Remarks
Chen et al. [81]	$\mu_{nf} = \mu_o\left(1+10.6\phi+(10.6\phi)^2\right)$ $In\left(\mu_{nf}\right) = A+\frac{1000B}{(T+C)}$	0-8[a]	25	20-60	◦ TiO_2-EG nanofluid. ◦ Newtonian nanofluid. ◦ Agglomerated size is 70-100 nm. ◦ μ_{nf} predicted the experimental data with R^2 = 0.9989. ◦ *A*, *B* and *C* are empirical curve fit parameters with deviation ~ 1.7%.
Tseng and Chen [82]	$\mu_{nf} = \mu_o \times 0.4513e^{0.6965\phi}$	3-10	300	25	◦ Ni-terpineol nanofluid. ◦ Dispersant concentration 0.5-10% of Ni weight. ◦ μ_{nf} predicted the experimental with R^2 = 0.9952.
Tseng and Lin [83]	$\mu_{nf} = \mu_o \times 13.47e^{35.98\phi}$	5-12	7-20	25	◦ TiO_2-DI-water nanofluid. ◦ μ_{nf} predicted the experimental with R^2 = 0.98. ◦ μ_{nf} was obtained at shear rate of 100 s^{-1}.
Horri et al. [85]	$\mu_{nf} = \mu_o\left(1+2.5\phi+A\phi\left(\frac{\phi}{\phi_m-\phi}\right)^2\right)$	0-40			◦ NiO/YSZ-furfuryl alcohol suspension. ◦ Reconciles the models of Einstein [47], Chen et al. [68] and Browers' model using mobility parameters $(\phi/\phi_m-\phi)$. ◦ Shear rate ranging from 10-1000 s^{-1}. ◦ *A* and ϕ_m are obtainable from experimental data.
Sahoo et al. [86]	$\mu_{nf} = Ae^{(B/T+C\phi)}$	1-10	53	-35-90	◦ Al_2O_3-EG/water (60:40) nanofluid. ◦ Non-Newtonian nanofluid shear thinning (-35 – 0°C). ◦ Newtonian nanofluid (0-90 °C). ◦ *T* is the absolute temperature in Kelvin. ◦ *A*, *B* and *C* are empirical curve fit parameters with R^2 = 0.99.
Nguyen et al. [87]	$\mu_{nf} = \mu_o \times 0.904e^{0.1483\phi}$	0.15-13	47	22-25	◦ Al_2O_3-water nanofluid. ◦ No information on the dispersant used.
Nguyen *et al.* [87]	$\mu_{nf} = \mu_o\left(1-0.025\phi+0.015\phi^2\right)$	0.15-12	36	22-25	◦ Al_2O_3-water nanofluid. ◦ No information on the dispersant used.

Table 3 Continued

Investigators	Empirical Models	Concentration (%)	Size (nm)	Temperature (°C)	Remarks
Nguyen et al. [87]	$\mu_{nf} = \mu_o \begin{pmatrix} 1.475 - 0.319\phi + 0.051\phi^2 \\ +0.009\phi^3 \end{pmatrix}$	0.15-12	29	22-25	◦ CuO-water nanofluid. ◦ No information on the dispersant used.
Nguyen et al. [87]	$\mu_{nf} = \mu_o(1.125 - 0.0007T)$ $\mu_{nf} = \mu_o(2.1275 - 0.0215T + 0.0002T^2)$	1 and 4	29, 36 and 47	20-70	◦ Al_2O_3-water and CuO-water nanofluid.
Garg et al. [90]	$\mu_{nf} = \mu_o(1+11\phi)$	0.5-2	200	–	◦ Cu-EG nanofluid. ◦ Newtonian nanofluid. ◦ A linear fit following Einstein's model [47].
Godson et al. [91]	$\mu_{nf} = \mu_o(1.005 + 0.497\phi - 0.1149\phi^2)$	0.3-0.9	60	50-90	◦ Ag-DI-water nanofluid.
Duangthongsuk and Wongwises [92]	$\mu_{nf} = \mu_o(A + B\phi + C\phi^2)$	0.2-2	21	15, 25 and 35	◦ TiO_2-water nanofluid. ◦ A, B and C are empirical constants obtained from curve fitting for the three different temperatures.
Chevalier et al. [94]	$\mu_{nf} = \mu_o(1+8.3\phi)$	0-6	190 nm	25	◦ SiO2-Ethanol nanofluid. ◦ Clearly a linear fit of the type of classical work of Einstein [47].
Chevalier et al. [94]	$\mu_{nf} = \mu_o\left(1 - \frac{\phi_a(d_p)}{\phi_m}\right)^{-2}$ $\phi_a(d_p) = \left(\frac{D_a}{d_p}\right)^{1.2}\phi$	0-7	35 and 94	25	◦ SiO_2-ethanol nanofluid. ◦ Correlated based on Krieger and Dougherty model. ◦ Fitted for the particle sizes with D_a as the aggregated diameter (195 and 352 nm) corresponding to the nanoparticle diameters. ◦ ϕ_m is crowding factor as detailed by Prasher et al. [191]. D_a is the aggregate diameter.
Kulkarni et al. [101]	$In(\mu_{nf}) = A\left(\frac{1}{T}\right) - B$	5-15	29	5-50	◦ CuO-water nanofluid. ◦ Non-Newtonian nanofluid showing pseudoplastic and shear-thinning behaviour. ◦ T is the absolute temperature in Kelvin. ◦ A and B are empirical constants and are dependent on the particle volume fraction.

Table 3 Continued

Investigators	Empirical Models	Concentration (%)	Size (nm)	Temperature (^oC)	Remarks
Syam Sundar et al. [109]	$\mu_{nf} = \mu_o\left(1+\frac{\phi}{12.5}\right)^{6.356}$	0-2%	13	20 – 60	◦ Fe_3O_4-water nanofluid. ◦ Newtonian nanofluids.
Phuoc and Massoudi [110]	$\mu_{nf} = \mu_\infty + \left(\frac{\psi e^{n\phi}}{\dot{\gamma}}\right)^{1/2}\left[\left(\frac{\psi e^{n\phi}}{\dot{\gamma}}\right)^{1/2} + 2\mu_\infty^{1/2}\right]$	0-4	20-40	25	◦ Fe_2O_3-DI-water. ◦ Modelled to express the dependent of viscosity on shear rate and volume fraction. ◦ Shear rates are 26.4, 79.2, 132, and 211 s^{-1}. ◦ Non-Newtonian shear thinning at $\phi \geq 2$ %. ◦ Dispersant.
Corcione [111]	$\mu_{nf} = \mu_o\left(\frac{1}{1-34.87(d_p/d_f)^{-0.3}\phi^{1.03}}\right)$ $d_f = 0.1\left(\frac{6M}{N\pi\rho_f}\right)^{1/3}$	0.01-7.1	25-200	20-50	◦ Correlated for a wide range of data from the literature. ◦ Nanofluids consisting of Al_2O_3, TiO_2, SiO_2 and Cu nanoparticles were used. ◦ d is the diameter. ◦ M is the molar mass of the base fluid. ◦ N is the Avogadro's number.
Sekhar and Sharma [112]	$\mu_{nf} = 0.935\mu_0\left(1+\frac{T_{nf}}{70}\right)^{0.5602}\left(1+\frac{d_p}{80}\right)^{-0.05915}\left(1+\frac{\phi}{100}\right)^{10.51}$	0.01-5	13-100	20-70	◦ Al_2O_3-water nanofluid. ◦ Regression model based on experimental data from the literature. ◦ Deviations of -10% – +18%.
Kitano *et al.* [113]	$\mu_{nf} = \mu_o\left(1-\frac{\phi}{\Phi}\right)^{-2}$	0-6.2	–	–	◦ Modelled for polymer melts (for?) different inorganic fillers. ◦ Based on Maron-Pierce's equation $\eta_r = (1-\phi/\Phi)^{-2}$, Φ is a constant for packing geometry. ◦ Φ is related to packing geometry of various inorganic materials that fill the polymer melts; $\Phi = 0.54 - 0.0125\bar{p}$, where $\bar{p}$ is the average aspect ratio. ◦ The equation is only applicable above the shear) stress of 10^4 dyne/cm^2.
Bobbo et al. [114]	$\mu_{nf} = \mu_o\left(1+A\phi+B\phi^2\right)$	0.01-1%	21-60	10-80	◦ TiO_2-water nanofluids (21 nm). ◦ SWCNT-water nanofluids (60 nm). ◦ Newtonian nanofluids. ◦ A and B are empirical parameters based on present experimental data. ◦ Dispersant used (SDS and PEG).

Table 4 Overview of classification of methods of preparation of nanoparticles

Classification	Methods	Nanostructures	Ref.
Physical	Ball milling	γ-Fe_2O_3	[133]
		Fe_2S_4, Fe_2S	[134]
		Si	[135]
	Pulsed laser ablation	Fe_2O_4 and Fe_3C	[136]
		Pd	[137]
		Au	[138]
	Laser deposition and MAPLE	TiO	[130, 139]
Chemical	Chemical precipitation	CdS	[140]
		$CaCo_3$, $Al(OH)_3$,	[141]
		$SrCO_3$, NiCuZn	[142]
	Sonoelectrochemical synthesis	Ag	[143]
		CdSe	[144]
		PbSe	[145]
		Pt	[146]
		Tungsten	[147]
	Spray pyrolysis	SiO_2	[149]
		TiO	[150]
	Chemical vapour deposition	SWCNT	[151, 152]
		SiO_2	[153]
	Thermal decomposition	Tungsten	[154]
Biological	Algae	Au	[161]
	Fungi	Ag	[162, 163]
	Plant and plant extracts	Ag	[164–166]
		Au	[166–168]
	Bacteria	Ag	[169]
		Au	[170, 171]
	Yeast	Au	[172–175]
	Marine sponge	Ag	[176]

Table 5 Summary of equipment for nanoviscosity and their measurement bases

Nanofluids	Equipment type & Manufacturer	SP (hr)	Temp. (^oC)	Basis of measurement	Ref.
Al_2O_3 – water	Oscillation Viscometer VM – 10A (CBC Co Ltd.)	5	21-39	Resonating vibration	[17]
ZnO – EG	LVDV – II + Viscometer (Brookfield Engr. Lab, USA)	3	60-20	Shear rate	[18]
Al_2O_3 – water	LVDV – I – Prime C/P Viscometer (Brookfield Engr. Lab, USA)	6	300[a]	Shear rate	[32]
ZnO – EG and ZnO – G	Glass Capillary Viscometer (Ostwald viscometer)	NA	25 ^oC	Gravity induced	[42]
α–Fe_2O_3– glycol	LVDV – II + Pro EXTRA Viscometer (Brookfield Engr. Lab, USA)	0.5	NA	Viscous drag	[43]
CuO–Gear Oil	LVDV – II – Pro Viscometer (Brookfield Engr. Lab, USA)	4	-20-100	Viscous drag	[44]
EG – TiO_2	Bohlin CVO Rheometer (Malvern Instrument UK)	20	20-60	Controlled shear stress	[68]
Al_2O_3 – water/EG	LVDV – II – Pro Viscometer (Brookfield Engr. Lab, USA)	4	20-100	Shear rate	[76]
TiO_2 – EG	Bohlin CVO Rheometer (Malvern Instrument UK)	20	10-90	Controlled shear stress	[81]
Ni– tevpineol	VT550 Viscometer (Gerbruder HAAKE Gmbh, Germany)	24	25	Shear rate	[82]
FA – NiO/YSZ	HAAKE Mars III Rheometer (Thermo Fisher Sci. Inc.)	24	22 ± 1	Shear rate	[85]
Al_2O_3 – water/EG	LVDV – II + Viscometer (Brookfield Engr. Lab, USA)	1.5	-35-90	Shear rate	[86]
Al_2O_3 – water	ViscoLab450 Model (Cambridge Applied Systems, USA)	NA	20-85	Piston-type (Couette flow)	[87]
SiO_2 – ethanol	Capillary microviscometer	-	-	-	[94]
SiC – DI-water	SV-10 Vibro-viscometer (A&D Company, Japan)	12	20 – 80	Resonating vibration	[182]
Fe_2O_3 – DDW	LDDV – II Pro Viscometer (Brookfield Engr. Lab, USA)	NA	-20-150	Viscous drag	[183]
Al_2O_3 – water TiO_2 – water	AR 1000 Rheometer (TA Instrument, USA)	3min	20 ± 0.1	Shear rate	[184]
CNT – water/EG	Bohlin CVO Rheometer (Malvern Instrument, UK)	NA	0 – 40	Controlled shear stress	[185]
EG – TNT	Bohlin CVO Rheometer (Malvern Instrument, UK)	NA	20 – 60	Controlled shear stress	[186]
Cu - VEF	Kinexus Pro (Malvern Instrument, UK)	3	225-325[*]	Controlled shear stress	[187]

[*] Temperature is given in ^oK, SP – Sonication period, EG – Ethylene Glycol, G – Glycerol, DDW – Double Distilled Water, VEF – viscoelastic fluid.

List of figure captions

Figure 1 Inconsistency in suspension viscosity predictions by different available models. Al_2O_3-DI-water nanofluids prediction at 20 ^oC. Insets at points (1) and (2) depict the level of discordance in the predicted relative viscosity values even for models built around particle volume concentration.

Figure 2 Underprediction of Al_2O_3-DI-water nanofluids by classical models.

Figure 3 Underprediction of TiO_2-DI-water nanofluids by classical models.

Figure 4 Instability sequence in nanofluids. At time t_o, the nanofluid is stable just after preparation by ultrasonication or HPH, at t_1, flocculation sets in and degenerates to agglomeration at t_2, which finally sediments at time t_3. As ϕ also increases, the tendency of the instability sequence is high.

Figure 5 Effect of temperature on the viscosity of Al_2O_3-glycerol nanofluid.

Figure 6 Effect of shear rate on the rheology of suspension: (a) the stress (τ)-shear rate ($\dot{\gamma}$) curve of TiO_2-water nanofluid at different particle volume fractions; (b) the suspension viscosity (μ_{nf})-shear rate ($\dot{\gamma}$) curve of TiO_2-water nanofluid at different particle volume fractions [83].

Figure 7 Effect of shearing time water-based nanofluids of CNT and Al_2O_3 at 5 ^oC: (a) CNT – water nanofluid showing shear thinning, thixotropic; (b) Al_2O_3-water nanofluid showing shear thickening, thixotropic [108].

Figure 8. Effect of nanoparticle size on the relative viscosity of SiO_2-DI water nanofluid [211].

Figure 9 Criteria and selection flow chart for the implementation of search and sort algorithm.

Figure 10 Generic algorithms for selection of appropriate nanofluid viscosity models. R, S,…V are available nanofluid viscosity models with attributes R1, R2, …V5, V6 and sub-array attributes r1, r2, …v5,v6.

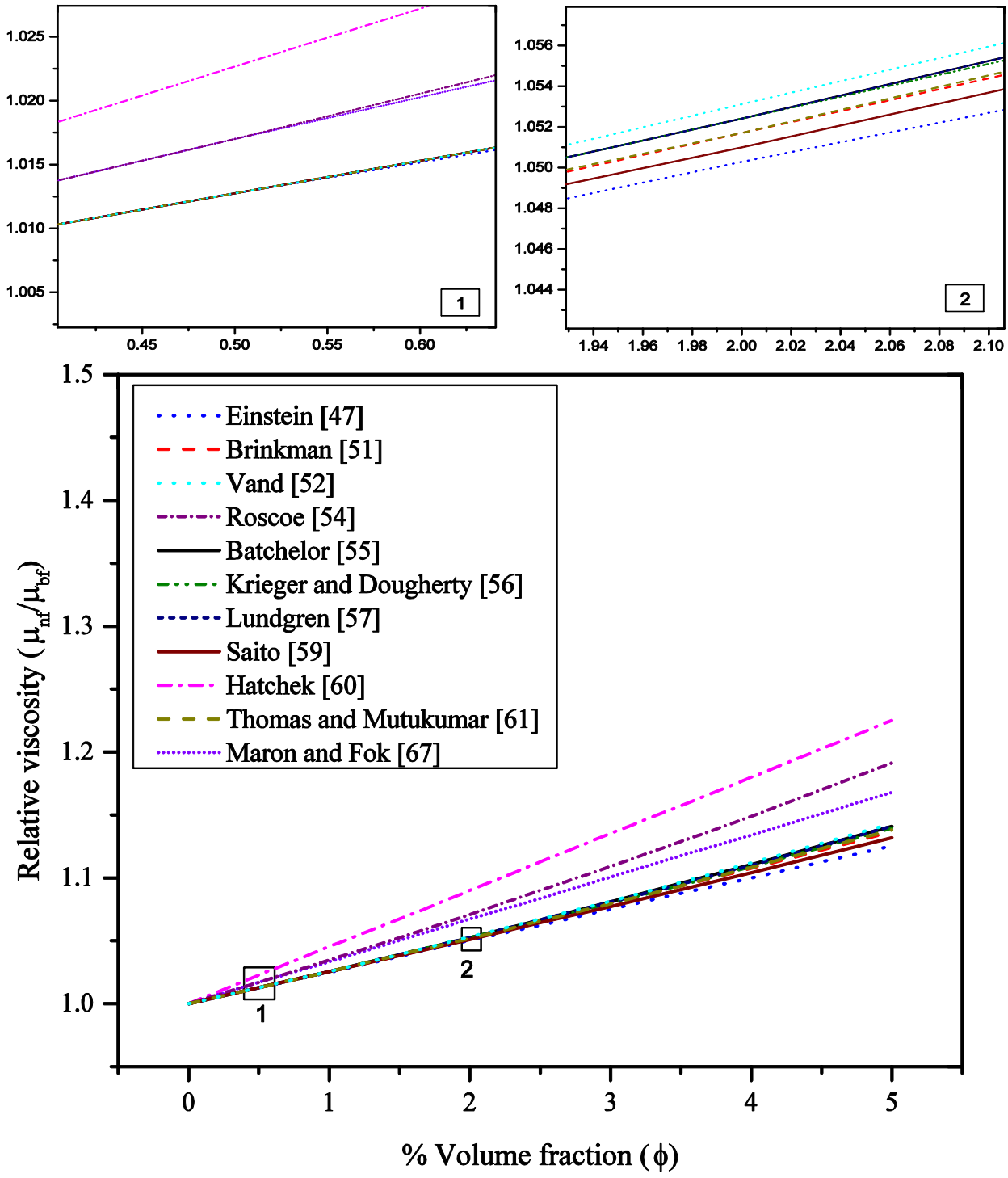

Figure 1 Inconsistency in suspension viscosity predictions by different available models. Al_2O_3-DI-water nanofluids prediction at 20 ^oC. Insets at points (1) and (2) depict the level of discordance in the predicted relative viscosity values even for models built around particle volume concentration.

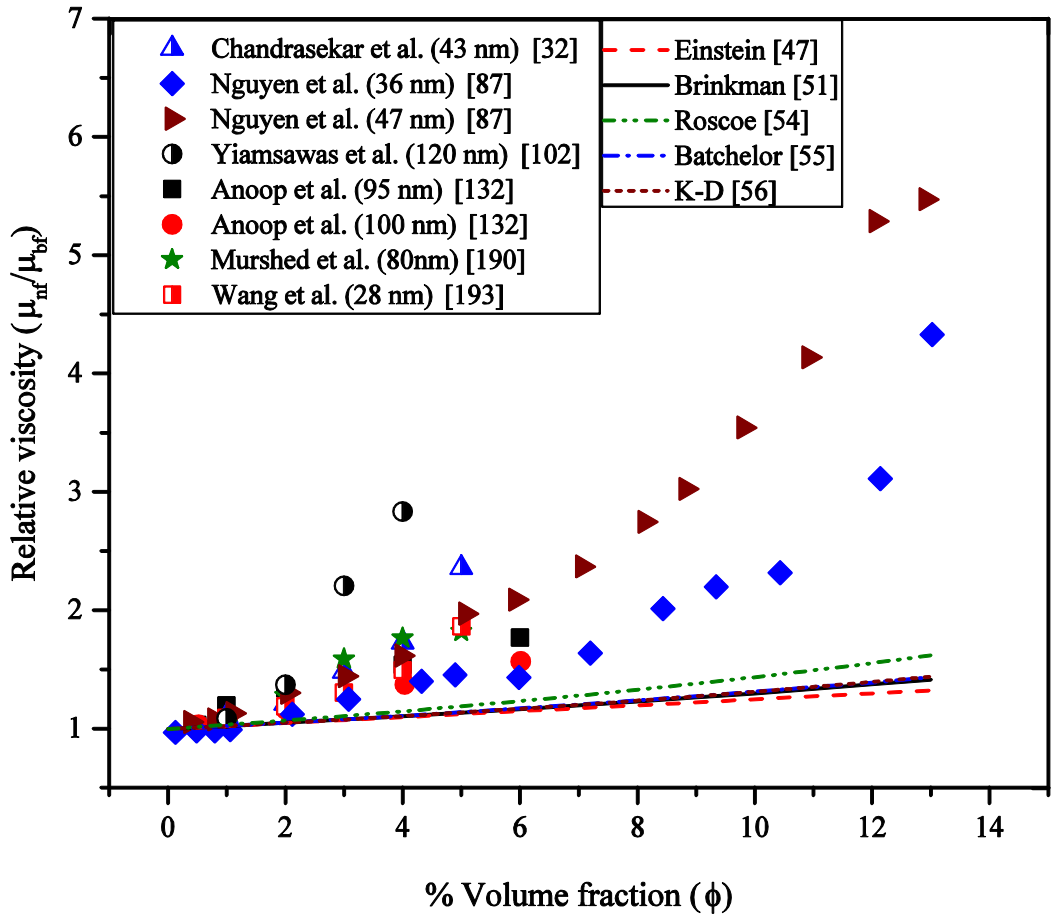

Figure 2 Underprediction of Al_2O_3-DI-water nanofluids by classical models.

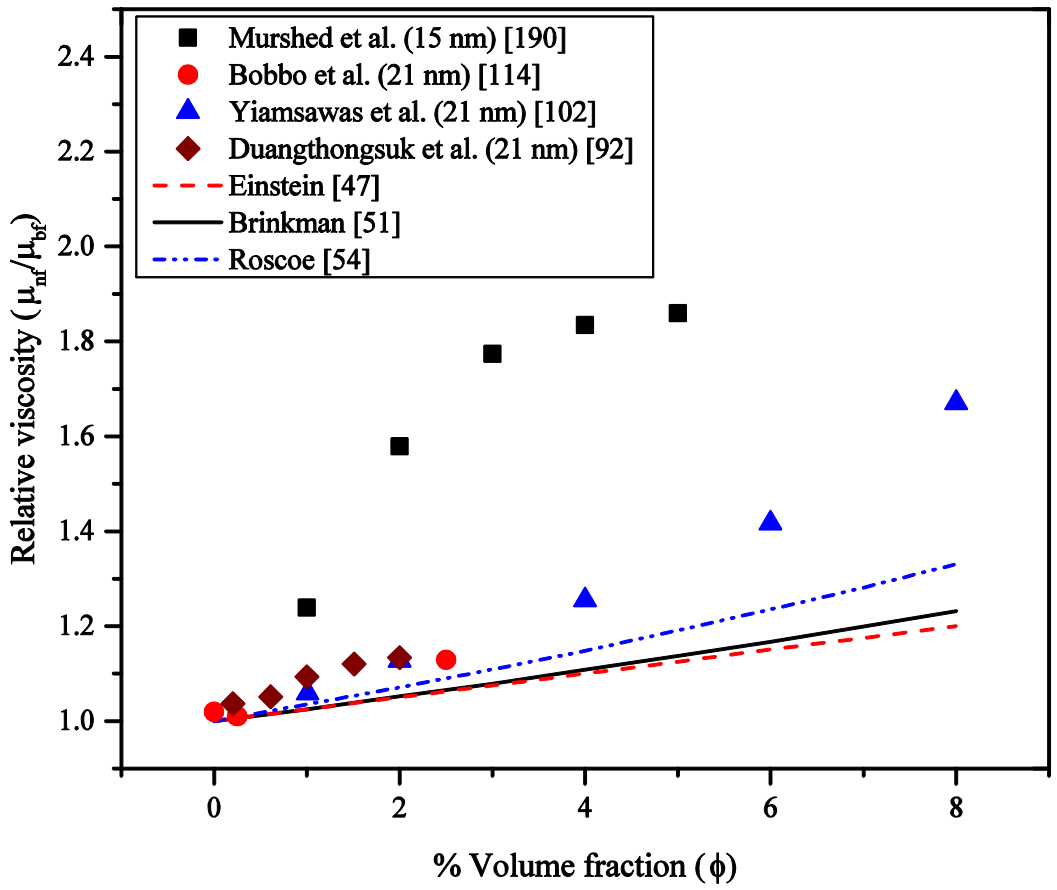

Figure 3 Underprediction of TiO_2-DI-water nanofluids by classical models.

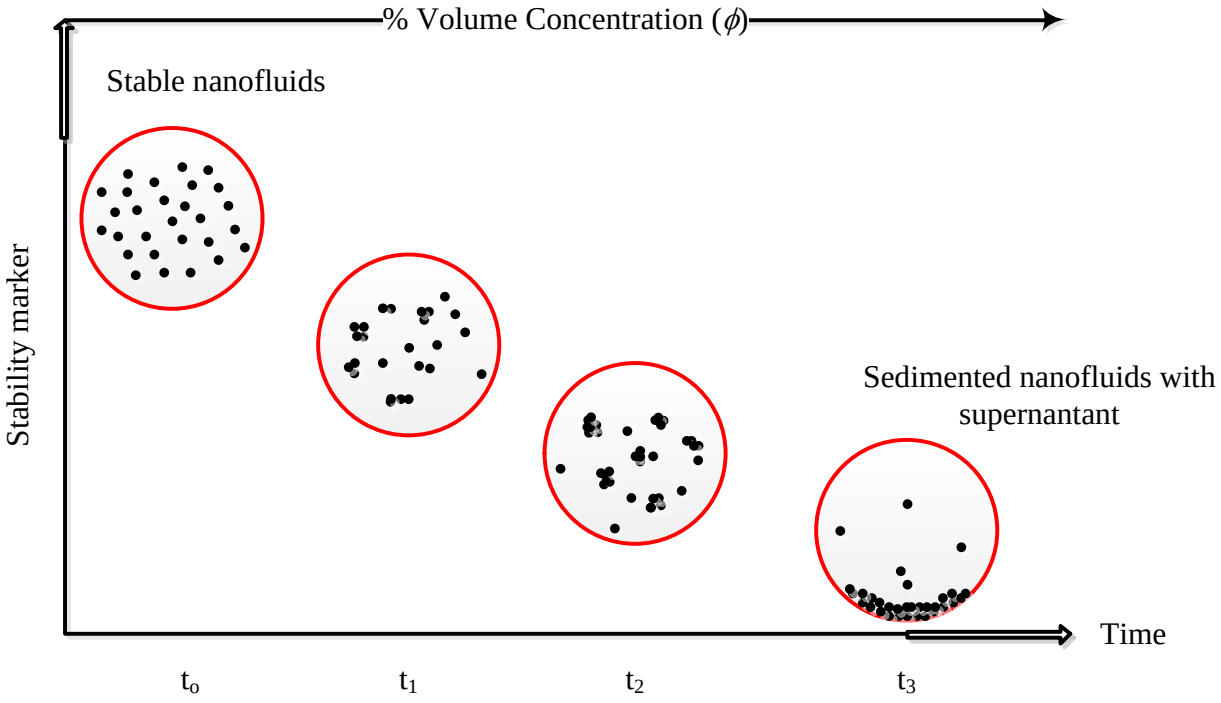

Figure 4 Instability sequence in nanofluids. At time t_o, the nanofluid is stable just after preparation by ultrasonication or HPH, at t_1, flocculation sets in and degenerates to agglomeration at t_3, which finally sediments at time t_3. As ϕ also increases, the tendency of the instability sequence is high.

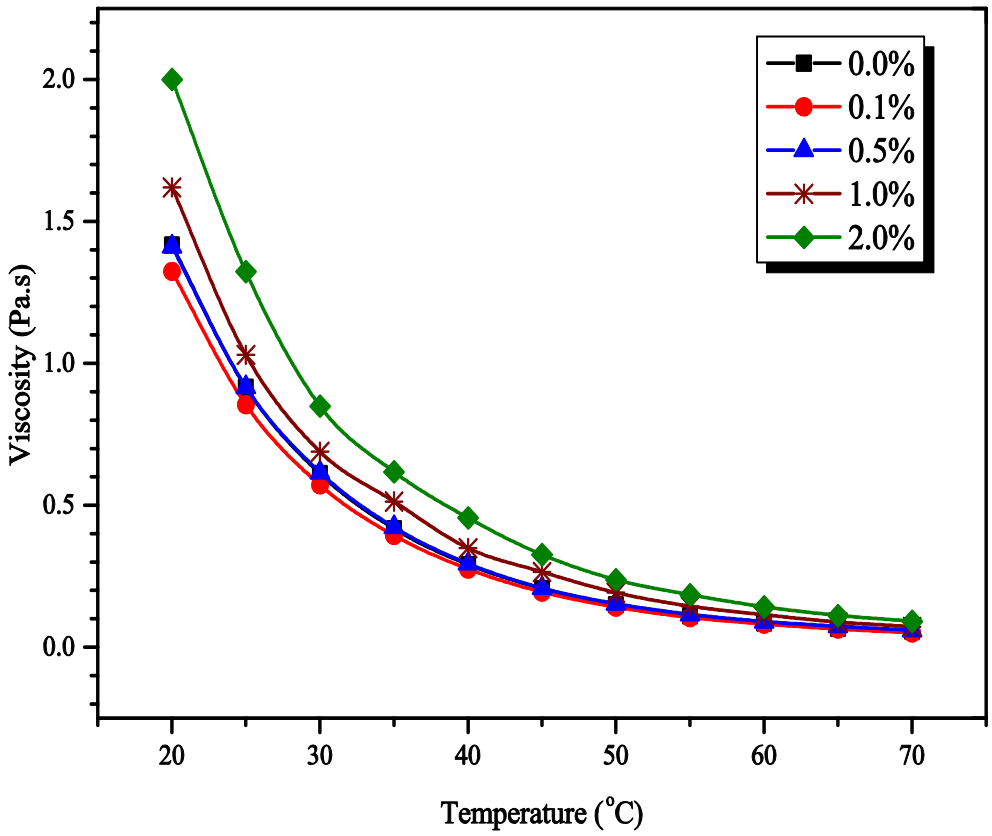

Figure 5 Effect of temperature on the viscosity of Al_2O_3-glycerol nanofluid [189].

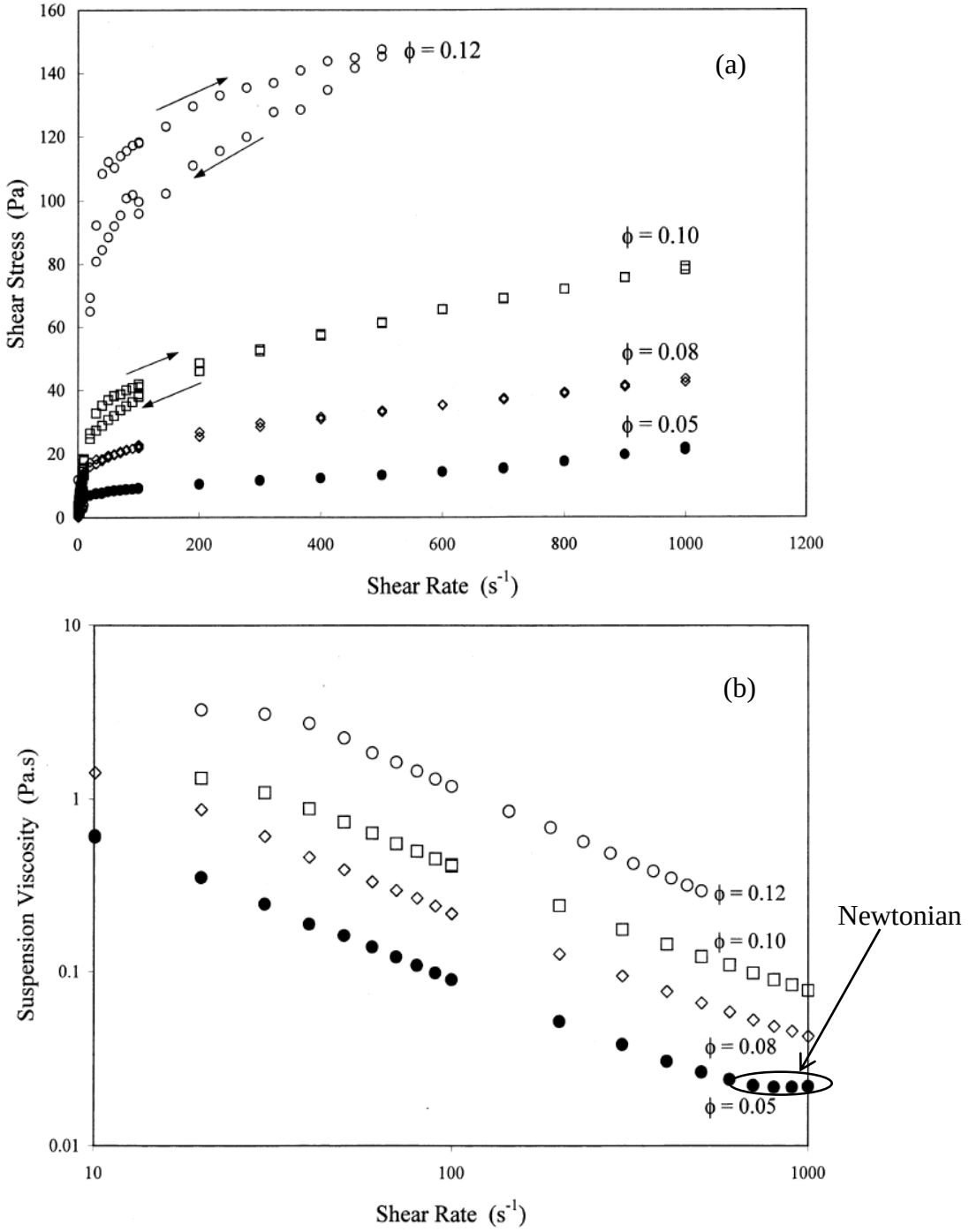

Figure 6 Effect of shear rate on the rheology of suspension: (a) the shear stress (τ)-shear rate ($\dot{\gamma}$) curve of TiO_2-water nanofluid at different particle volume fractions; (b) the nanofluid viscosity (μ_{nf})-shear rate ($\dot{\gamma}$) curve of TiO_2-water nanofluid at different particle volume fractions [83].

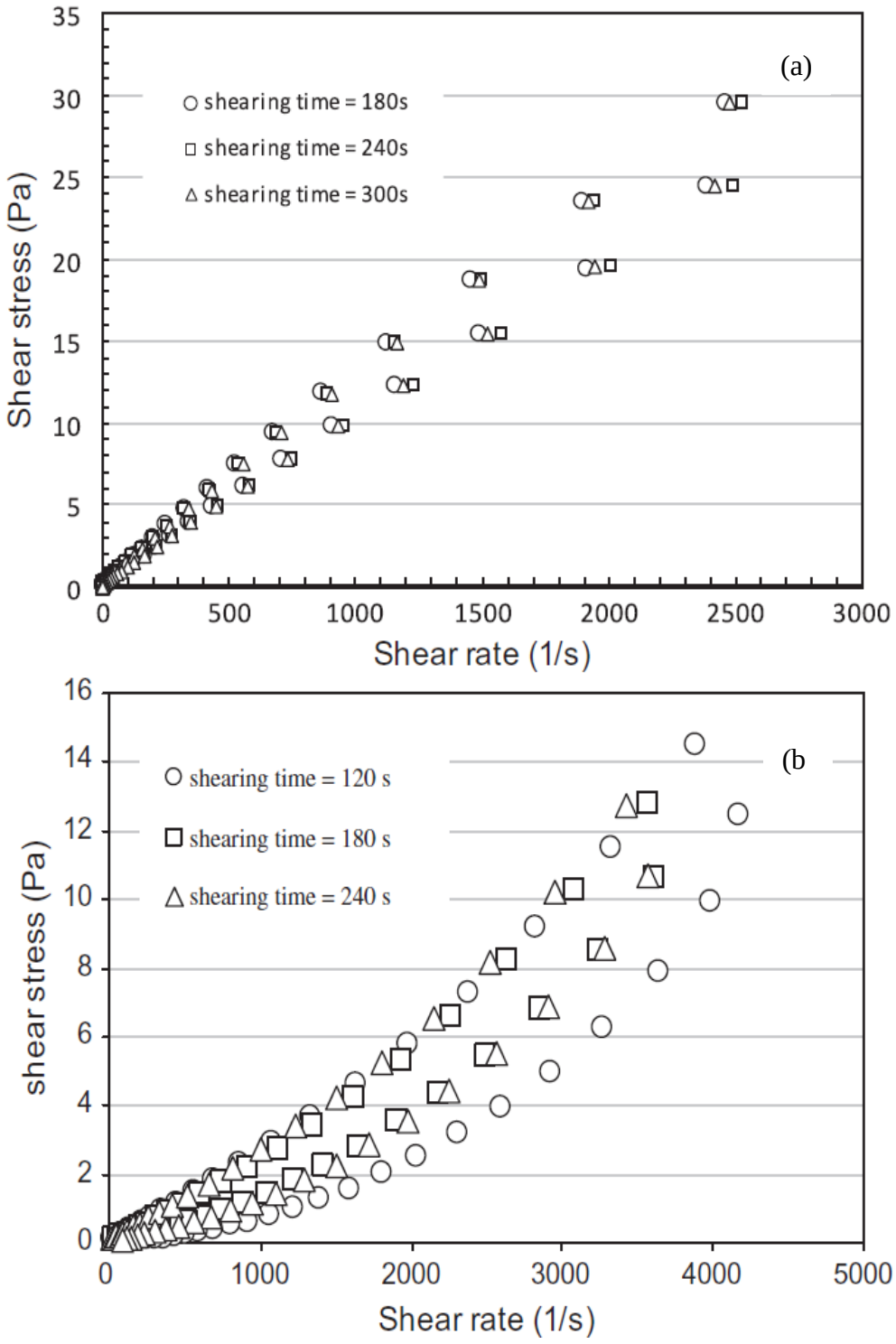

Figure 7 Effect of shearing time water-based nanofluids of CNT and Al_2O_3 at 5 ^oC: (a) CNT-water nanofluid showing shear thinning, thixotropic; (b) Al_2O_3-water nanofluid showing shear thickening, thixotropic [108].

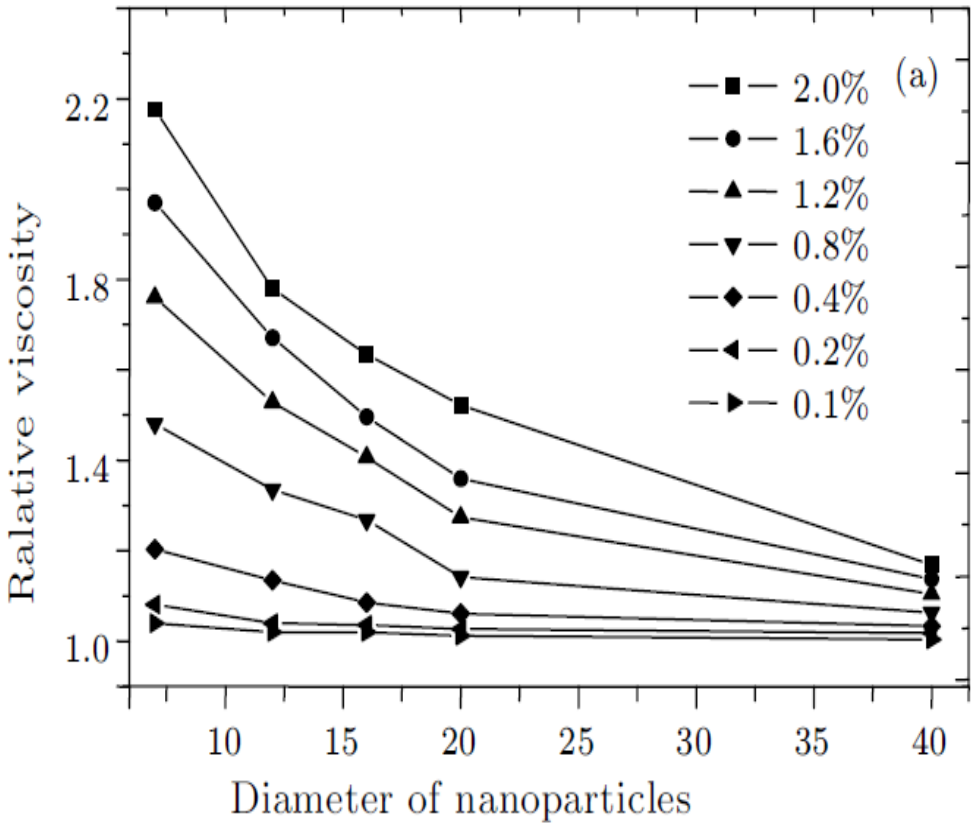

Figure 8. Effect of nanoparticle size on the relative viscosity of SiO_2-DI-water nanofluid [211].

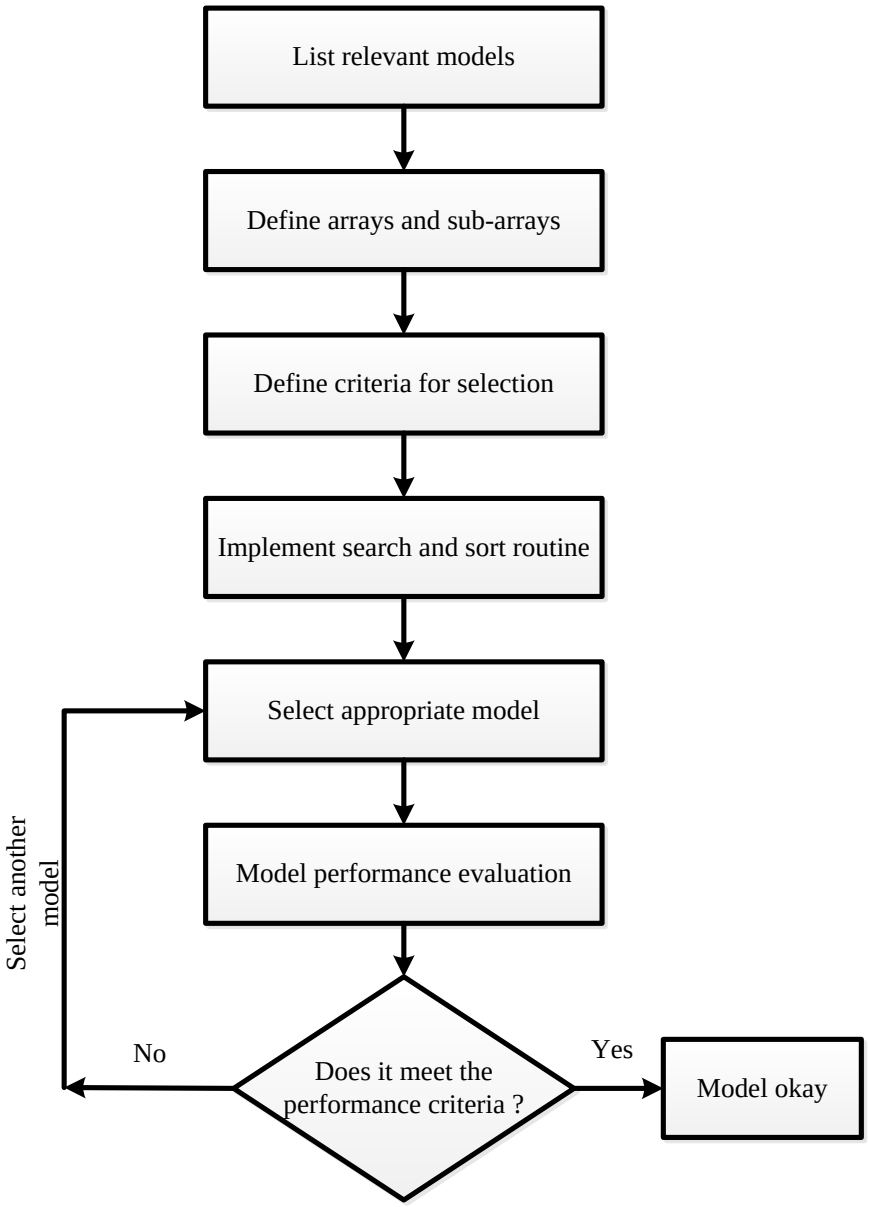

Figure 9 Criteria and selection flow chart for the implementation of search and sort algorithm.

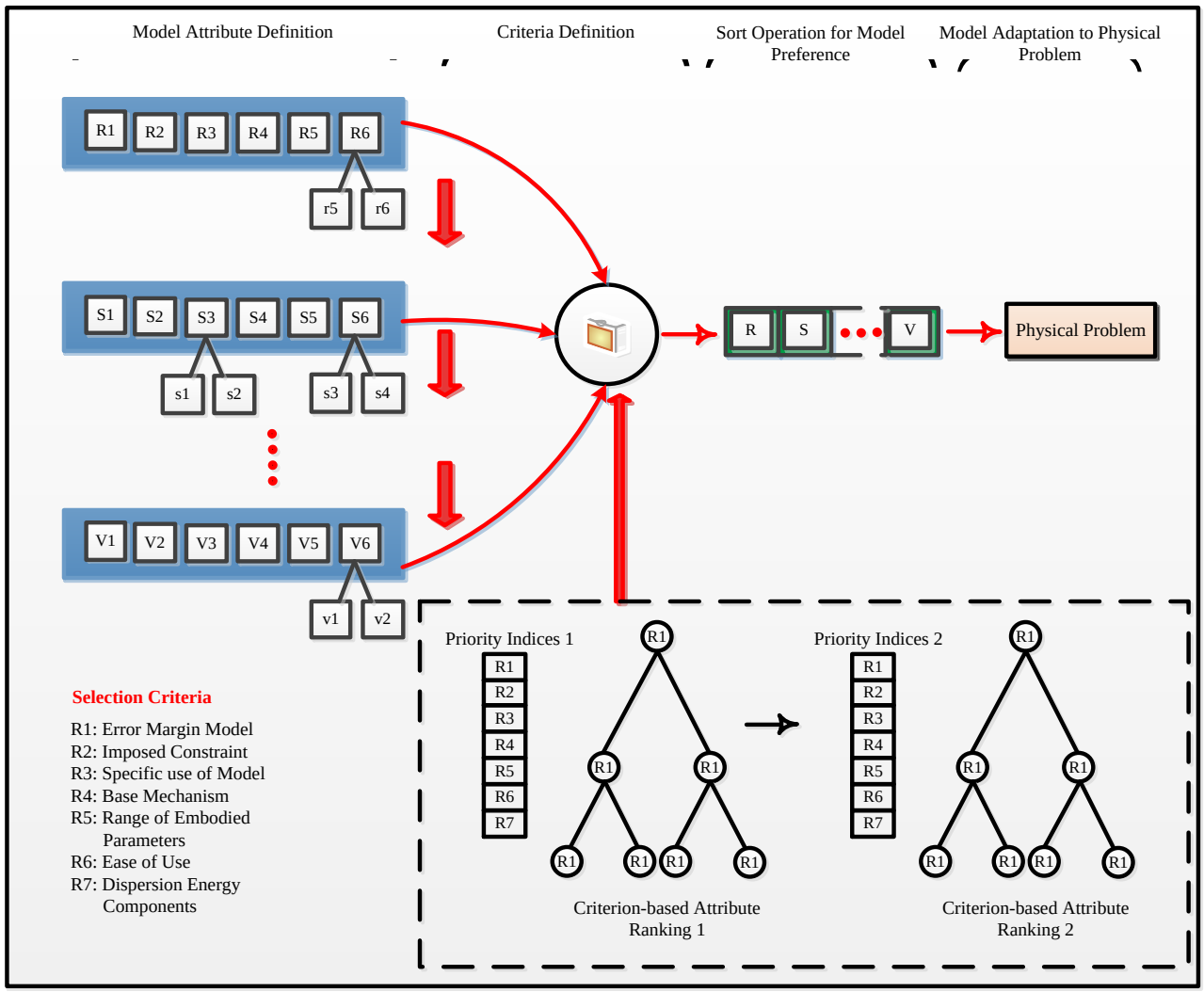

Figure 10 Generic algorithm for selection of appropriate nanofluid viscosity models. R, S,…V are available nanofluid viscosity models with attributes R1, R2,…V5, V6 and sub-array attributes r1, r2,…v5, v6.

Josua Meyer obtained his BEng (cum laude) in 1984, MEng (cum laude) in 1986, and his PhD in 1988, all in mechanical engineering from the University of Pretoria and is registered as a professional engineer. After his military service (1988-1989), he accepted a position as Associate Professor in the Department of Mechanical Engineering at the Potchefstroom University in 1990. He was Acting Head and Professor in Mechanical Engineering before accepting a position as Professor in the Department of Mechanical and Manufacturing Engineering at the Rand Afrikaans University in 1994. He was Chairman of Mechanical Engineering from 1999 until the end of June 2002, after which he was appointed Professor and Head of the Department of Mechanical and Aeronautical Engineering at the University of Pretoria from 1 July 2002. At present, he is the Chair of the School of Engineering. He specialises in heat transfer, fluid mechanics and thermodynamic aspects of heating, ventilation and air-conditioning. He is the author and co-author of more than 450 articles, conference papers and patents and has received various prestigious awards for his research. He is also a fellow or member of various professional institutes and societies such as the South African Institute for Mechanical Engineers, South African Institute for Refrigeration and Air-Conditioning, American Society for Mechanical Engineers, American Society for Air-Conditioning, Refrigeration and Air-Conditioning, and is regularly invited as a keynote speaker at local and international conferences. He has also received various teaching and exceptional achiever awards. He is an associate editor of *Heat Transfer Engineering* and Editor of the *Journal of Porous Media*.

Saheed A. Adio is currently a PhD student in the Department of Mechanical and Aeronautical Engineering, University of Pretoria, South Africa. He obtained his BSc(Hons) degrees in mechanical engineering at the Obafemi Awolowo University, Ile-Ife, Nigeria in 2005 with a second class upper mark and after a few

years of working, he obtained his MSc in 2010 with distinction from the same university. He is currently working on the mathematical modelling and experimental investigation into the effective viscosity of nanofluids under the supervision of Dr M. Sharifpur and Professor J.P. Meyer.

Mohsen Sharifpur is a senior lecturer and also responsible for the nanofluids research laboratory in the Department of Mechanical and Aeronautical Engineering at the University of Pretoria. He received his BSc in mechanical engineering from Shiraz University, Iran. He completed his MSc in nuclear engineering, and then received a full scholarship for PhD study in mechanical engineering (thermal fluid) from Eastern Mediterranean University. He was the only postgraduate student who received four out of four for the CGPA when he received his PhD. He is the author and co-author of more than 40 articles and conference papers. His research interests include convective multiphase flow, thermal fluid behaviour of nanofluids, porous media, CFD and waste heat to work in thermal systems. He is also a reviewer for notable accredited journals.

Paul N. Nwosu obtained a PhD degree in mechanical engineering at the University of Nigeria in 2011. He did a stint as a postdoctoral fellow at the Mechanical and Aeronautical Engineering Department (Thermofluids Research Group), University of Pretoria, South Africa, and Energy Technology Department (Internal Combustion Engine Research Group), Aalto University, Finland. His research interests are in renewable energy systems, nanofluids, mechatronics (with embedded software development), finite element modelling and computer simulation.